Chapter 4

Results and discussion

Chapter 4A

Characterization of flours from underutilized *Dioscorea* species and its utilization in cookies enriched with almond protein isolate

4A.1   Introduction

The present chapter deals with the characterization of flours from three yam species, viz., *Dioscorea esculenta* (Y1), *Dioscorea alata* (purple yam, Y2) and *Dioscorea alata* (yellow yam, Y3), and its utilization in the preparation of cookies. The native yam flours were not found suitable for the preparation of cookies due to their low protein content and structural breakage of cookies during trial experiments. The native yam flours were mixed with almond protein isolate (API) in an attempt to get the qualities of gluten in gluten-free food such as cookies. Hence, the flours Y1, Y2, and Y3 were mixed with 10 % of API, and the blends were named PY-1, PY-2, and PY-3, respectively. The characterization of all the native flours and their blends with API was done. Consequently, PY-1, PY-2, and PY-3, which represents the flour and API blends, were used in the formulation of cookies. The nutritional composition, physical characteristics, texture and color of the prepared cookies were checked. Sensory analysis of the cookies was also conducted.

4A.2   Flour characteristics

4A.2.1 Proximate analysis and antioxidant properties of almond protein isolate and flours

The proximate composition and antioxidant properties of almond protein isolate (API) are shown in **Table 4A.1**. The protein content of API was 82.79 ± 0.31 %, which was found to be higher than protein content (64 to 79 %) isolated from almond flour as reported by **de Almeida et al. [19]**, and lower than protein (89.95 %) extracted from almond seed **[58]**. Carbohydrate and fat content of 4.72 ± 0.05 % and 2.30 ± 0.14 %, respectively, were found to be higher than 3.15 % and 0 %, reported by **Yusuf [58]**. The extraction process and the drying methods can affect the functionality, composition, structure, and conformation of proteins **[18]**.

Table 4A.1: Proximate composition (on dry weight basis) and antioxidant properties of flours, almond protein isolate and their blends

Compositions	Samples							
	WF	API	YF-1	YF-2	YF-3	PY-1	PY-2	PY-3
Moisture (%)	13.15 ± 0.23^a	7.12 ± 0.16^d	9.06 ± 0.11^c	9.00 ± 0.15^c	10.71 ± 0.40^b	8.95 ± 0.39^c	9.11 ± 0.15^c	10.57 ± 0.43^b
Protein (%)	12.98 ± 0.12^d	82.79 ± 0.31^a	5.21 ± 0.13^f	5.71 ± 0.19^f	7.56 ± 0.12^e	13.46 ± 0.30^{cd}	13.72 ± 0.16^c	16.12 ± 0.23^b
Crude fat (%)	1.60 ± 0.15^c	2.30 ± 0.14^a	1.47 ± 0.21^c	1.61 ± 0.08^c	1.58 ± 0.10^c	1.73 ± 0.08^{bc}	2.12 ± 0.17^{ab}	1.84 ± 0.22^{bc}
Crude fiber (%)	1.99 ± 0.15^c	1.98 ± 0.13^c	2.18 ± 0.10^{bc}	2.51 ± 0.19^b	2.43 ± 0.11^b	2.46 ± 0.10^b	3.27 ± 0.07^a	2.95 ± 0.23^a
Ash (%)	1.71 ± 0.11^e	1.09 ± 0.09^f	2.42 ± 0.03^d	2.96 ± 0.17^{ab}	2.53 ± 0.05^{cd}	2.56 ± 0.05^{cd}	3.04 ± 0.12^a	2.75 ± 0.06^{bc}
Carbohydrate (%)	68.57 ± 0.08^e	4.72 ± 0.05^g	79.66 ± 0.06^a	78.21 ± 0.43^b	75.17 ± 0.41^c	70.84 ± 0.51^d	68.73 ± 0.48^e	65.77 ± 0.95^f
TPC (mg GAE/g)	1.33 ± 0.15^a	0.51 ± 0.07^b	0.12 ± 0.03^d	0.18 ± 0.03^d	0.39 ± 0.07^{bc}	0.15 ± 0.04^d	0.25 ± 0.06^{cd}	0.43 ± 0.01^{bc}
DPPH (% Inhibition)	71.14 ± 0.19^c	80.48 ± 1.02^a	15.36 ± 0.56^h	24.84 ± 0.42^g	43.51 ± 0.29^e	33.69 ± 0.31^f	52.44 ± 0.85^d	76.25 ± 0.76^b

Data values are presented as mean ± standard deviation. Data with different alphabetic superscript in the same row are statistically significant (p<0.05). WF: wheat flour; YF-1: *D. esculenta* flour; YF-2: *D. alata* (purple yam) flour; YF-3: *D. alata* flour; PY-1: *D. esculenta* (yellow yam) flour and almond protein isolate blend; PY-2: *D. alata* (purple yam) flour and almond protein isolate blend; PY-3: *D. alata* (yellow yam) flour and almond protein isolate blend.

High total phenolic content (TPC) and DPPH scavenging activity (% inhibition) of 0.51 ± 0.07 mg GAE/g and 80.48 ± 1.02 %, respectively, were found in API. High TPC and antioxidant activity in API could be explained by the higher presence of polyphenols such as proanthocyanidins, hydrolyzable tannins, and flavonoids in almonds [14, 48]. A similar high value of TPC and antioxidant activity was observed for almond proteins isolated through aqueous and enzyme-assisted aqueous extraction processes [20].

Proximate composition and antioxidant properties of native and blend flours are presented in **Table 4A.1**. No significant difference in the moisture content was noticed due to the inclusion of API in the native flours. The inclusion of API in the native yam flours resulted in a significant increase in protein content. The highest protein content of 7.56 ± 0.12 % and 16.12 ± 0.23 % was recorded for yellow yam flour (YF-3) and yellow yam flour and API blend (PY-3), respectively. The protein content of yam flours reported in this study is consistent with the protein content of $2.66 - 9.02$ % and $0.91 - 10.16$ % reported for *D. esculenta* and *D. alata* flours, respectively [21, 39, 46, 53]. Higher protein content in the blends was due to the inclusion of API in native yam flours, and as a consequence, a significant decrease in carbohydrate content of yam flour-API blends was observed.

No significant increase in the TPC values was observed in the blends compared to native yam flour. Meanwhile, a significant increase in the antioxidant activity (DPPH scavenging activity, % inhibition) was observed in blends compared to the respective native yam flours due to the inclusion of API, which possibly could increase the antioxidant activity [14, 20, 48].

4A.2.2 Functional properties of flours

The data related to the functional properties of flours are shown in **Table 4A.2**. The bulk density of the yam flour decreased with the addition of API. The lowering of bulk density can be an advantage for consumers who can get more nutrients from the consumption of lighter food items [40]. The water adsorption capacity (WAC) and oil adsorption capacity (OAC) of the yam flour increased significantly ($p<0.05$) with the addition of API. This increase in WAC and OAC can be attributed to the hydrophilic and hydrophobic side chains in amino acids available in the protein isolate, resulting in increased interactions with water and oil [40, 41]. The swelling power of the blends of yam flour and API was observed to be lower than the native yam flour. This reduction in

swelling power with the addition of API could be linked to the reduction in amylose content on account of the decrease in the carbohydrate content of the blends [16, 49]. The foaming capacity (FC) of the flours increased significantly ($p<0.05$) with the addition of API, whereas the foaming stability (FS) decreased with the addition of API. The increase in FC can be attributed to the increase in protein content of the flours due to the addition of API, and protein content was found to be positively correlated with FC [27, 40]. The inverse relation between FC and FS may be due to the formation of large air bubbles with thin and less flexible protein film in flours with high foam capacity that eventually collapses easily, resulting in low FS [10].

Table 4A.2: Functional properties of flours from different *Dioscorea* species and their blends with almond protein isolate

Sample	BD (g/ml)	WAC (g/g)	OAC (g/g)	SP (g/g)	FC (%)	FS (%)
WF	0.72 ± 0.01[d]	1.27 ± 0.03[f]	1.27 ± 0.01[b]	5.25 ± 0.04[b]	9.26 ± 0.08[c]	41.23 ± 0.54[d]
YF-1	0.82 ± 0.01[a]	1.51 ± 0.03[e]	0.82 ± 0.01[d]	5.90 ± 0.02[a]	3.55 ± 0.32[e]	66.10 ± 0.78[b]
YF-2	0.80 ± 0.01[a]	1.51 ± 0.02[e]	0.99 ± 0.02[c]	4.45 ± 0.03[c]	3.68 ± 0.13[e]	68.44 ± 0.63[a]
YF-3	0.78 ± 0.01[b]	1.94 ± 0.02[d]	1.01 ± 0.03[c]	3.85 ± 0.01[f]	5.12 ± 0.07[d]	52.42 ± 0.60[c]
PY-1	0.75 ± 0.01[c]	2.05 ± 0.02[c]	1.31 ± 0.02[b]	4.15 ± 0.02[d]	11.67 ± 0.30[b]	34.63 ± 0.91[e]
PY-2	0.72 ± 0.01[d]	2.16 ± 0.03[b]	1.57 ± 0.01[a]	4.03 ± 0.02[e]	11.51 ± 0.25[b]	33.22 ± 0.76[e]
PY-3	0.68 ± 0.01[e]	2.95 ± 0.03[a]	1.56 ± 0.02[a]	3.03 ± 0.03[g]	14.93 ± 0.16[a]	21.61 ± 0.81[f]

Data values are presented as mean ± standard deviation. Data with different alphabetic superscript in the same column are statistically significant ($p<0.05$). WF: wheat flour; YF-1: *D. esculenta* flour; YF-2: *D. alata* (purple yam) flour; YF-3: *D. alata* flour; PY-1: *D. esculenta* (yellow yam) flour and almond protein isolate blend; PY-2: *D. alata* (purple yam) flour and almond protein isolate blend; PY-3: *D. alata* (yellow yam) flour and almond protein isolate blend.

4A.2.3 Pasting properties of flours

The pasting properties of the flours measured by RVA are shown in **Table 4A.3**. Pasting properties refers to the changes during the gelatinization of starch granules, which swell and rupture due to the combined effect of heat and water during heating and cooling.

Table 4A.3: Pasting properties of flours

Sample	PT (ºC)	PV (cP)	HPV (cP)	FV (cP)	BD (cP)	SB (cP)	Stability ratio	Setback ratio	Relative breakdown
WF	66.23 ± 1.02[c]	4192 ± 26.06[a]	706 ± 18.03[a]	1472 ± 27.40[a]	3486 ± 36.04[a]	766 ± 45.40[a]	0.17 ± 0.01[e]	2.09 ± 0.09[b]	4.56 ± 0.23[a]
YF-1	65.87 ± 0.60[c]	672 ± 8.19[b]	263 ± 10.58[b]	528 ± 15.39[b]	409 ± 5.20[b]	265 ± 8.54[b]	0.39 ± 0.01[d]	2.01 ± 0.04[bc]	1.54 ± 0.07[b]
YF-2	68.22 ± 1.26[c]	328 ± 17.06[c]	197 ± 13.08[d]	422 ± 4.58[c]	131 ± 30.05[c]	225 ± 9.17[b]	0.60 ± 0.07[c]	2.15 ± 0.12[ab]	0.58 ± 0.11[c]
YF-3	76.08 ± 0.84[b]	257 ± 6.56[d]	233 ± 4.00[c]	397 ± 11.53[c]	24 ± 2.65[d]	164 ± 7.55[c]	0.91 ± 0.01[a]	1.70 ± 0.02[bc]	0.15 ± 0.01[d]
PY-1	74.91 ± 1.03[b]	76 ± 5.57[f]	58 ± 6.08[f]	151 ± 12.77[e]	18 ± 2.65[d]	93 ± 18.00[d]	0.76 ± 0.04[b]	2.63 ± 0.45[a]	0.20 ± 0.03[d]
PY-2	74.73 ± 1.33[b]	143 ± 3.51[e]	132 ± 2.00[e]	195 ± 4.58[d]	11 ± 3.21[d]	63 ± 3.61[de]	0.92 ± 0.02[a]	1.48 ± 0.03[c]	0.18 ± 0.04[d]
PY-3	80.72 ± 0.51[a]	56 ± 4.36[f]	45 ± 2.65[f]	83 ± 3.61[f]	11 ± 6.56[d]	38 ± 4.58[e]	0.81 ± 0.11[ab]	1.85 ± 0.14[bc]	0.29 ± 0.16[cd]

Data values are presented as mean ± standard deviation. Data with different alphabetic superscript in the same column are statistically significant ($p<0.05$). WF: wheat flour; YF-1: *D. esculenta* flour; YF-2: *D. alata* (purple yam) flour; YF-3: *D. alata* flour; PY-1: *D. esculenta* (yellow yam) flour and almond protein isolate blend; PY-2: *D. alata* (purple yam) flour and almond protein isolate blend; PY-3: *D. alata* (yellow yam) flour and almond protein isolate blend.

The pasting properties of the yam flour, and the blends of yam flour and almond protein isolate were significantly (p<0.5) different. The peak viscosity of the yam flours reduced significantly with the incorporation of almond protein isolate. The decrease in peak viscosity could be correlated to the lowering of carbohydrates (mainly starch) as well as the interactions between the components such as fat, protein, and starch of the blends [40]. The addition of protein isolate can restrict the swelling behaviour of the starch granules, consequently restricting the gelatinization of the starch granules. Similar results were reported for oat starch and corn starch added with whey protein isolates [29, 56]. The final viscosities of the blends showed a similar reduction due to the addition of the almond protein isolate to yam flour.

Low breakdown viscosity exhibited by the blends of yam flour-protein isolate compared to native flours, indicates the higher stability of the pastes to high shear and temperature. A lower breakdown can be linked to the presence of a protein that leads to a lower disruption of starch granules or the reduction in starch concentrations due to protein addition, thereby, can increase the paste stability. Lower setback values of the blends reflect a lower degree of retrogradation compared to the respective native flours. Thus, somehow the protein isolate interfered with and delayed the retrogradation process. Lower setback values were shown by the blends of yam flour and almond protein isolate making them suitable for food applications such a refrigerated and frozen products, where a lower syneresis rate is desired [51]. During starch gelatinization, higher the thermal energy required to break the hydrogen bonds between starch molecules and form new hydrogen bonds between starch and water, the higher the pasting temperature. It is also influenced by the proteins present in the gel system that may compete with the starch molecules for water and can form their own gel [37]. A higher pasting temperature was exhibited by the blends of yam flour and almond protein isolate compared to the native flours. Similar reports on the increase in pasting temperature due to the addition of proteins were reported by **Nogueira et al. [37]**, **Chinma et al. [17]**, and **Indrani et al. [24]**.

The stability ratio (hot paste viscosity: peak viscosity) of the yam flours (except YF-3) was found to increase with the addition of almond protein isolates, which indicated that the proteins prevented swelling and breakdown of the starch granules. The setback ratio (final viscosity: hot paste viscosity) of the yam flours (except YF-2) increased significantly with the addition of almond protein isolate, which indicated the

retrogradation behavior and the formation of junction zones between starch molecules. Relative breakdown (breakdown: setback) of the yam flours (except YF-3) was found to be lower with the addition of almond protein isolate, which indicated a lower disruption of starch granules and high integrity of starch granules after retrogradation. Moreover, it is worth mentioning that a higher degree of rupture of granules during heating and holding may not always lead to a weaker gel after retrogradation. At the same time, a firm viscoelastic paste can be formed by the higher amount of leached amylose fractions during the setback stage which can help in the formation of 3-dimensional networks in the gel **[29]**.

Almond protein isolate addition to the yam flour increased the pasting temperature and decreased the peak viscosity, hot paste viscosity, final viscosity, breakdown, and setback. A similar reduction of the peak viscosity, hot paste viscosity, final viscosity, breakdown, and setback as well as an increase in pasting temperature was reported for premixes of groundnut protein concentrate and wheat flour **[40]**, Bambara groundnut protein concentrate and wheat/plantain flour **[26]**, and soy protein isolate and rice flour **[41]**. The reduction in the pasting properties (except pasting temperature) of the blends may be attributed to the increase in protein content that may affect the starch granules and induce dilution effect.

4A.2.4 ATR-FTIR spectra of flours

ATR-FTIR spectra of the flour samples are presented in **Fig. 4A.1 (A)**, which provides information on short-range crystalline order in starch and can detect a wide range of functional groups that are visible in the form of peaks. The changes due to any modification of flour can be identified on a structural level using FTIR. Native yam flours and yam flours added with almond protein isolate showed similar FTIR spectra, suggesting no synergistic interactions and the addition of API did not alter the structure of the yam flours. However, a difference in the intensities of absorbance was observed in the FTIR spectra due to the addition of protein isolate to yam flours.

Absorbance intensities in the region 3000 – 3700 cm^{-1} represent OH stretches of inter- and intramolecular H-bonds **[34, 59]**. The broadband with a peak at 3277 cm^{-1} representing OH stretch was observed in all the sample flours, and it can be associated with the moisture content of samples **[35]**.
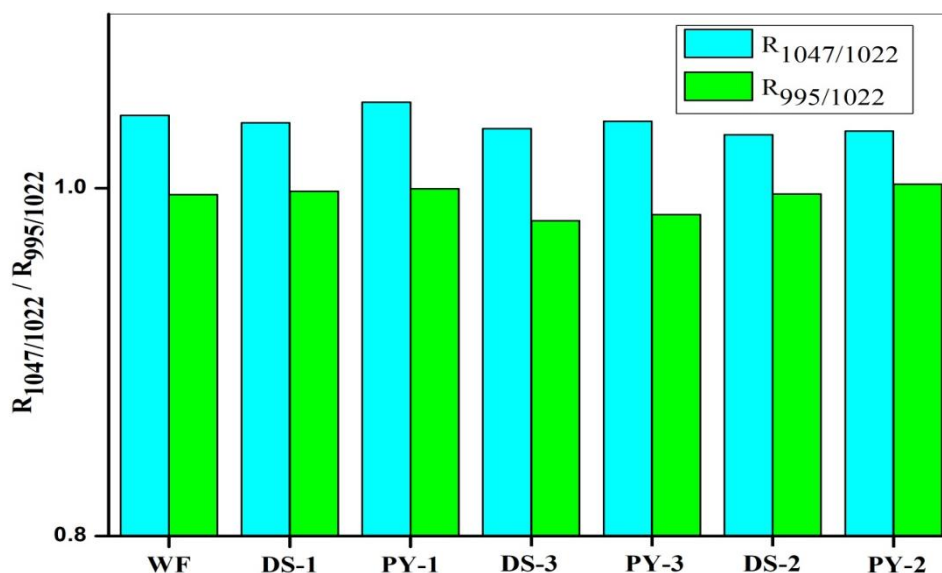
(A)
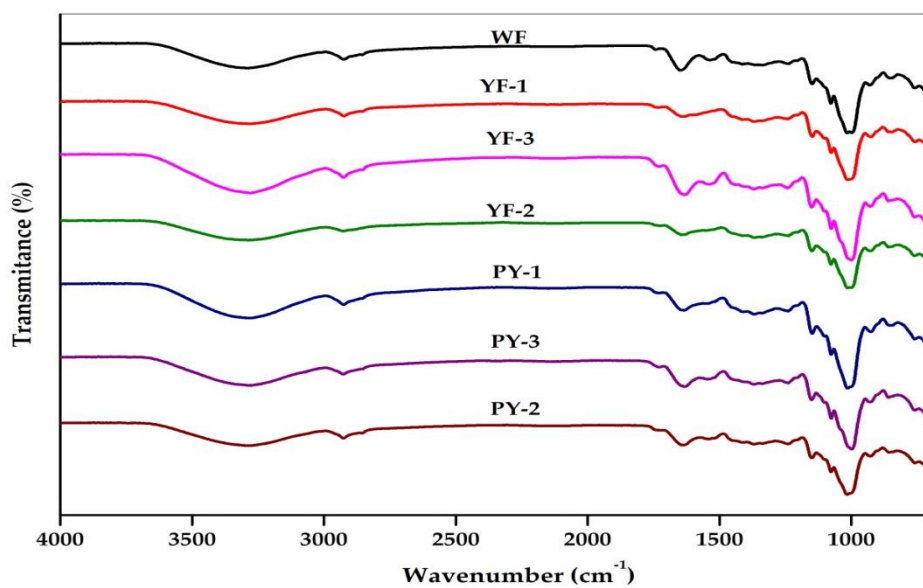
(B)

Fig. 4A.1: (A) ATR-FTIR spectra of flours, and (B) absorbance ratio of 1047/1022 cm^{-1} and 995/1022 cm^{-1}. WF: wheat flour; YF-1: *D. esculenta* flour; YF-2: *D. alata* (purple yam) flour; YF-3: *D. alata* (yellow yam) flour; PY-1: *D. esculenta* flour and almond protein isolate blend; PY-2: *D. alata* (purple yam) flour and almond protein isolate blend; PY-3: *D. alata* (yellow yam) flour and almond protein isolate blend.

The absorbance band in the range of 3000 – 2800 cm^{-1} can be related to the lipid content of samples [35]. A greater intensity of peak at 2925 cm^{-1}, which is associated with asymmetric stretches of the CH$_2$ group present in the aliphatic chains of fatty acids, could be correlated with the lipid content of sample flours. Strong absorbance bands at 1600 – 1700 cm^{-1} (amide I band) and 1550 – 1570 cm^{-1} (amide II band) indicate a higher

110

protein content [5]. All the yam flours mixed with almond protein isolate showed a higher absorbance peak at 1632 and 1551 cm^{-1} indicating a higher level of protein than the native yam flours. This result was obvious due to the addition of almond protein isolate to native yam flours. Peaks in the band at 800 - 1200 cm^{-1} are the fingerprint region used to characterize starch [5, 35]. No difference in the shape of the peaks was observed in the samples. However, the observed difference in the intensity of peaks could be due to the milling methods employed to obtain flours, granule size, and amount of damaged starch in flours [8, 15].

FTIR spectrum could be used to determine the degree of order and the degree of double helix of starch granules using the ratio of absorbance at 1047/1022 cm^{-1} and 995/1022 cm^{-1}, respectively [60, 61]. **Fig. 4A.1 (B)** shows that the ratio of 1047/1022 cm^{-1} was higher for all the yam flours enriched with API than the respective native yam flour. This indicated an increase in the degree of order due to the perfection in the degree of crystallinity in starch granules [23, 31]. A similar increase in the ratio of 995/1022 cm^{-1} was observed for all the yam flours enriched with API compared to their respective native yam flours. This observation suggests a more effective organization of double helices within the crystalline lamellae of starch granules [4, 57].

4A.3 Cookie characteristics

4A.3.1 Rheological characteristics of cookie dough

The rheological characteristics of the cookie dough prepared from the blend of yam flour and almond protein isolate were measured by a dynamic frequency sweep test within the linear viscoelastic region. **Fig. 4.2 (A) & (B)** depicts the variation of G´ (storage modulus) and G´´ (loss modulus) and shows the dependence of both the modulus (G´ and G´´) on frequency. In all the dough samples, G´ (storage modulus) was found to be greater than G´´ (loss modulus) which implies that all the sample dough tends to be more elastic than viscous. The dough strength (G´) increased in the following order: PY-3 < PY-2 < PY-1 < Control. These results confirmed the viscoelastic nature of the samples [44].
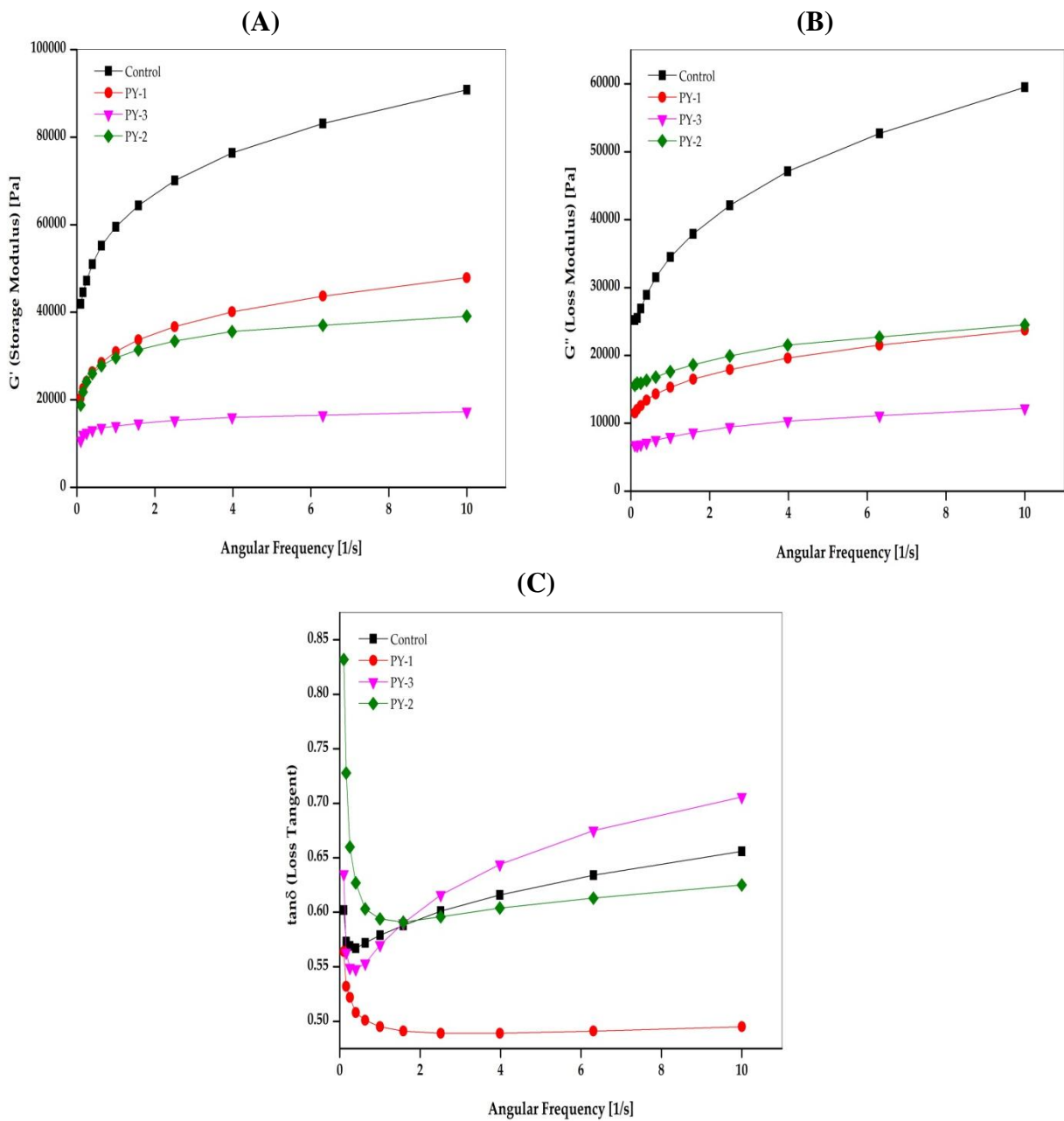
Fig. 4A.2: Dynamic rheological characteristics of cookie doughs. (A) The storage modulus; (B) the loss modulus; and (C) tanδ. WF: wheat flour cookie dough; PY-1: *D. esculenta* flour-almond protein isolate cookie dough; PY-2: *D. alata* (purple yam)-almond protein isolate cookie dough; PY-3: *D. alata* (yellow yam) flour-almond protein isolate cookie dough.

In a rheological study, G´ refers to the solid-like property and toughness of a sample which is linked to the extent of crosslinking in a dough. A higher value of G´ and G´´ was noticed for the wheat flour dough compared to the dough prepared from blends of yam flour and almond protein isolate, indicating a low viscoelastic behaviour of the dough prepared from blends. The absence of gluten in the blends of yam flour and almond protein isolate makes the dough less cohesive and elastic, and have a major impact on the rheological properties

The variation of loss tangent ($\tan\delta = G´´/ G´$) as a function of frequency at 25 ℃ is presented in **Fig. 4.2 (C)**. All the doughs showed a higher tanδ value at higher frequencies indicating an increase in the viscous characteristics with the increase in frequency. The tanδ value increased in the following order: PY-1 < PY-2 < Control < PY-3. The tanδ value of PY-1 cookie dough was found to be the lowest indicating more elasticity in nature and a stronger gel network (gel strength) compared to all other dough samples. This could be because protein or other non-starch ingredients played an important role in the interactions of flour constituents **[42]**.

A similar study reported a higher G´ and G´´ for wheat flour dough than dough prepared from a blend of wheat flour and soy protein isolate **[50]**. Corn flour substituted with pea proteins also presented lower G´ and G´´ values than control corn flour dough **[45]**. The prevalence of G´ over G´´ in cookie dough may be due to the high fat and protein content, and low moisture content **[12]**. The changes in the gel strength observed may be due to the macromolecular organization as a result of interactions between the protein and polysaccharides leading to changes in the profile of G´ and G´´ **[22, 52]**. Moreover, the rheological properties of flour depend on various substances such as water, D_2O, esterifying agents for glutamine residues, urea, salts, agents affecting disulphide bonds, and the protein subunits that are present or added in the flour **[7]**. Meanwhile, in this study, the rheological properties of the dough samples were consistent with the physical parameters of the cookies and the RVA results of the flours.

4A.3.2 Proximate analysis and antioxidant properties of cookies

The proximate composition of the cookies (**Fig. 4A.3**) made from the blend of yam flour and almond protein isolate is presented in **Table 4A.4**.
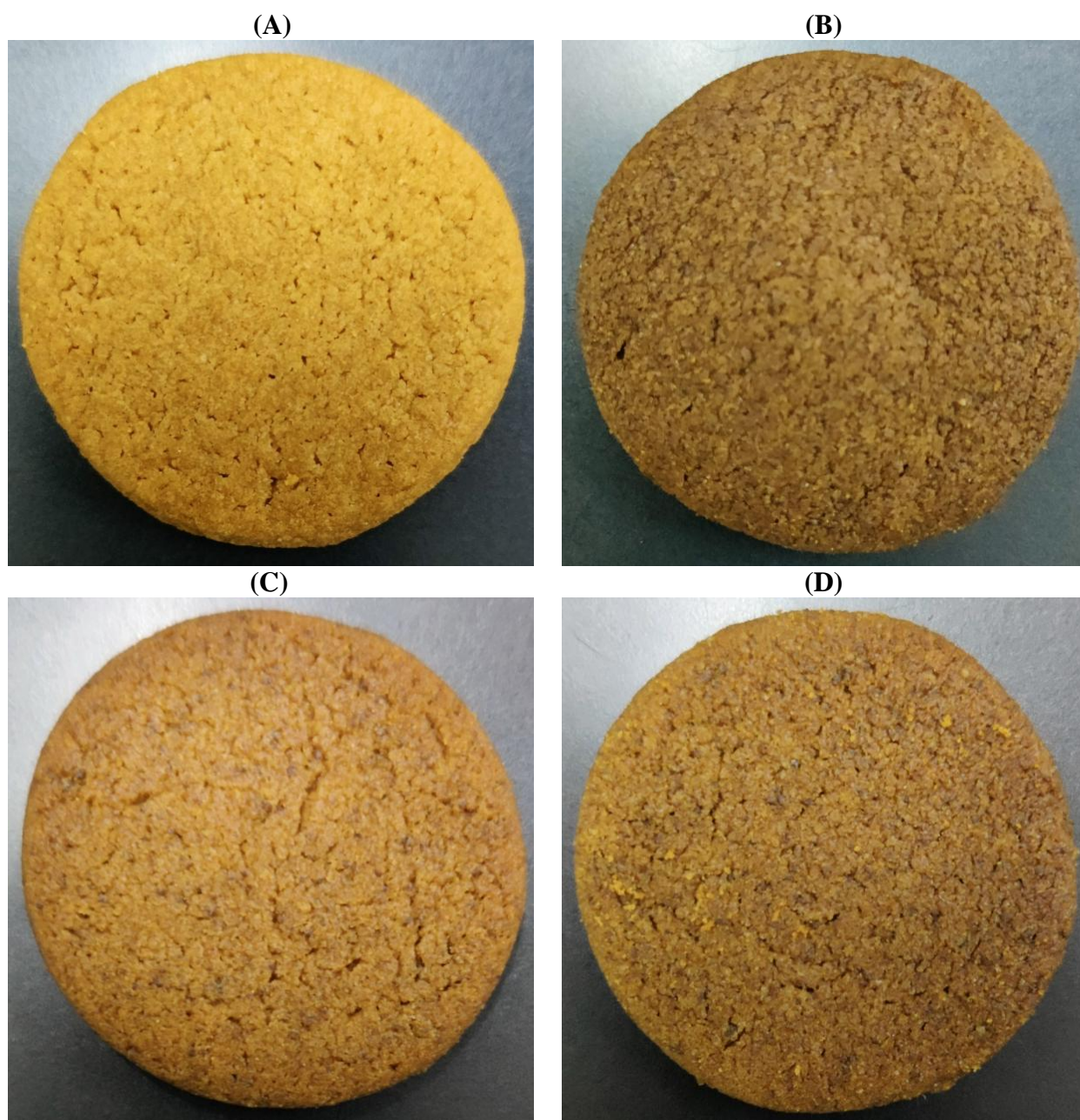
(A)

(B)

(C)

(D)

Fig. 4A.3: Cookies from (A) WF: wheat flour cookie dough; (B) PY-1: *D. esculenta* flour-almond protein isolate cookie dough; (C) PY-2: *D. alata* (purple yam)-almond protein isolate cookie dough; and (D) PY-3: *D. alata* (yellow yam) flour-almond protein isolate cookie dough.

The moisture content of yam flour-API cookies ranged from 1.88 to 2.28 %, which was lower than the control (wheat flour cookies). Meanwhile, it was found to be lower than the range of moisture content (3.28 – 5.33 %) reported for cookies from rice flour and soy protein isolate (SPI) blends [41]. The relatively lower moisture content of

cookies in this study may be useful for the higher shelf-life of the cookies. The protein content of PY-3 cookies was the highest (8.08 ± 0.04 %) compared to all other cookies, and the moisture content decreased due to the decrease in protein content of cookies. A similar reduction in moisture content of cookies from wheat flour blended with buckwheat flour was reported due to a decrease in protein content [25]. The crude fat, crude fiber, and ash content of the cookies from yam flour and API blends were found to be higher than the control. This increase in fat content could be attributed to the high OAC of the yam flour and API blends. A similar increase in the fat content of cookies from rice flour and SPI blends due to fat-binding properties of SPI was reported [41]. Due to the lower carbohydrate content of the cookies from yam flour and API blends as compared to control, it could be used in the diet for obese and diabetic patients.

Table 4A.4: Proximate composition (on dry basis) and antioxidant properties of cookies

Compositions	Samples			
	Control	PY-1	PY-2	PY-3
Moisture (%)	3.31 ± 0.08^a	1.88 ± 0.03^c	2.21 ± 0.06^b	2.28 ± 0.10^b
Protein (%)	7.18 ± 0.03^b	6.47 ± 0.06^d	7.00 ± 0.08^c	8.08 ± 0.04^a
Crude fat (%)	19.13 ± 0.05^d	21.67 ± 0.08^c	25.96 ± 0.03^a	25.67 ± 0.03^b
Crude fiber (%)	2.65 ± 0.01^d	3.78 ± 0.04^c	4.94 ± 0.02^a	4.53 ± 0.05^b
Ash (%)	0.71 ± 0.01^d	1.87 ± 0.01^c	1.55 ± 0.01^a	1.37 ± 0.02^b
Carbohydrate (%)	67.01 ± 0.05^a	65.01 ± 0.08^b	58.33 ± 0.12^c	58.07 ± 0.14^c
TPC (µg GAE/g)	1.18 ± 0.02^a	0.13 ± 0.03^d	0.22 ± 0.02^c	0.35 ± 0.03^b
DPPH (% Inhibition)	89.73 ± 0.09^b	47.21 ± 0.13^d	61.22 ± 0.10^c	94.25 ± 0.07^a

Data values are presented as mean ± standard deviation. Data with different alphabetic superscript in the same row are statistically significant (p<0.05). Control: wheat flour cookies; PY-1: *D. esculenta* flour and almond protein isolate blend cookies; PY-2: *D. alata* (purple yam) flour and almond protein isolate blend cookies; PY-3: *D. alata* (yellow yam) flour and almond protein isolate blend cookies.

The TPC of the cookies from yam flour and API blends significantly decreased compared to the control. This suggests the susceptibility of the phenolics present in the cookies from yam flour and API blends to high temperatures during baking. This decrease in the TPC values may be due to the decarboxylation of phenolic acids and

depolymerization of polyphenols during baking at high temperatures [32]. However, an increase in DPPH scavemging activity (% inhibition) was observed after baking all the cookie dough which could be attributed to the formation of melanoidins (brown pigment) during baking that can increase the antioxidant activity of cookies [25, 47].

4A.3.3 Physical characteristics of cookies

The physical characteristics of the cookies made from the blend of yam flour and almond protein isolate are presented in **Table 4A.5**.

Cookies from purple yam flour-almond protein isolate had the lowest weight (5.79 ± 0.40 g). No significant difference ($p<0.05$) in the diameter, thickness, and spread ratio was observed in PY-1, PY-2, and PY-3 cookies in comparison to control cookies. The spread ratio which represents a ratio of diameter to thickness was found to be non-significant for cookies from corn flour incorporated with pea proteins, which may be the result of the non-significant difference in thickness and diameter, or both [45]. Similar studies were performed for rice, buckwheat, oat, spelt and kamut flours incorporated with lupin seed protein extract and no effect in the cookie diameter and area were reported [36]. Moreover, the variations observed in the thickness, diameter and spread ratio not only depends on the addition level of protein isolates but also on the processes and formulations used [38]. Overall, the incorporation of almond protein isolate in yam flour can lead to comparable physical or geometric characteristics to that of cookies made of wheat flour. **Mota et al. [36]** reported that the presence of gluten in flour does not influence the cookie area and no direct relationship with the expansion of structure could be established. Cookie diameter and spread ratio are considered desirable quality characteristics of cookies.

4A.3.4 Texture analysis of cookies

Cookie hardness measured by the Texture Analyzer is shown in **Table 4A.5**. Hardness of cookies represents the peak force required to snap the cookies, and is one of the most important textural properties for cookies [33]. The maximum cutting force (3.64 kg) to break the cookies was noticed for the wheat flour cookies and the lowest cutting force (2.24 kg) for PY-3 cookies, which is in concordance with the measured rheological properties of cookie dough. The difference in the cookie hardness of wheat flour cookies and yam flour-almond protein isolate cookies can be attributed to the gluten fractions, which provide a strong binding structure to dough [30]. The cookies with almond protein isolate with no gluten fractions showed a lower value of hardness compared to gluten-

containing wheat flour cookies and resulted in cookies with a soft texture. A similar lower value of hardness of cookies from blends of rice flour-potato protein isolate was reported as compared to wheat flour cookies [54]. A higher value of hardness was observed with the addition of potato protein concentrate which may be due to the association of polysaccharides with concentrate. Moreover, the hardness of cookies is related to the particle size of the flours used [3, 13, 43]. In addition, the difference in the texture of the cookies may be linked to the difference in the protein-protein interaction or protein-carbohydrate interactions [55].

Table 4A.5: Physical characteristics and hardness of cookies

Sample	Weight (g)	Diameter (cm)	Thickness (cm)	Spread ratio	Cookie hardness (kg)
Control	6.30 ± 0.40^{ab}	4.43 ± 0.06^{ab}	0.70 ± 0.05^{a}	6.32 ± 0.40^{a}	3.64 ± 0.37^{a}
PY-1	6.39 ± 0.54^{a}	4.41 ± 0.06^{b}	0.74 ± 0.03^{a}	5.95 ± 0.22^{a}	3.01 ± 0.28^{ab}
PY-2	5.85 ± 0.21^{bc}	4.44 ± 0.11^{ab}	0.74 ± 0.06^{a}	6.06 ± 0.53^{a}	2.65 ± 0.17^{bc}
PY-3	5.79 ± 0.40^{c}	4.63 ± 0.30^{a}	0.75 ± 0.04^{a}	6.18 ± 0.62^{a}	2.24 ± 0.16^{c}

Data values are presented as mean ± standard deviation. Data with different alphabetic superscript in the same column are statistically significant (p<0.05). Control: wheat flour cookies; PY-1: *D. esculenta* flour and almond protein isolate blend cookies; PY-2: *D. alata* (purple yam) flour and almond protein isolate blend cookies; PY-3: *D. alata* (yellow yam) flour and almond protein isolate blend cookies.

4A.3.5 Color analysis of cookies

Color is an aesthetically important parameter in the quality of cookies. Color values of the cookies (**Fig. 4A.3**) made from the blends of yam flour and almond protein isolate are shown in **Table 4A.6**. *L** and *b** values of the yam flour-almond protein isolate cookies significantly (p<0.05) decreased in comparison to control cookies, indicating that the color of PY-1, PY-2, and PY-3 cookies became increasingly bluish-black. The *a** value of PY-1 and PY-2 cookies significantly increased in comparison to the control indicating an increase in the redness of the cookies. A higher degree of browning in the cookies prepared from blends of yam flour and almond protein isolate may be due to a high degree of non-enzymatic browning that takes place between amino acids and sugars [55]. Moreover, yam flour and almond protein isolate contain the amino acid lysine which promotes non-enzymatic browning by reacting with carbonyl groups of

reducing sugar and might result in darker color cookies **[6, 28]**. Cookies from PY-1 were lighter in color compared to PY-2 and PY-3, which may be due to the lower amount of lysine in *D. esculenta* than *D. alata* **[28]**.

Table 4A.6: Color attributes of cookies

Sample	L^*	a^*	b^*	c	h
Control	51.49 ± 1.60^a	12.78 ± 0.89^b	26.35 ± 0.57^a	29.29 ± 0.33^a	64.12 ± 1.96^a
PY-1	43.50 ± 1.73^b	14.97 ± 0.83^a	19.87 ± 1.54^b	24.91 ± 0.98^b	52.89 ± 3.39^b
PY-2	41.57 ± 2.82^b	15.03 ± 0.71^a	19.49 ± 2.24^b	24.65 ± 1.70^b	52.14 ± 3.78^b
PY-3	33.41 ± 0.59^c	12.06 ± 0.22^b	14.32 ± 1.08^c	18.73 ± 0.88^c	49.80 ± 2.11^b

Data values are presented as mean ± standard deviation. Data with different alphabetic superscript in the same column are statistically significant (p<0.05). Control: wheat flour cookies; PY-1: *D. esculenta* flour and almond protein isolate blend cookies; PY-2: *D. alata* (purple yam) flour and almond protein isolate blend cookies; PY-3: *D. alata* (yellow yam) flour and almond protein isolate blend cookies.

The chroma and hue angle were found to be lower in the yam flour-almond protein isolate cookies when compared with the control. A similar decrement in L^* value (brightness) was observed in fermented and unfermented yam flour when compared with wheat flour **[9]**. Additionally, drying conditions, milling parameters, chemical composition, and polyphenol content tends to affect the color of flour **[1, 9]**.

4A.4   Sensory evaluation of cookies

Cookies prepared from WF, PY-1, PY-2, and PY-3 were evaluated for their color, flavor, texture, aroma and overall acceptability using the sensory analysis method based on a 9-point hedonic scale (**Fig. 4A.4**). Sensory panelist rated the highest score for the cookies prepared from PY-1 in terms of color, flavor, aroma, and overall acceptability. The lowest score rated was for the cookies prepared from PY-3 in terms of flavor, texture, aroma, and overall acceptability. The sensory scores assigned to the cookies for texture by the judges were in good agreement with the texture analysis data of the cookies, and were in the following order: Control > PY-1 > PY-2 > PY-3. The lower preference for cookies prepared from a blend of *D. alata* flours and almond protein isolate (PY-2 and PY-3) was due to the texture, aroma, and slightly bitter taste. A similar observation was made for yam flour cookies in terms of taste **[11]**. The bitter taste of *D.*

alata flour may be due to the presence of higher content of saponin, alkaloid, and phenol compared to other flours used in this study **[2]**.
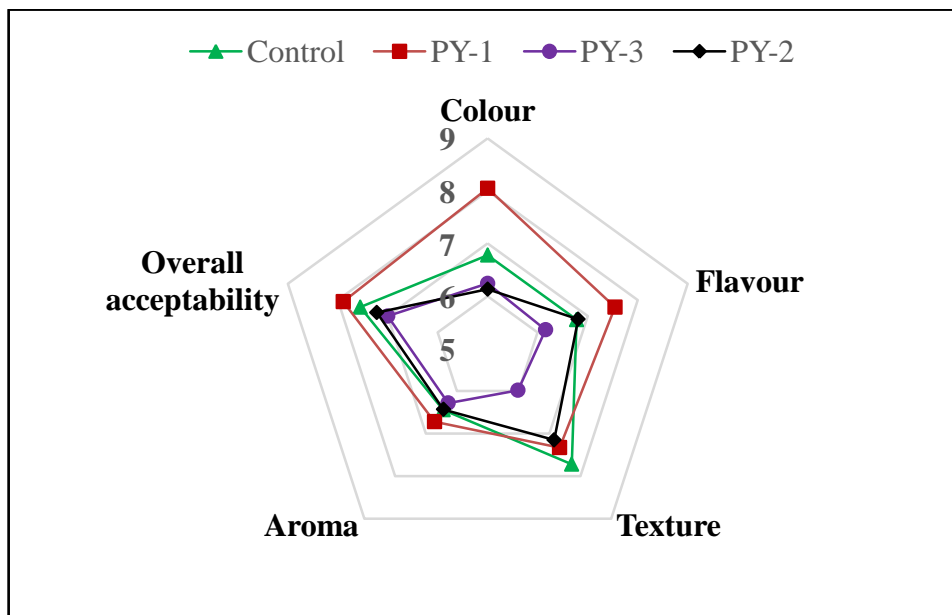

Fig. 4A.4: Radar plot representing the sensory attributes of cookies. Control: wheat flour cookies; PY-1: *D. esculenta* flour and almond protein isolate blend cookies; PY-2: *D. alata* (purple yam) flour and almond protein isolate blend cookies; PY-3: *D. alata* (yellow yam) flour and almond protein isolate blend cookies.

4A.5 Bibliography

[1]   Abiodun, O. and Akinoso, R., Textural and sensory properties of trifoliate yam (*Dioscorea dumetorum*) flour and stiff dough 'amala'. *Journal of Food Science and Technology,* 52(5):2894-2901, 2015.

[2]   Adebowale, A.R.A., Wahab, A.B., Sobukola, P.O., Obadina, A.O., Kajihausa, E.O., Adegunwa, O.M., Sanni, O.L., and Tomlins, K., The antinutritional and vitamin composition of high-quality yam flour as affected by yam species, pretreatment, and drying method. *Food Science & Nutrition,* 6(8):1985-1990, 2018.

[3]   Ai, Y., Jin, Y., Kelly, J.D., and Ng, P.K., Composition, functional properties, starch digestibility, and cookie-baking performance of dry bean powders from 25 Michigan-grown varieties. *Cereal Chemistry,* 94(3):400-408, 2017.

[4]   Ambigaipalan, P., Hoover, R., Donner, E., Liu, Q., Jaiswal, S., Chibbar, R., Nantanga, K., and Seetharaman, K., Structure of faba bean, black bean and pinto bean starches at different levels of granule organization and their

physicochemical properties. *Food Research International,* 44(9):2962-2974, 2011.

[5]   Amir, R.M., Anjum, F.M., Khan, M.I., Khan, M.R., Pasha, I., and Nadeem, M., Application of Fourier transform infrared (FTIR) spectroscopy for the identification of wheat varieties. *Journal of Food Science and Technology,* 50(5):1018-1023, 2013.

[6]   Amirshaghaghi, Z., Rezaei, K., and Habibi Rezaei, M., Characterization and functional properties of protein isolates from wild almond. *Journal of Food Measurement and Characterization,* 11(4):1725-1733, 2017.

[7]   Amjid, M.R., Shehzad, A., Hussain, S., Shabbir, M.A., Khan, M.R., and Shoaib, M., A comprehensive review on wheat flour dough rheology. *Pakistan Journal of Food Sciences,* 23(2):105-123, 2013.

[8]   Ao, Z. and Jane, J.-l., Characterization and modeling of the A-and B-granule starches of wheat, triticale, and barley. *Carbohydrate Polymers,* 67(1):46-55, 2007.

[9]   Asiyanbi-Hammed, T.T. and Simsek, S., Comparison of physical and chemical properties of wheat flour, fermented yam flour, and unfermented yam flour. *Journal of Food Processing and Preservation,* 42(12):e13844, 2018.

[10]   Awuchi, C.-G., Igwe, V.S., and Echeta, C.K., The functional properties of foods and flours. *International Journal of Advanced Academic Research,* 5(11):139-160, 2019.

[11]   Bansod, P.N., Ningot, E.P., Panchbhai, D., and Gawande, S., Storage studies of aerial yam (*Dioscorea bulbifera* L.) flour cookies. *Journal of Pharmacognosy and Phytochemistry,* 9(3):1428-1433, 2020.

[12]   Bashir, S., Yaseen, M., Sharma, V., Purohit, S.R., Barak, S., and Mudgil, D., Rheological and textural properties of gluten free cookies based on pearl millet and flaxseed. *Biointerface Research in Applied Chemistry,* 10:6565-6576, 2020.

[13]   Belorio, M., Sahagún, M., and Gómez, M., Influence of flour particle size distribution on the quality of maize gluten-free cookies. *Foods,* 8(2):83, 2019.

[14]   Bolling, B.W., Almond polyphenols: Methods of analysis, contribution to food quality, and health promotion. *Comprehensive Reviews in Food Science and Food Safety,* 16(3):346-368, 2017.

[15]   Cai, C., Lin, L., Man, J., Zhao, L., Wang, Z., and Wei, C., Different structural properties of high-amylose maize starch fractions varying in granule size. *Journal of Agricultural and Food Chemistry,* 62(48):11711-11721, 2014.

[16]   Chinma, C.E., Ariahu, C.C., and Abu, J.O., Chemical composition, functional and pasting properties of cassava starch and soy protein concentrate blends. *Journal of Food Science and Technology,* 50(6):1179-1185, 2013.

[17]   Chinma, C.E., Ilowefah, M., Shammugasamy, B., Mohammed, M., and Muhammad, K., Effect of addition of protein concentrates from natural and yeast fermented rice bran on the rheological and technological properties of wheat bread. *International Journal of Food Science & Technology,* 50(2):290-297, 2015.

[18]   Cui, L., Bandillo, N., Wang, Y., Ohm, J.-B., Chen, B., and Rao, J., Functionality and structure of yellow pea protein isolate as affected by cultivars and extraction pH. *Food Hydrocolloids,* 108:106008, 2020.

[19]   de Almeida, N.M., FG Dias, F., Rodrigues, M.I., and LN de Moura Bell, J.M., Effects of processing conditions on the simultaneous extraction and distribution of oil and protein from almond flour. *Processes,* 7(11):844, 2019.

[20]   de Souza, T.S., Dias, F.F., Oliveira, J.P.S., de Moura Bell, J.M., and Koblitz, M.G.B., Biological properties of almond proteins produced by aqueous and enzyme-assisted aqueous extraction processes from almond cake. *Scientific Reports,* 10(1):1-12, 2020.

[21]   Harijono, T.E., Saputri, D.S., and Kusnadi, J., Effect of blanching on properties of water yam (*Dioscorea alata*) flour. *Advance Journal of Food Science and Technology,* 5(10):1342-1350, 2013.

[22]   Harrington, J., Foegeding, E., Mulvihill, D., and Morris, E., Segregative interactions and competitive binding of Ca2+ in gelling mixtures of whey protein isolate with Na+ κ-carrageenan. *Food Hydrocolloids,* 23(2):468-489, 2009.

[23]   Hu, Y., He, C., Zhang, M., Zhang, L., Xiong, H., and Zhao, Q., Inhibition from whey protein hydrolysate on the retrogradation of gelatinized rice starch. *Food Hydrocolloids,* 108:105840, 2020.

[24]   Indrani, D., Prabhasankar, P., Rajiv, J., and Rao, G.V., Influence of whey protein concentrate on the rheological characteristics of dough, microstructure and

quality of unleavened flat bread (parotta). *Food Research International,* 40(10):1254-1260, 2007.

[25]   Jan, U., Gani, A., Ahmad, M., Shah, U., Baba, W.N., Masoodi, F., Maqsood, S., Gani, A., Wani, I.A., and Wani, S., Characterization of cookies made from wheat flour blended with buckwheat flour and effect on antioxidant properties. *Journal of Food Science and Technology,* 52(10):6334-6344, 2015.

[26]   Kiin-Kabari, D., Eke-Ejiofor, J., and Giami, S., Functional and pasting properties of wheat/plantain flours enriched with bambara groundnut protein concentrate. *International Journal of Food Science and Nutrition Engineering,* 5(2):75-81, 2015.

[27]   Kouakou, B., N'Da-Kouassi, A.M., Halbin, K.J., Tagro, G., N'Guessan, K.F., and Dago, G., Biochemical characterization and functional properties of weaning food made from cereals (millet, maize) and legumes (beans, soybeans). *Journal of Food Chemistry and Nutrition,* 1(1):22-32, 2013.

[28]   Kouassi, B., Diopoh, J., Leroy, Y., and Fournet, B., Total amino acids and fatty acids composition of yam (*Dioscorea*) tubers and their evolution during storage. *Journal of the Science of Food and Agriculture,* 42(3):273-285, 1988.

[29]   Kumar, L., Brennan, M., Brennan, C., and Zheng, H., Influence of whey protein isolate on pasting, thermal, and structural characteristics of oat starch. *Journal of Dairy Science,* 105(1):56-71, 2022.

[30]   Li, P.-H., Huang, C.-C., Yang, M.-Y., and Wang, C.-C., Textural and sensory properties of salted noodles containing purple yam flour. *Food Research International,* 47(2):223-228, 2012.

[31]   Luo, Y., Xiao, Y., Shen, M., Wen, H., Ren, Y., Yang, J., Han, X., and Xie, J., Effect of *Mesona chinensis* polysaccharide on the retrogradation properties of maize and waxy maize starches during storage. *Food Hydrocolloids,* 101:105538, 2020.

[32]   Mahloko, L.M., Silungwe, H., Mashau, M.E., and Kgatla, T.E., Bioactive compounds, antioxidant activity and physical characteristics of wheat-prickly pear and banana biscuits. *Heliyon,* 5(10):e02479, 2019.

[33]   Mancebo, C.M., Picón, J., and Gómez, M., Effect of flour properties on the quality characteristics of gluten free sugar-snap cookies. *LWT-Food Science and Technology,* 64(1):264-269, 2015.

[34]   Marta, H., Cahyana, Y., Bintang, S., Soeherman, G.P., and Djali, M., Physicochemical and pasting properties of corn starch as affected by hydrothermal modification by various methods. *International Journal of Food Properties,* 25(1):792-812, 2022.

[35]   Marti, A., Bock, J.E., Pagani, M.A., Ismail, B., and Seetharaman, K., Structural characterization of proteins in wheat flour doughs enriched with intermediate wheatgrass (*Thinopyrum intermedium*) flour. *Food Chemistry,* 194:994-1002, 2016.

[36]   Mota, J., Lima, A., B. Ferreira, R., and Raymundo, A., Lupin seed protein extract can efficiently enrich the physical properties of cookies prepared with alternative flours. *Foods,* 9(8):1064, 2020.

[37]   Nogueira, A.d.C., OLIVEIRA, R.A.d., and Steel, C.J., Protein enrichment of wheat flour doughs: empirical rheology using protein hydrolysates. *Food Science and Technology,* 40:97-105, 2020.

[38]   Nogueira, A.d.C. and Steel, C.J., Protein enrichment of biscuits: A review. *Food Reviews International,* 34(8):796-809, 2018.

[39]   Obadina, A.O., Babatunde, B.O., and Olotu, I., Changes in nutritional composition, functional, and sensory properties of yam flour as a result of presoaking. *Food Science & Nutrition,* 2(6):676-681, 2014.

[40]   Ocheme, O.B., Adedeji, O.E., Chinma, C.E., Yakubu, C.M., and Ajibo, U.H., Proximate composition, functional, and pasting properties of wheat and groundnut protein concentrate flour blends. *Food Science & Nutrition,* 6(5):1173-1178, 2018.

[41]   Ogunbusola, E.M., Alabi, O.O., Sanni, T.A., Seidu, K.T., Oke, H.O., and Akinwale, O.R., Assessment of gluten-free cookies made from rice and soy protein isolate blends. *Journal of Microbiology, Biotechnology and Food Sciences,* 2021:907-912, 2021.

[42]   Pareyt, B. and Delcour, J.A., The role of wheat flour constituents, sugar, and fat in low moisture cereal based products: a review on sugar-snap cookies. *Critical Reviews in Food Science and Nutrition,* 48(9):824-839, 2008.

[43]   Rao, B.D., Anis, M., Kalpana, K., Sunooj, K., Patil, J., and Ganesh, T., Influence of milling methods and particle size on hydration properties of sorghum flour and quality of sorghum biscuits. *LWT-Food Science and Technology,* 67:8-13, 2016.

[44]   Ronda, F., Pérez-Quirce, S., and Villanueva, M., *Rheological properties of gluten-free bread doughs: relationship with bread quality*, in *Advances in food rheology and its applications.* Elsevier, 297-334, 2017.

[45]   Sahagún, M. and Gómez, M., Influence of protein source on characteristics and quality of gluten-free cookies. *Journal of Food Science and Technology,* 55(10):4131-4138, 2018.

[46]   Senanayake, S., Ranaweera, K., Bamunuarachchi, A., and Gunaratne, A., Proximate analysis and phytochemical and mineral constituents in four cultivars of yams and tuber crops in Sri Lanka. *Tropical Agricultural Research and Extension,* 15(1):32-36, 2012.

[47]   Sharma, P. and Gujral, H.S., Cookie making behavior of wheat–barley flour blends and effects on antioxidant properties. *LWT-Food Science and Technology,* 55(1):301-307, 2014.

[48]   Smeriglio, A., Barreca, D., Bellocco, E., and Trombetta, D., Proanthocyanidins and hydrolysable tannins: occurrence, dietary intake and pharmacological effects. *British Journal of Pharmacology,* 174(11):1244-1262, 2017.

[49]   Sun, Q. and Xiong, C.S.L., Functional and pasting properties of pea starch and peanut protein isolate blends. *Carbohydrate Polymers,* 101:1134-1139, 2014.

[50]   Tang, X. and Liu, J., A comparative study of partial replacement of wheat flour with whey and soy protein on rheological properties of dough and cookie quality. *Journal of Food Quality,* 2017, 2017.

[51]   Thory, R. and Sandhu, K.S., A Comparison of mango kernel starch with a novel starch from litchi (*Litchi chinensis*) kernel: Physicochemical, morphological, pasting, and rheological properties. *International Journal of Food Properties,* 20(4):911-921, 2017.

[52]   Torbica, A., Hadnađev, M., and Dapčević, T., Rheological, textural and sensory properties of gluten-free bread formulations based on rice and buckwheat flour. *Food Hydrocolloids,* 24(6-7):626-632, 2010.

[53]   Ukpabi, U.J., Farmstead bread making potential of lesser yam ('*Dioscorea esculenta*') flour in Nigeria. *Australian Journal of Crop Science,* 4(2):68-73, 2010.

[54]   Waglay, A. and Karboune, S., Predictive consumer acceptance models and quality attributes for cookies enriched with potato protein isolate and concentrate. *Food and Bioprocess Technology,* 13(9):1645-1660, 2020.

[55]   Wani, A.A., Sogi, D., Singh, P., and Khatkar, B., Influence of watermelon seed protein concentrates on dough handling, textural and sensory properties of cookies. *Journal of Food Science and Technology,* 52(4):2139-2147, 2015.

[56]   Yang, C., Zhong, F., Goff, H.D., and Li, Y., Study on starch-protein interactions and their effects on physicochemical and digestible properties of the blends. *Food Chemistry,* 280:51-58, 2019.

[57]   Yu, B., Li, J., Tao, H., Zhao, H., Liu, P., and Cui, B., Physicochemical properties and in vitro digestibility of hydrothermal treated Chinese yam (*Dioscorea opposita* Thunb.) starch and flour. *International Journal of Biological Macromolecules,* 176:177-185, 2021.

[58]   Yusuf, A., Physico-chemical properties of almond seed protein concentrate. *Italian Journal of Food Science,* 15(4):531-540, 2003.

[59]   Zeng, H., Chen, P., Chen, C., Huang, C., Lin, S., Zheng, B., and Zhang, Y., Structural properties and prebiotic activities of fractionated lotus seed resistant starches. *Food Chemistry,* 251:33-40, 2018.

[60]   Zhang, Y., Chen, C., Chen, Y., and Chen, Y., Effect of rice protein on the water mobility, water migration and microstructure of rice starch during retrogradation. *Food Hydrocolloids,* 91:136-142, 2019.

[61]   Zheng, Y., Guo, Z., Zheng, B., Zeng, S., and Zeng, H., Insight into the formation mechanism of lotus seed starch-lecithin complexes by dynamic high-pressure homogenization. *Food Chemistry,* 315:126245, 2020.

Chapter 4B

Native and physically modified starches of underutilized yam species, and their functional, thermal, pasting, morphological and rheological properties

4B.1   Introduction

This chapter deals with the isolation of starch from *Dioscorea esculenta* (Y1), *Dioscorea alata* (purple yam, Y2), and *Dioscorea alata* (yellow yam, Y3), and the isolated starches were named as 1YNS, 2YNS, and 3YNS, respectively. Meanwhile, there is no report on the comparative study of HMT and ANN treatments on yam starch, and the effect of moisture levels during these treatments on yam starch. Therefore, the starches from the three yam species were subjected to heat moisture treatment (HMT) with 20 and 30 % moisture at 110 ºC for 3 h, and annealing (ANN) with 1:2 and 1:4 starch to water ratio at 50 ºC for 24 h. The HMT treated starches were named 1HMT-20, 1HMT-30, 2HMT-20, 2HMT-30, 3HMT-20, and 3HMT-30, where the prefix '1', '2', and '3' indicate the yam species *D. esculenta*, *D. alata* (purple yam), and *D. alata* (yellow yam) respectively, and the suffix -20 and -30 indicate moisture levels. The annealed starches were named 1ANN-12, 1ANN-14, 2ANN-12, and 2ANN-14, 3ANN-12, and 3ANN-14, where the prefix '1', '2', and '3' indicate the yam species *D. esculenta*, *D. alata* (purple yam), and *D. alata* (yellow yam) respectively, and the suffix -12 and -14 indicate starch to water ratio of 1:2 and 1:4, respectively. The effect of both the hydrothermal modifications on functional, thermal, pasting, morphological, and rheological properties and *in vitro* digestibility was investigated. A comparative study between HMT and ANN treatments with different moisture levels, and the yam species on the properties of starches was attempted.

4B.2   Proximate composition (on dry basis) of native starches

The proximate composition of the starches 1YNS, 2YNS, and 3YNS from *Dioscorea esculenta* (Y1), *Dioscorea alata* (purple yam, Y2), and *Dioscorea alata* (yellow yam, Y3), respectively, are shown in **Table 4B.1**.

126

Table 4B.1: Proximate composition (on dry weight basis) of native starches isolated from the three yam species

Proximate compositions	Native starches		
	1YNS	2YNS	3YNS
Moisture (%)	11.04 ± 0.11^a	10.79 ± 0.13^a	10.86 ± 0.10^a
Protein (%)	0.85 ± 0.01^b	1.53 ± 0.03^a	0.92 ± 0.07^b
Lipid (%)	0.32 ± 0.04^b	0.41 ± 0.05^b	0.57 ± 0.05^a
Ash (%)	0.16 ± 0.01^b	0.15 ± 0.01^b	0.20 ± 0.02^a
Yield (%)	21.52 ± 1.14^a	16.48 ± 0.86^b	17.52 ± 0.88^b

Data values are presented as mean ± standard deviation. Data with different alphabetic superscript in the same column are statistically significant (p<0.05).

The small percentage of protein content (0.85 – 1.53 %) in all the native starches prove that the isolated starches from the yam species are of high quality and purity [34]. The moisture content of the starches is less than the recommended moisture content (< 13 %) for safe storage [17]. The ash content (0.16 – 0.20 %) was found to be lower than the recommended ash content (< 0.5 %) in the industry [32]. Amongst all the three varieties, *Dioscorea esculenta* (Y1) showed the maximum yield (21.52 ± 1.14 %), which may be due to the presence of lower amount of lipid and protein.

4B.3 Total amylose content, amylose leaching, water and oil absorption capacity

The data on amylose content, amylose leaching (AML), water absorption capacity (WAC), and oil absorption capacity (OAC) of native and modified starches of yam species are presented in **Table 4B.2**.

Amylose content of native and modified starches of *D. esculenta* (Y1), *D. alata* (purple yam, Y2), and *D. alata* (yellow yam, Y3) ranged from 21.34 to 29.53 %, 26.58 to 33.93 %, and 32.71 to 38.17 %, respectively. The above values of amylose content were within the range (9.9-47 %) of amylose content reported for *Dioscorea* starches [50]. Amylose content of 2YNS and 3YNS was found to be higher than 1YNS, and the species *D. alata* tend to have higher amounts of amylose compared to *D. esculenta* [2]. Various factors such as method of quantification, endogenous lipid content, environmental and agronomic practices may affect the content of amylose in yam starches [50]. A significant (p<0.5) increase in amylose content was induced by HMT and ANN and with

moisture levels of treatment. A similar increase in amylose content after HMT has been reported for buckwheat starches [13], and this increase in amylose content can be attributed to the interactions between amylose (AM) and amylopectin (AP) in the amorphous regions and degradation of AP during HMT or ANN [26, 27]. However, the amylose content was found to be higher after ANN compared to HMT. In hydrothermal treatments, heat and moisture disrupt the crystalline matrix of starch granules leading to AP degradation and causing an increase in the interactions within the amorphous matrix [6].

Table 4B.2: Total amylose content, amylose leaching (AML), water absorption capacity (WAC) and oil absorption capacity (OAC) of native and modified starches of Y1, Y2 and Y3.

Sample	Amylose content (%)	AML (%)	WAC (g/g)	OAC (g/g)
1YNS	21.34 ± 0.56^l	15.46 ± 0.22^d	2.10 ± 0.04^f	1.68 ± 0.02^{bc}
1HMT-20	24.55 ± 0.33^k	5.62 ± 0.08^j	2.64 ± 0.01^b	1.59 ± 0.03^{cde}
1HMT-30	25.61 ± 0.21^j	2.75 ± 0.17^l	2.77 ± 0.02^a	1.16 ± 0.03^i
1ANN-12	26.97 ± 0.13^i	12.14 ± 0.35^f	2.31 ± 0.00^d	1.31 ± 0.02^{gh}
1ANN-14	29.53 ± 0.39^g	9.86 ± 0.17^h	2.48 ± 0.02^c	1.25 ± 0.01^{ghi}
2YNS	26.58 ± 0.17^i	17.23 ± 0.36^b	2.16 ± 0.01^{ef}	1.94 ± 0.04^a
2HMT-20	28.12 ± 0.15^h	6.81 ± 0.19^i	2.66 ± 0.03^b	1.65 ± 0.04^{bcd}
2HMT-30	29.25 ± 0.32^g	3.63 ± 0.18^k	2.76 ± 0.03^a	1.22 ± 0.05^{hi}
2ANN-12	31.45 ± 0.19^f	12.66 ± 0.11^f	2.38 ± 0.02^d	1.56 ± 0.04^{de}
2ANN-14	33.93 ± 0.14^d	10.95 ± 0.25^g	2.52 ± 0.07^c	1.46 ± 0.02^f
3YNS	32.71 ± 0.40^e	21.54 ± 0.19^a	2.20 ± 0.01^e	1.86 ± 0.03^a
3HMT-20	34.63 ± 0.18^{cd}	9.62 ± 0.10^h	2.51 ± 0.03^c	1.74 ± 0.01^b
3HMT-30	35.12 ± 0.29^c	7.15 ± 0.17^i	2.73 ± 0.06^{ab}	1.32 ± 0.02^g
3ANN-12	37.28 ± 0.13^b	16.33 ± 0.13^c	2.34 ± 0.01^d	1.69 ± 0.01^b
3ANN-14	38.17 ± 0.38^a	14.77 ± 0.11^e	2.35 ± 0.04^d	1.52 ± 0.04^{ef}

Data values are presented as mean ± standard deviation. Data with different alphabetic superscript in the same column are statistically significant (p<0.05).

A significant (p<0.5) reduction in the AML and OAC with an increase in the WAC was observed after HMT and ANN and with increase in moisture levels of

treatment. Similar trends of WAC and OAC have been reported for HMT-modified buckwheat starch [36], amaranth starch [35], and sohphlang starch [29]; and ANN-modified maize starch [27] and white yam starch [11]. The decrease in AML after HMT treatment may be due to additional interactions between the amylose-amylopectin and the amylose-amylose chain during HMT [9]. The observed difference in AML of Y1, Y2 and Y3 starches was due to the total amylose content of the starches.

4B.4   Scanning electron microscopy

Fig. 4B.1 illustrates the SEM images of the native, heat moisture treated, and annealed yam starches. *D. esculenta* (Y1) starches micrographs showed the presence of irregular polygonal or polyhedral shaped granules with smooth surfaces, and the length of the granules ranged in size from 1.6 to 6.2 μm. *D. alata* (purple yam, Y2) and *D. alata* (yellow yam, Y3) starches micrographs showed the presence of oval, elongated or lenticular shaped starch granules with smooth surface. The length of the granules ranged in size from 10.6 to 48.7 μm and 6.5 to 57.9 μm for Y2 and Y3 starches, respectively.

1HMT-20 and 1HMT-30 starch granules showed the presence of cavities and fissures (**Fig. 4B.2**) on starch granules and granular aggregation, which may be linked to the partial gelatinization of starch induced by HMT. Similar studies have been reported for heat moisture-treated elephant foot yam starch [39] and pearl millet starch [31]. No cavities and fissures were found on the starch granules of 2HMT-20, 2HMT-30, 3HMT-20 and 3HMT-30 except for granular aggregation. A more aggregated structure of starch granules was observed for HMT granules compared to native and ANN granules. This changes in granular morphology might be due to the exposure of starch granules to high moisture content during hydrothermal treatment, which promotes the partial gelatinization and morphological changes of starch [10]. Similar observation on more aggregated HMT starch granules than ANN starch granules was reported on buckwheat starch by **Liu et al. [26]**. HMT and ANN starch granules had higher number of smaller granules in comparison to the native starches. These changes might be due to the compaction of granular matter induced by heating and pressure during HMT [26, 45]. Lower size of the ANN starch granules than native samples might be due to the strengthening of the granular structure and perfection of crystalline structure due to the thermal treatment [28]. Moreover, the morphology of starch depends on the treatment conditions of HMT and ANN, and starch source [27].
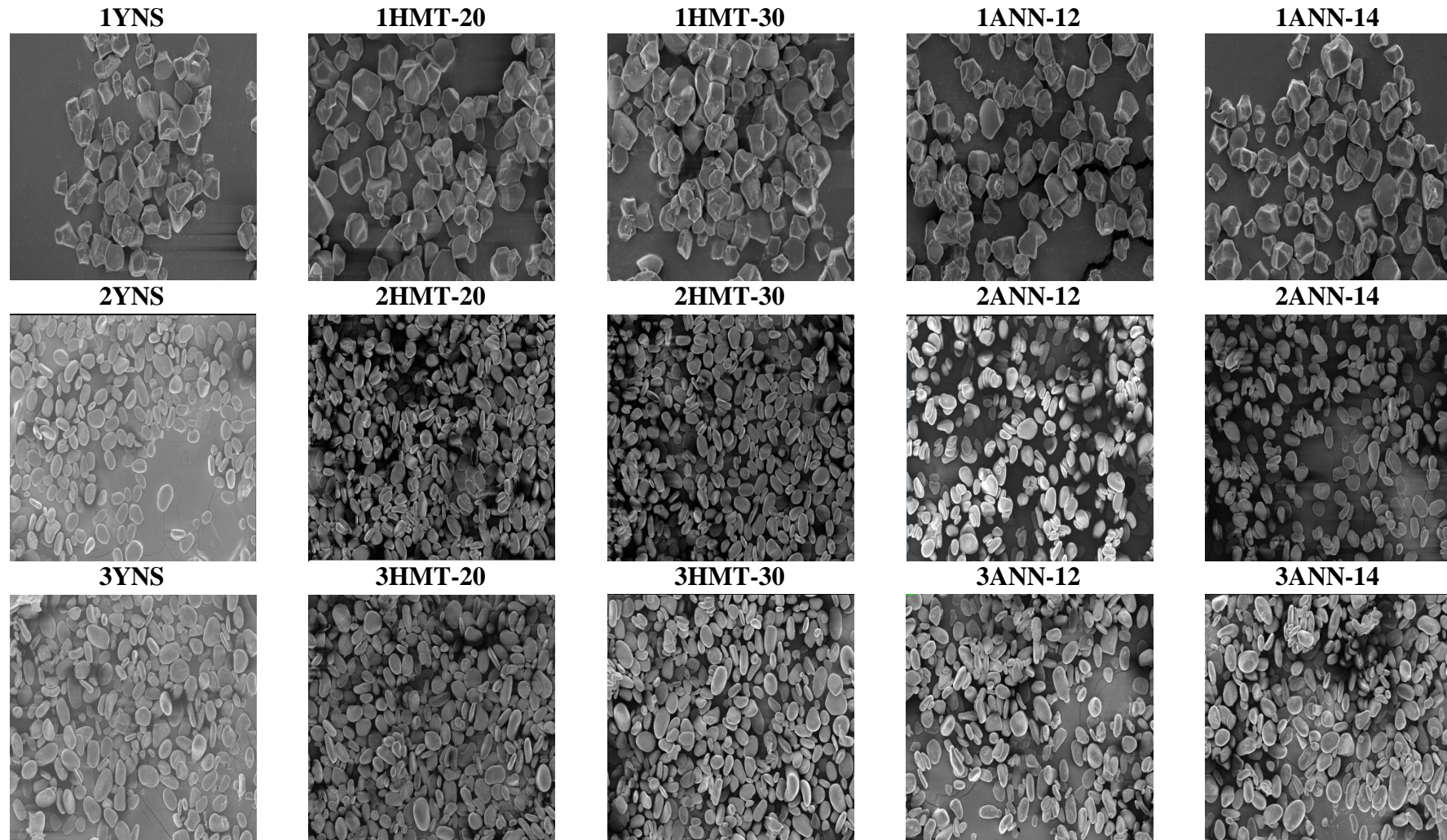
Fig. 4B.1: Scanning electron microscopy (SEM) of native and modified yam starches at 5000x for yam species 1, and 500x for yam species 2 and 3. YNS, HMT, and ANN indicate native, heat-moisture treated, and annealed yam starch, respectively. Prefix 1, 2 & 3 indicate the three yam species. Suffix –20, –30, –12 and –14 indicate 20% moisture level, 30% moisture level, 1:2 starch to moisture ratio and 1:4 starch to moisture ratio, respectively.
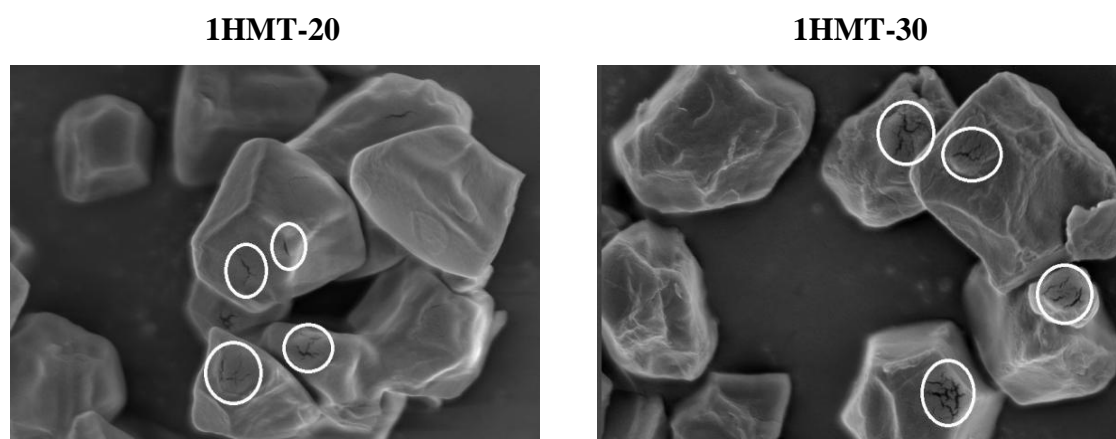
1HMT-20   **1HMT-30**

Fig. 4B.2: Scanning electron microscopy (SEM) of 2HMT-20 and 2HMT-30 starch granules at 15000x magnification. Highlighted circles indicate fissures and cavities.

4B.5   ATR-FTIR spectroscopy

Fig. 4B.3 illustrates the ATR-FTIR spectra of the native, heat moisture treated, and annealed yam starches. HMT and annealing did not alter the ATR-FTIR spectra of the starch granules and exhibited similar vibration peaks at 2924 cm^{-1} (C-H stretching vibration), 1641 cm^{-1} (H-O-H bending vibration), 1150 cm^{-1} and 1077 cm^{-1} (C-O, C-C, and C-O-H stretching), 930 cm^{-1} (skeletal mode vibration of α-(1–4) glycosidic linkage), and 860 cm^{-1} (C–H and CH2 deformations) **[21, 39, 44]**. However, some variations in the peak intensities were observed in the ATR-FTIR spectra of the HMT and ANN starch granules. Higher intensities of the peak at 3293 cm^{-1} representing O-H stretching vibrations were observed in the annealed starches, and it indicates a stronger interaction of hydrogen bonds and more crystalline perfection **[38]**. HMT starches showed a decrease in the intensities of the peak at 3293 cm^{-1} indicating a weaker interaction of hydrogen bonds. HMT modification led to a decrease in the intensities of the peak at 1641 cm^{-1} which indicates lower moisture content in the amorphous region of HMT-modified starch granules, while no change in the intensities of the peak at 1641 cm^{-1} was observed for annealed starches **[38]**. A reduction in the intensities of the peak at 1000 cm^{-1} was observed in HMT and ANN starches indicating the breakdown of C-H bonding **[3]**.

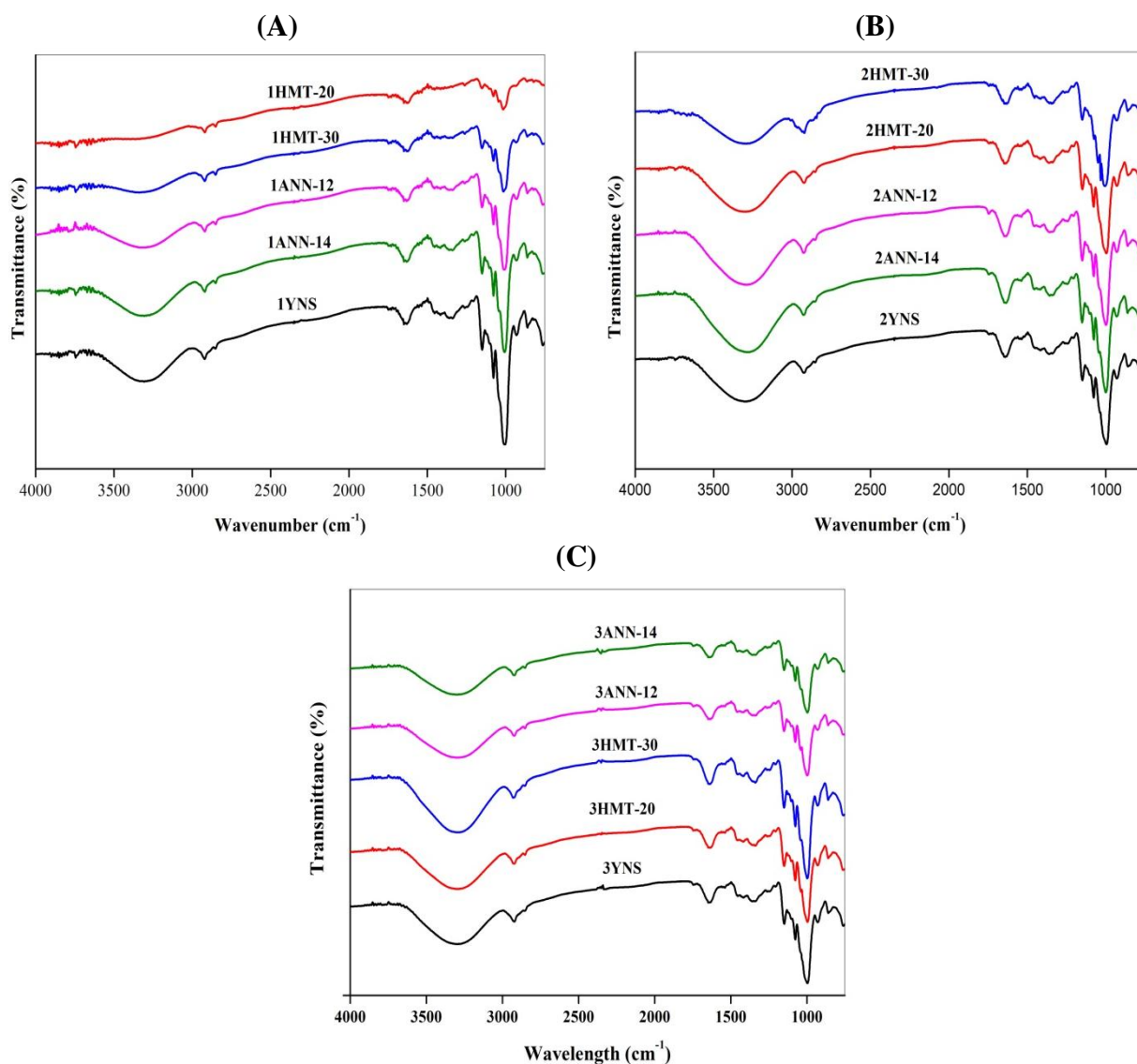**(A)**

(B)

(C)

Fig. 4B.3: ATR-FTIR spectra of native and physically modified yam starches. YNS, HMT, and ANN indicate native, heat-moisture treated, and annealed yam starch, respectively. Prefix 1, 2 & 3 indicate the three yam species. Suffix –20, –30, –12 and –14 indicate 20% moisture level, 30% moisture level, 1:2 starch to moisture ratio and 1:4 starch to moisture ratio, respectively.

4B.6   Swelling power and solubility

The effect of temperature on swelling power and solubility of the native and modified starches of the yam species is presented in **Fig. 4B.4 (A)-(F)**. The swelling power and solubility of all the starches increased as the temperature increased from 55 to 95 °C, due to the gelatinization of starch.
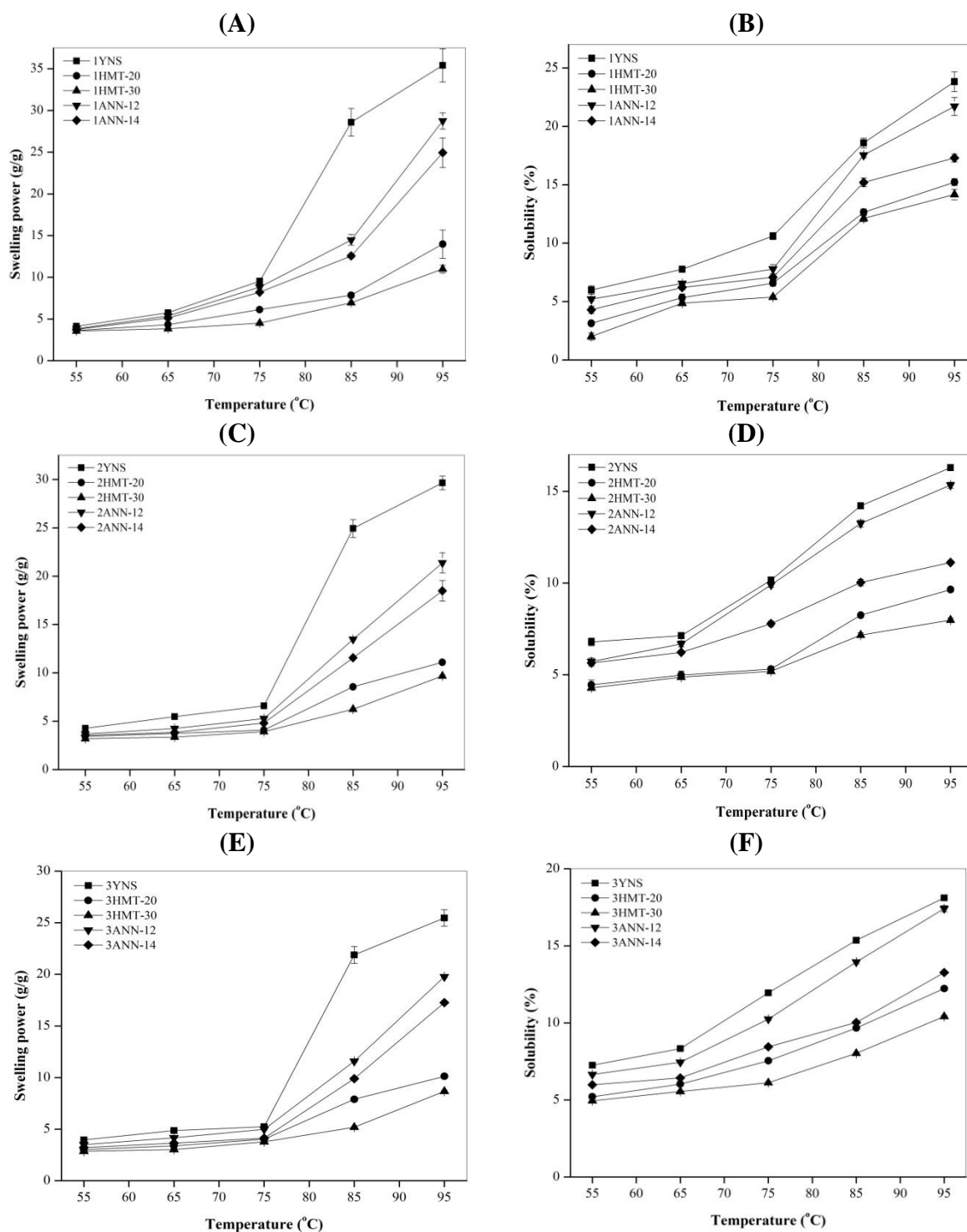
132

Fig. 4B.4: Effect of temperature on the swelling power and solubility of native and modified yam starches. (A), (C), and (E) are the swelling power vs. temperature curve of Y1, Y2, and Y3 yam starches, respectively. (B), (D), and (F) are the solubility vs. temperature curve of Y1, Y2, and Y3 yam starches, respectively.

Native starches exhibited greater swelling power and solubility than the HMT and ANN-treated starches as the treatment temperature increased. The reduction in swelling power and solubility of HMT-treated starch in comparison to native counterparts might be due to the decrease in the amylose leaching as a result of increased interactions between amylose-amylose chains and amylose-amylopectin chains, and the formation of amylose-lipid complex or highly ordered amylopectin side-chain clusters leading to a stable and rigid granular structure of starch after HMT that prevents amylose leaching [9, 13, 39]. Furthermore, a decrease in the swelling power and solubility was noticed along with the increase in moisture levels of the HMT treatment of starch due to the greater mobility of the amylose chains resulting in enhanced amylose-amylose and amylose-amylopectin interactions [8, 40]. Similar observations on the decline of swelling power and solubility after HMT were noticed for mango kernel starches [5], maize starch [27], buckwheat starch [13], oat starch [22], and purple yam flour [40].

The decrease in swelling power and solubility of ANN-treated starch in comparison to their native counterparts might be due to the degree of crystalline perfections and interactions between amylose/amylose and/or amylose-amylopectin, which decreases the hydration of the amorphous regions of starch granules [24]. The strengthening of bonds between amylose/amylopectin or amylopectin/amylopectin molecules prevents amylose leaching, thereby reducing the solubility of the granules [37]. The increase in the moisture levels of ANN-treated starch decreased the swelling power and solubility and similar results on sohphlang starch [29] have been reported. The higher swelling power and solubility of ANN than HMT treated starch at higher temperatures might be due to the destruction of the starch's internal structure at high temperatures and weaker interactions between the functional groups of starch [41]. The higher swelling power shown by Y1 starches than Y2 and Y3 starches is probably influenced by crystallinity (*D. esculenta* > *D. alata*) and extent of interaction between AM-AP and AM-AM chains (*D. esculenta* > *D. alata*) [19].

4B.7   Thermal properties

Gelatinization, which is modulated by water and heat, can determine the starch quality. In the presence of an appropriate amount of water and high temperature, the semicrystalline regions in starch change to amorphous form; and induce changes in the functional properties such as viscosity and gel-forming ability of starch, which are

desired for industrial food applications **[48]**. **Table 4B.3** presents the information on the gelatinization properties of the native starches, HMT, and ANN-treated starches. The gelatinization onset (T_o), peak (T_p) and conclusion (T_c) temperature for 1YNS were 72.34 ± 0.19 ºC, 77.22 ± 0.18 ºC, and 82.67 ± 0.11 ºC, respectively, with a transition enthalpy (ΔH) of 17.87 ± 0.12 J/g. The gelatinization onset (T_o), peak (T_p) and conclusion (T_c) temperature for 2YNS were 71.16 ± 0.23 ºC, 78.52 ± 0.18 ºC, and 84.08 ± 0.19 ºC, respectively, with a transition enthalpy (ΔH) of 17.58 ± 0.15 J/g. The gelatinization onset (T_o), peak (T_p) and conclusion (T_c) temperature for 3YNS were 71.60 ± 0.11 ºC, 75.50 ± 0.16 ºC, and 79.32 ± 0.15 ºC, respectively, with a transition enthalpy (ΔH) of 16.33 ± 0.09 J/g. The gelatinization parameters of the native starches were in the range or close to that for *Dioscorea esculenta* (T_o, 72.30–72.55 ºC; T_p, 75.00–75.73 ºC; T_c, 81.65–85.40 ºC; ΔH, 17.32–18.07 J/g) **[19]**, *Dioscorea alata* (T_o, 68.80–75.80 ºC; T_p, 73.50–82.40 ºC; T_c, 79.90–88.40 ºC; ΔH, 11.80–18.00 J/g) **[16]**, and *Dioscorea bulbifera* (T_o, 71.50–75.26 ºC; T_p, 75.69–78.10 ºC; T_c, 82.50–93.05 ºC) **[20]**.

Table 4B.3: Thermal properties of native and physically modified yam starches

Sample	T_o (ºC)	T_p (ºC)	T_c (ºC)	ΔH (J/g)
1YNS	72.34 ± 0.19[g]	77.22 ± 0.18[j]	82.67 ± 0.11[h]	17.87 ± 0.12[cd]
1HMT-20	75.29 ± 0.14[de]	81.71 ± 0.26[d]	86.74 ± 0.14[d]	15.51 ± 0.10[g]
1HMT-30	77.25 ± 0.30[b]	84.77 ± 0.21[b]	89.37 ± 0.36[c]	11.39 ± 0.14[j]
1ANN-12	74.77 ± 0.24[ef]	80.93 ± 0.09[ef]	84.62 ± 0.13[fg]	18.95 ± 0.15[b]
1ANN-14	76.34 ± 0.41[bc]	81.58 ± 0.11[de]	85.62 ± 0.08[e]	20.25 ± 0.12[a]
2YNS	71.16 ± 0.23[h]	78.52 ± 0.18[i]	84.08 ± 0.19[g]	17.58 ± 0.15[d]
2HMT-20	76.04 ± 0.34[cd]	83.50 ± 0.23[c]	90.07 ± 0.39[b]	15.97 ± 0.22[fg]
2HMT-30	79.05 ± 0.33[a]	86.81 ± 0.45[a]	93.33 ± 0.24[a]	12.37 ± 0.19[i]
2ANN-12	72.05 ± 0.53[gh]	79.71 ± 0.11[h]	85.06 ± 0.25[ef]	18.12 ± 0.14[c]
2ANN-14	73.84 ± 0.42[f]	80.45 ± 0.13[fg]	86.79 ± 0.26[d]	19.18 ± 0.32[b]
3YNS	71.60 ± 0.11[gh]	75.50 ± 0.16[k]	79.32 ± 0.15[j]	16.33 ± 0.09[ef]
3HMT-20	74.56 ± 0.37[ef]	78.68 ± 0.50[i]	82.33 ± 0.26[h]	13.26 ± 0.14[h]
3HMT-30	76.63 ± 0.26[bc]	80.13 ± 0.22[gh]	84.56 ± 0.10[fg]	11.54 ± 0.29[j]
3ANN-12	72.51 ± 0.59[g]	76.18 ± 0.17[k]	79.76 ± 0.17[j]	16.82 ± 0.21[e]
3ANN-14	74.37 ± 0.21[ef]	77.05 ± 0.26[j]	81.45 ± 0.13[i]	17.52 ± 0.10[d]

Data values are presented as mean ± standard deviation. Data with different alphabetic superscript in the same column are statistically significant (p<0.05).

The gelatinization parameters in yam starches are found to be higher than in starches of potato, cassava, and sweet potato [50]. The long interblock chain length, external chain length, and a low number of building blocks per cluster of amylopectin in *Dioscorea esculenta* promote the parallel organization of adjacent double helices and lead to better packing of amylopectins in the starch granules with less branched backbone, thereby increasing ΔH and T_o [42]. HMT and ANN-treated starches had significantly higher T_o, T_p and T_c compared to their respective native starches. HMT treatments are reported to increase the gelatinization temperatures by a broadening of gelatinization range and decreasing the swelling power [46]. The reduced mobility of starch chains in the amorphous regions due to the interactions between amylose-amylose, amylose-amylopectin, and amylose-lipids could increase the gelatinization temperatures [14]. ANN reduces the swelling power and hydration capacity of the starch granules, leading to an increase in gelatinization temperature and narrowing of the gelatinization range, due to the higher alignment of amylopectin double helices and higher content of glassy amorphous regions in annealed starch [46].

There was a significant decline and increase in the ΔH of starch after HMT and ANN, respectively, compared to their respective native starches and with moisture levels. HMT treatments decrease the enthalpy of gelatinization, and reflect the unraveling of the double helix structure present in crystalline and non-crystalline regions of starch granules [36], whereas, the increase of ΔH in ANN indicates a more ordered arrangement of the double helices which forms a tighter starch network with higher crystallinity [48]. Meanwhile, partial gelatinization of less stable amylose and amylopectin molecules can also be linked with a reduced value of ΔH in HMT [27]. Similar results are reported after HMT for maize [27], elephant foot yam [39], and amaranth [35] starches; and after ANN for potato [47], wheat [37], and maize [27] starches. There was no gelatinization of native, HMT, and ANN starches below 70 ºC; therefore, the starches can have potential applications in dough and bread making where an increase in dough volume and higher final bread volume is desired [30].

4B.8 Pasting properties

The pasting parameters of the native and modified yam starches are summarized in **Table 4B.4** and the pasting curves are shown in **Fig. 4B.5**.

Table 4B.4: Pasting properties of native and physically modified yam starches

Sample	PT (^{o}C)	PV (cP)	HPV (cP)	BD (cP)	SB (cP)	FV (cP)
1YNS	82.7 ± 0.75^{cde}	5813 ± 64^{a}	5548 ± 49^{a}	265 ± 25^{c}	1679 ± 32^{i}	7227 ± 22^{f}
1HMT-20	85.3 ± 0.30^{abc}	1872 ± 33^{l}	1760 ± 19^{k}	112 ± 15^{gh}	1003 ± 25^{l}	2763 ± 10^{i}
1HMT-30	86.2 ± 0.53^{a}	1156 ± 17^{o}	1140 ± 13^{n}	16 ± 8^{i}	755 ± 23^{n}	1895 ± 24^{k}
1ANN-12	83.1 ± 0.89^{bcde}	5216 ± 20^{b}	5027 ± 19^{b}	189 ± 2^{def}	2341 ± 37^{h}	7368 ± 55^{de}
1ANN-14	85.6 ± 0.35^{ab}	4965 ± 35^{c}	4838 ± 11^{c}	127 ± 26^{fgh}	2574 ± 15^{g}	7412 ± 26^{cde}
2YNS	77.3 ± 1.28^{ij}	4648 ± 42^{d}	4224 ± 15^{d}	424 ± 54^{b}	3083 ± 44^{f}	7307 ± 50^{ef}
2HMT-20	82.2 ± 1.04^{def}	2988 ± 6^{j}	2830 ± 3^{i}	158 ± 6^{efg}	887 ± 18^{m}	3717 ± 21^{g}
2HMT-30	83.9 ± 0.82^{abcd}	1526 ± 37^{m}	1473 ± 13^{l}	53 ± 29^{hi}	1223 ± 69^{j}	2696 ± 64^{i}
2ANN-12	79.5 ± 0.44^{ghi}	4258 ± 21^{f}	4002 ± 27^{e}	256 ± 14^{cd}	3453 ± 21^{e}	7455 ± 15^{bcd}
2ANN-14	80.7 ± 0.61^{efgh}	4115 ± 18^{g}	3928 ± 8^{f}	187 ± 11^{def}	3595 ± 38^{d}	7523 ± 45^{b}
3YNS	75.4 ± 1.31^{j}	4428 ± 17^{e}	3429 ± 28^{h}	999 ± 11^{a}	4052 ± 13^{c}	7481 ± 39^{bc}
3HMT-20	79.7 ± 1.22^{fghi}	2537 ± 31^{k}	2415 ± 10^{j}	122 ± 22^{fgh}	1109 ± 18^{k}	3524 ± 28^{h}
3HMT-30	81.5 ± 0.87^{defg}	1345 ± 20^{n}	1250 ± 22^{m}	95 ± 15^{gh}	883 ± 17^{m}	2133 ± 18^{j}
3ANN-12	77.6 ± 0.69^{ij}	3839 ± 35^{h}	3613 ± 17^{g}	226 ± 52^{cde}	4172 ± 19^{b}	7785 ± 31^{a}
3ANN-14	78.8 ± 1.13^{hi}	3651 ± 29^{i}	3486 ± 23^{h}	165 ± 10^{efg}	4380 ± 12^{a}	7866 ± 34^{a}

Data values are presented as mean $\pm$ standard deviation. Data with different alphabetic superscript in the same column are statistically significant ($p<0.05$).
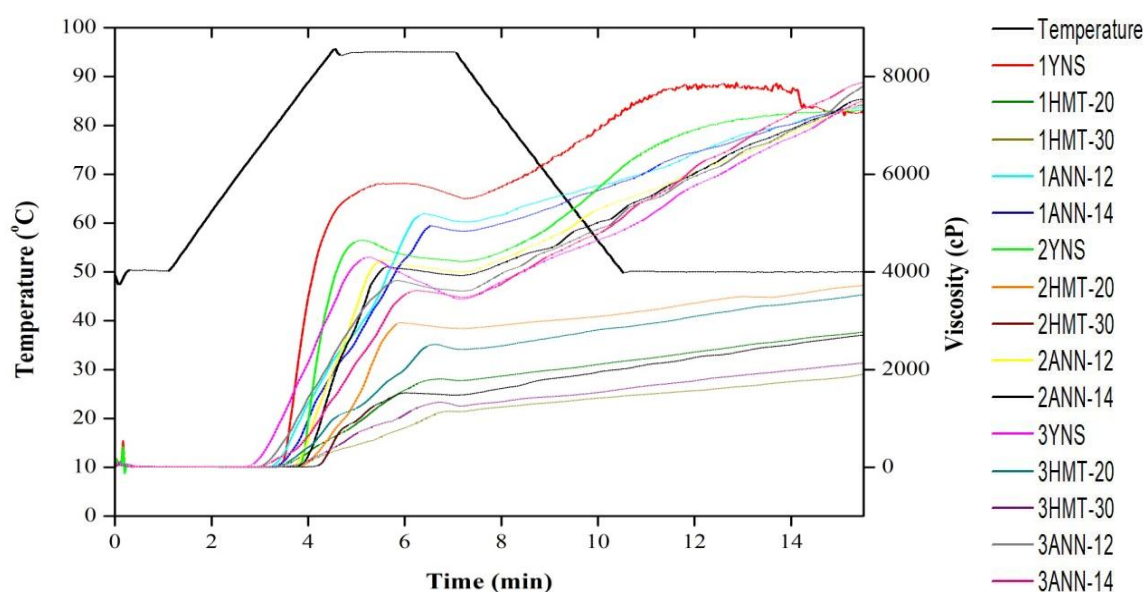
Fig. 4B.5: Pasting curves of native and physically modified starches.

After HMT and with moisture levels, a significant (p<0.5) increase in the pasting temperature and decrease in the PV, HPV, BD, SB, and FV values was observed (except SB for 2HMT-30). Similar trends were reported for HMT normal potato and pearl millet starches, which could be attributed to the decrease in swelling power and amylose leaching of starch granules, and stronger bonding between starch chains (AM-AM, AM-AMP, AMP-AMP) leading to increased granular rigidity [9, 33]. HMT promotes granular rigidity by strengthening granular bonding due to increased intermolecular association of starch chains, restricts swelling power and AML, and thus indicates a higher temperature requirement to disrupt the HMT starch granules to form paste [9, 14, 39]. The increase in moisture levels of HMT was found to increase the PT in elephant foot yam starch [39].

After ANN and with moisture levels, an increase in the PT, SB, and FV values with a decrease in the PV, HPV, and BD was observed. The increase in PT of ANN granules might be due to the complex changes in the crystalline regions and strengthening of intragranular binding forces in the granules, thereby rendering better thermal resistance [14, 47]. A remarkably higher decrease in the PV values was observed after HMT than ANN compared to native starch. This reduction in PV could be attributed to the reduction in the swelling power and AML of the starch granules induced by HMT and ANN. BD indicates the thermal stability and resistivity to shear or deformation of the starch granules during gelatinization at 95 ºC under constant mixing and agitation. BD values were found to be significantly (p<0.5) lower after HMT than ANN compared to the native starch, and with moisture levels. These results indicated the increased thermal stability of the HMT and ANN modified starches, and thus the extent of granular rupture was more pronounced in the native starches compared to the HMT and ANN modified starches. In comparison to the native starch, a decrease in moisture content and HPV of the starch granules after HMT and ANN was observed. Setback (retrogradation) depends on the extent of viscosity breakdown and size of the granules, and the presence of rigid and large granules embedded in leached amylose network can show a higher degree of SB [14, 19]. After ANN, the setback viscosity increased steadily, whereas a decrease in SB was observed after HMT, compared to the native starch. The final viscosity was found to be higher for ANN starches and lower for HMT starches as compared to the native starch granules. An increase in the FV after ANN could be attributed to insufficient gelatinization, decreased swelling power, and

increased rigidity of the ANN granules that can cause the amount of leaching out starches to remain unchanged, leading to the formation of a continuous gel structure, and hence increased FV [1, 18]. These differences in the pasting and viscosity properties between the starches could be explained more clearly with molecular insights on the change of amylose/amylopectin ratio, chain length distribution, and internal helix arrangements during the modification processes, and hence needs further research.
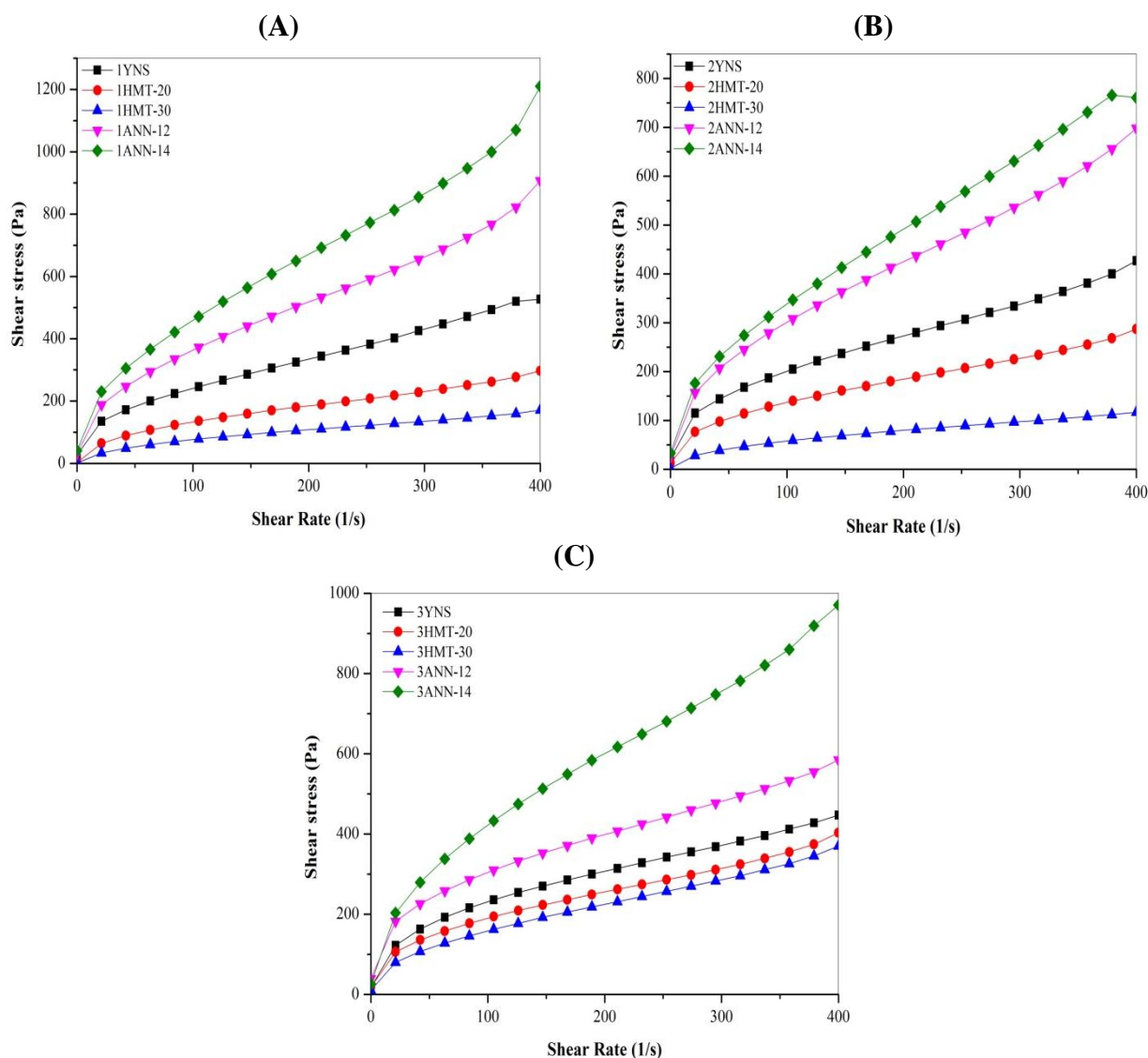
(A)

(B)

(C)

Fig. 4B.6: (A), (B) and (C) are the flow curves of steady shear testing of Y1, Y2 and Y3 yam starches, respectively. YNS, HMT, and ANN indicate native, heat-moisture treated, and annealed yam starch, respectively. Prefix 1, 2 & 3 indicate the three yam species. Suffix −20, −30, −12 and −14 indicate 20% moisture level, 30% moisture level, 1:2 starch to moisture ratio and 1:4 starch to moisture ratio, respectively.

Table 4B.5: Power law fitted parameters of steady flow and oscillatory testing of Y1, Y2 and Y3 starches, respectively

Sample	Flow behavior			G´			G´´		
	k (Pa.s^n)	n	R^2	$k´$	$n´$	R^2	$k´´$	$n´´$	R^2
1YNS	19.84 ± 0.73^g	0.54 ± 0.005^e	0.9851	161.90 ± 0.89^k	0.12 ± 0.000^b	0.9605	33.14 ± 1.24^{gh}	0.25 ± 0.005^{defg}	0.9989
1HMT-20	10.70 ± 0.35^i	0.54 ± 0.005^e	0.9907	150.03 ± 1.05^l	0.12 ± 0.001^b	0.9651	29.98 ± 1.15^{hi}	0.26 ± 0.005^{def}	0.9987
1HMT-30	5.73 ± 0.29^j	0.56 ± 0.007^{de}	0.9954	53.62 ± 2.09^o	0.06 ± 0.002^f	0.8184	4.38 ± 0.98^k	0.48 ± 0.046^a	0.9840
1ANN-12	22.50 ± 0.43^{ef}	0.60 ± 0.003^b	0.9789	232.67 ± 3.34^j	0.09 ± 0.001^c	0.9238	35.16 ± 2.67^g	0.25 ± 0.013^{defg}	0.9942
1ANN-14	24.43 ± 0.49^d	0.63 ± 0.003^a	0.9787	315.62 ± 5.70^h	0.05 ± 0.001^g	0.8496	25.55 ± 1.94^{ij}	0.36 ± 0.015^b	0.9958
2YNS	20.86 ± 0.56^{fg}	0.49 ± 0.004^f	0.9856	262.30 ± 2.14^i	0.07 ± 0.000^e	0.9494	26.89 ± 0.65^i	0.31 ± 0.004^c	0.9976
2HMT-20	14.70 ± 0.59^h	0.48 ± 0.006^f	0.9869	134.79 ± 2.29^m	0.12 ± 0.001^b	0.9684	25.44 ± 1.29^{ij}	0.24 ± 0.007^{efg}	0.9987
2HMT-30	6.04 ± 0.55^j	0.49 ± 0.014^f	0.9980	115.58 ± 1.60^n	0.12 ± 0.001^b	0.9673	21.38 ± 0.58^j	0.29 ± 0.005^{cd}	0.9989
2ANN-12	22.10 ± 0.60^{ef}	0.57 ± 0.004^{cd}	0.9871	408.83 ± 5.35^g	0.07 ± 0.001^e	0.9137	45.78 ± 2.02^f	0.25 ± 0.007^{defg}	0.9978
2ANN-14	23.66 ± 0.36^{de}	0.58 ± 0.002^c	0.9920	648.60 ± 3.28^d	0.08 ± 0.000^d	0.9402	92.71 ± 3.58^c	0.21 ± 0.005^{gh}	0.9906
3YNS	28.87 ± 0.99^c	0.45 ± 0.005^g	0.9950	985.64 ± 0.91^c	0.05 ± 0.000^g	0.8816	133.67 ± 0.55^a	0.17 ± 0.001^i	0.9432
3HMT-20	19.94 ± 0.43^g	0.49 ± 0.003^f	0.9842	601.65 ± 0.81^e	0.06 ± 0.000^f	0.8591	54.28 ± 0.36^e	0.23 ± 0.001^{fg}	0.9933
3HMT-30	11.32 ± 0.25^i	0.57 ± 0.003^{cd}	0.9891	500.20 ± 1.14^f	0.07 ± 0.000^e	0.9173	63.95 ± 0.29^d	0.27 ± 0.001^{cde}	0.9919
3ANN-12	43.12 ± 0.81^a	0.43 ± 0.002^h	0.9873	1758.05 ± 0.61^a	0.03 ± 0.000^h	0.9281	131.38 ± 0.84^a	0.18 ± 0.001^{hi}	0.9550
3ANN-14	30.71 ± 0.62^b	0.57 ± 0.003^{cd}	0.9912	1594.06 ± 0.55^b	0.16 ± 0.000^a	0.8202	110.03 ± 0.93^b	0.18 ± 0.001^{hi}	0.9921

Data values are presented as mean $\pm$ standard deviation. Data with different alphabetic superscript in the same column are statistically significant ($p < 0.05$).

4B.9 Steady shear testing

The steady-state flow behaviors of the native and modified starch pastes at 25 ⁰C are shown in **Fig. 4B.6 (A), (B) & (C)**. The experimental data fitted with power-law models were used to explain the flow behavior of the sample pastes with high R^2 values (0.9787 – 0.9980). Consistency coefficient (*k*), flow behavior index (*n*), and determination coefficient were the model parameters used to accurately analyze the flow curve of each starch paste (**Table 4B.5**).

The flow curves of all the sample pastes were non-linear and behaved as non-Newtonian fluids as shown in **Fig. 4B.6**. There was an increase in shear stress with an increase in the shear rate of all the sample pastes. However, after HMT treatment, there was a marked and significant decrease ($p<0.5$) in the shear stress compared to the native sample paste. This reduction in shear stress might be due to the limited water absorption by starch granules during HMT treatment which leads to partial gelatinization of the starch granules, resulting in weaker molecular interactions in the starch pastes.

Limited exudation of starch molecules, especially the amylose fractions, can also lower the shear stress required to achieve the same shear rate [7]. Compared to native starch, ANN-treated starch showed a significant ($p<0.5$) higher value of shear stress, indicating stronger molecular interactions among starch granules in the pastes.

All the sample pastes exhibited a pseudoplastic and shear-thinning fluid behavior ($n<1$), and the observed values of flow behavior index (*n*), which indicates the shear-thinning behavior ranged between 0.43 – 0.63. There was no significant ($p<0.5$) change in the *n* values of HMT treated starches (except 3HMT-20 and 3HMT-30) compared to native starches; however the *n* values of ANN treated starches increased significantly ($p<0.5$) compared to native starches, and also with moisture levels (except for 3ANN-12), indicating lower shear thinning behavior than native and HMT treated starches. Similar results on increase of *n* values have been reported for annealed starches of potato, lentil, and wheat; and this might be attributed to the decrease in swelling power of the modified starches, indicating reduced susceptibility of the starch granules towards shear deformation and disintegration [15]. 1ANN-14 had the highest *n* values of 0.63 ± 0.003. 2YNS and 3YNS exhibited a higher shear-thinning tendency compared to 1YNS, and this behavior could be attributed to the higher amylose content of *D. alata* starches.

Starch with higher amylose content contains more amylose pre-gel cluster, which contributes more micro-particles in the paste, and this eventually leads to higher severity of particle to shear thereby showing higher shear-thinning tendency [25]. The consistency coefficient (k) for native starch pastes was significantly reduced after the HMT treatment, indicating lower structural strength of the HMT-treated starch pastes. This reduction in the values of k may be due to the reduction in the swelling power of HMT-treated starch granules and a similar decrease was observed in HMT-treated potato, lentil, wheat, and pearl millet starches [15, 33]. Clearly, the results of this experiment showed a conspicuous decrease in swelling power for HMT-treated starches, and a reduction of k values can also be attributed to the decrease in AML from HMT-treated starches. Such flow properties contradicts earlier reports on sweet potato starch, where higher values of k and lower value of n has been reported [25]. This indicates that the type and source of starch can influence the flow properties, and efficient comparisons of consistency coefficient (k) between samples can only be done with a constant value of flow behavior index (n) in the samples. However, k values of all the ANN-modified starches (except for 2ANN-12) significantly ($p<0.5$) increased compared to native starches and with moisture levels, indicating stronger structural strength due to enhanced starch structure interactions during ANN. Similar trends for k values were observed for ANN-modified starches of potato despite lower swelling power and AML [15]. After the starch granules reach the maximum viscosity, the extent of granular collapse and disintegration under shear might be less pronounced for annealed starches than native starches, thereby increasing the thermal stability of ANN-treated starches during the holding cycle (at 95ºC), which could lead to higher k values of ANN treated starches than their native counterparts. These results were consistent with the results of RVA shown in **Table 4B.4**.

4B.10 Oscillatory testing

Dynamic rheological properties such as storage modulus (G´), loss modulus (G´´), and loss tangent (tan δ = G´´/ G´) as a function of frequency (ω) for the native and modified starch pastes at 25ºC are presented in **Fig. 4B.7 (A)-(I)**. Loss tangent (tan δ) > 1 indicates the predominance of viscous properties (behavior like liquid) whereas a tan δ < 1 indicates the predominance of elastic properties (behavior like solid) of a gel.

All the tested starch pastes showed a predominance of G´ over G´´ and no crossover was observed at the frequency range of 0.1-100 rad/s, and both G´ and G´´ increased with the increase in frequency, indicating weak gel characteristics of the starch pastes. Both the modulus (G´ and G´´) for native and modified starches for Y2 and Y3 were found to be higher than the moduli (G´ and G´´) for Y1 native and modified starches, possibly due to its reduced swelling power and AML, and indicated better viscoelastic properties (**Fig. 4B.7 (A)-(F)**). Tan δ values of the native and modified starches of Y2 and Y3 were found to be lower than the tanδ values (0.30-0.53) of the native and modified starches of Y1, respectively (**Fig. 4B.7 (G), (H) & (I)**). After HMT and with moisture levels, a conspicuous reduction in G´ (**Fig. 4B.7 (A), (C) & (E)**) and G´´ (**Fig. 4B.7 (B), (D) & (F)**) was observed compared to their native counterparts. In addition, the HMT samples (except 3HMT-20) were highly viscous compared to native samples as indicated by the higher tanδ values (**Fig. 4B.7 (G), (H) & (I)**) than native. A similar trend was reported for hydroxypropylated sweet potato starch where a reduction of G´ and G´´ was observed with an increase in water uptake capacity of the starch granules, indicating weaker granular integrity **[23]**.

Therefore, the results indicated that the decrease in moduli after HMT could be attributed to the decrease in granular integrity of the granules, and hence reduction of G´ and G´´ with increased tan δ was noticed. This observation can also be correlated with the RVA results of lower setback and final viscosities of starch after HMT (**Table 4B.4**), indicating lower retrogradation tendency (lower reassociation of amylose/amylopectin chains) leading to decreased gel strength. Moreover, granular rupture and increased water exudation from starch granules during gelatinization or shearing can reduce the frictional resistance to flow properties and make the adjacent starch granules easily slide each other, thereby can reduce G´ and G´´. After ANN and with moisture levels, there was a remarkable increase in the moduli (G´ and G´´) and decrease in tan δ, indicating stronger interactions between the starch chains in the starch pastes leading to increased gel strength. A higher value of G´ and G´´ (except 3ANN-14) after ANN compared to their native counterparts may be due to their higher retrogradation as indicated by the higher setback and final viscosity during RVA analysis (**Table 4B.4**). These findings are consistent with results reported for kithul starch after ANN, which could be associated with a higher rate of retrogradation due to stronger associations between

143

amylose/amylopectin chains leached from starch granules leading to increased gel strength of starch pastes **[38]**.
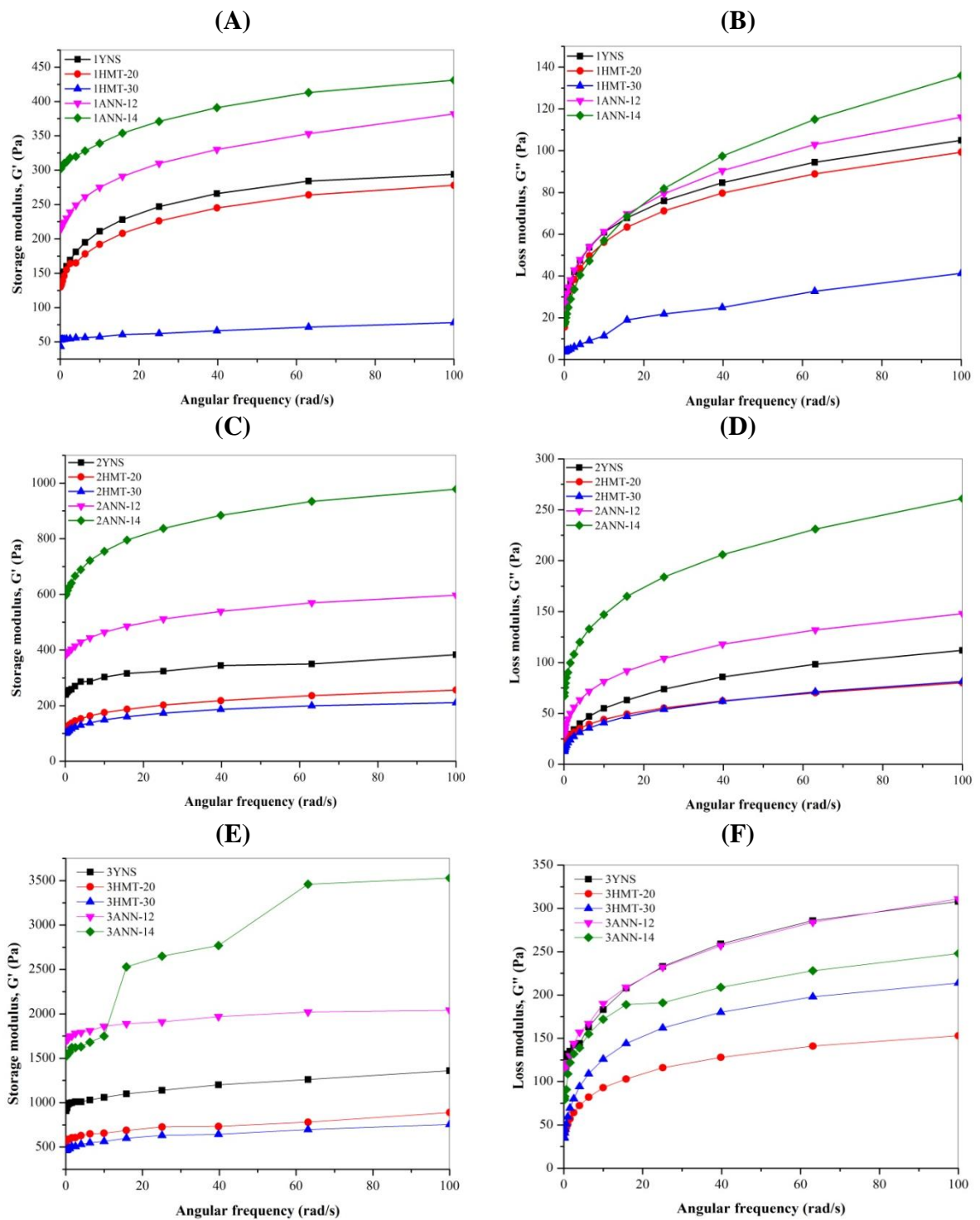

Fig. 4B.7: (A), (C) and (E) are the storage modulus vs. angular frequency curves for oscillatory testing of Y1, Y2 and Y3 starches, respectively. (B), (D) and (F) are the loss modulus vs. angular frequency curves for oscillatory testing of Y1, Y2 and Y3 starches, respectively.
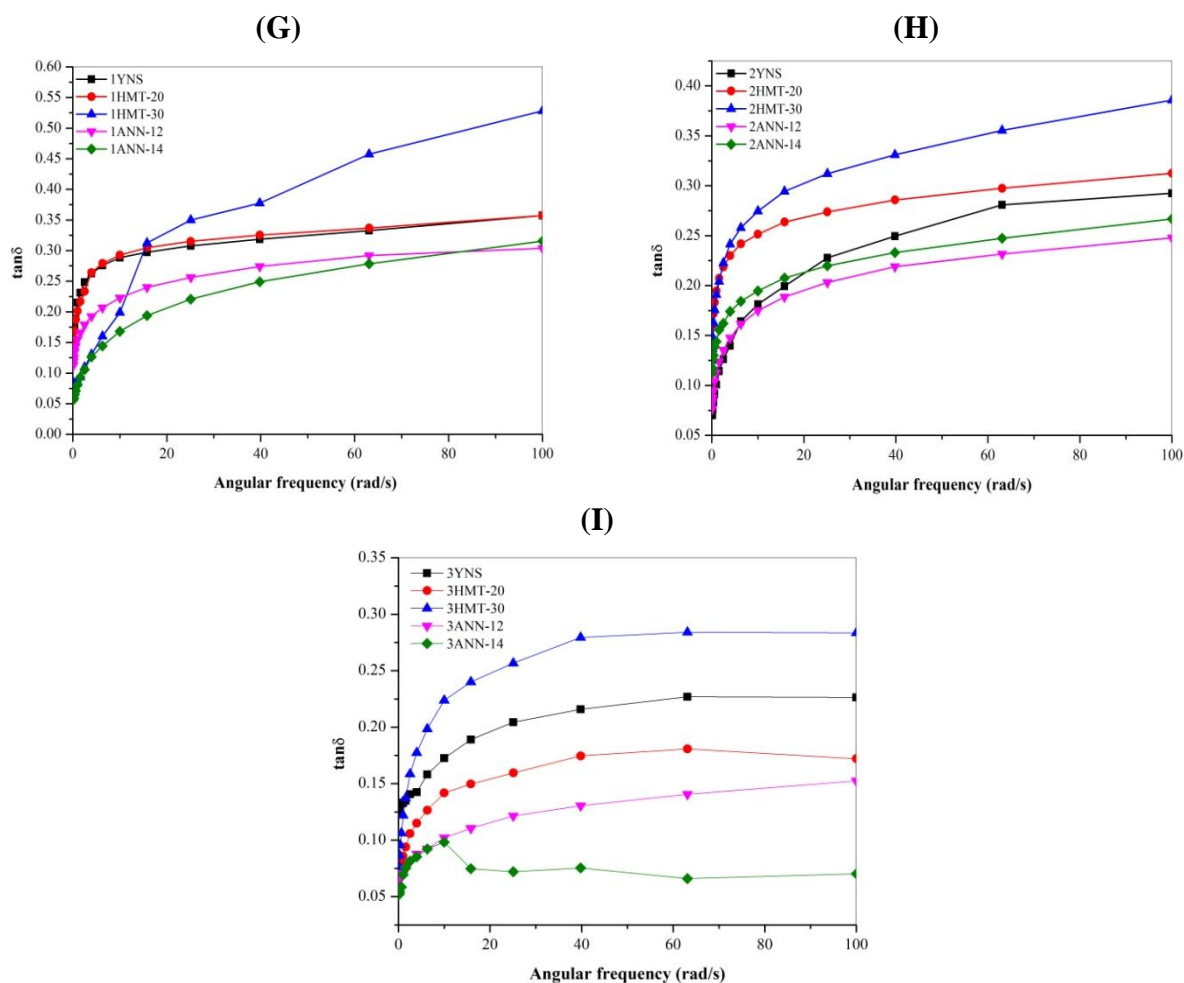
(G)

(H)

(I)

Fig. 4B.7: (continued) (G), (H) and (I) are the tanδ vs. angular frequency curves for oscillatory testing of Y1, Y2 and Y3 starches, respectively. YNS, HMT, and ANN indicate native, heat-moisture treated, and annealed yam starch, respectively. Prefix 1, 2 & 3 indicate the three yam species. Suffix –20, –30, –12 and –14 indicate 20% moisture level, 30% moisture level, 1:2 starch to moisture ratio and 1:4 starch to moisture ratio, respectively.

To further investigate the frequency dependence of G´ and G´´, the experimental data of G´ and G´´ were fitted to power-law models (**Eqs. 2 & 3**) to obtain the model parameters k´, k´´, n´ and n´´, with high coefficients of determination (R^2: 0.8184–0.9684 for G´ and R^2: 0.9432–0.9989 for G´´) as given in **Table 4B.5**. A linear decrease in k´ (elastic) and k´´ (viscous) was observed after HMT with increase in moisture levels (except k´´ for 3HMT-30) compared to native starch whereas an opposite phenomenon was observed for k´ (except for 3ANN-14) after ANN with increase in moisture levels

145

with decreasing k´´ (except for 2ANN-14). The n´ and n´´ values of the starch pastes represent the increased or decreased susceptibility of G´ and G´´, respectively, with changes in the angular frequency. An increase in the frequency dependence of G´ was noticed after HMT for Y2 and Y3 starches compared to native starch, and either constant or decrease after HMT for Y1 starch. After ANN, a decrease in the frequency dependence of G´ was noticed compared to native starch for Y1 starches, either constant or increase after HMT for Y2 starches. The frequency dependence of G´´ was found to be decreasing after HMT and ANN for all the starches of Y2 (except constant for 2HMT30). The frequency dependence of G´´ was found to be increasing at higher moisture levels after HMT and ANN for Y1 starches.

Therefore, based on the rheological results of the yam starches, HMT-modified yam starches can find suitable applications in food products such as bread making, ice-creams, puddings, salad dressing, etc., where a low viscosity is desired, whereas ANN-modified yam starches can be used in food products like jam, thickeners, etc. and more appropriately as an ingredient in making food products such as paneer to increase the viscosity as well as to improve the gel strength and consistency, which is the desired phenomenon to maintain the texture.

4B.11 *In vitro* starch digestibility

The data on *in vitro* digestibility of native and modified yam starches are presented in **Table 4B.6**. A significant ($p<0.5$) increase in the SDS and RS and a decrease in the RDS content were found after HMT and ANN.

ANN starches registered substantial increase in SDS and RS as compared to HMT starches. Among the ANN starches of Y1, Y2 and Y3, 1ANN-14 had the highest SDS content (24.18 %) and 3ANN-14 had the highest RS content (43.11 %), while, in comparison, their native forms recorded SDS content of 13.35% and RS content of 29.75 %, respectively. The increase in SDS and RS after HMT may be due to increased interactions between starch chains; perfection of existing starch crystallites; and reduced accessibility of enzymes for digestion [4, 33]. The decrease in RDS with an increase of SDS and RS after ANN could be attributed to a decrease in enzyme susceptibility; enhanced crystallites perfection; and increased amylose-amylose and/or amylose-amylopectin interactions [48]. An increase in starch granular porosity can decrease the content of RS during ANN, and no pores or fissures were seen on the ANN starch

granules in this study. Many reports on the increase of SDS with a decrease of RS and decrease of SDS with an increase of RS after HMT and ANN have been published **[8, 12, 26, 27, 43, 49]**. Thus, the amount of SDS and RS produced after hydrothermal modifications appeared to be dependent on the moisture levels of starch during treatment, treatment temperature, treatment time, and source of starch. Moreover, the enzyme hydrolysis of starch depends on various factors like starch crystallinity, the morphology of starch granules, polymorphism, and amylose/amylopectin content **[51]**. Higher RS content starches with low digestibility are desired for the production of food products with the low glycemic index.

Table 4B.6: *In vitro* starch digestibility of the native and hydrothermally treated starches

Sample	RDS (%)	SDS (%)	RS (%)
1YNS	70.22 ± 0.17^a	13.35 ± 0.55^h	15.51 ± 0.31^k
1HMT-20	61.13 ± 0.27^b	16.25 ± 0.46^{fg}	21.38 ± 0.58^j
1HMT-30	56.25 ± 0.11^c	19.53 ± 0.14^{de}	23.84 ± 0.23^i
1ANN-12	41.31 ± 0.56^i	20.72 ± 0.21^{bc}	36.72 ± 0.57^d
1ANN-14	34.23 ± 0.21^l	24.18 ± 0.35^a	41.01 ± 0.12^b
2YNS	61.11 ± 0.17^b	15.68 ± 0.88^g	22.32 ± 0.19^j
2HMT-20	55.71 ± 0.39^c	17.14 ± 0.44^f	26.13 ± 0.32^h
2HMT-30	46.37 ± 0.58^e	21.25 ± 0.18^b	31.51 ± 0.19^f
2ANN-12	45.29 ± 0.35^f	19.44 ± 0.26^{de}	34.67 ± 0.19^e
2ANN-14	37.83 ± 0.18^j	21.26 ± 0.16^b	40.63 ± 0.11^b
3YNS	56.25 ± 0.18^c	13.45 ± 0.29^h	29.75 ± 0.47^g
3HMT-20	51.17 ± 0.22^d	16.22 ± 0.17^{fg}	31.52 ± 0.12^f
3HMT-30	44.06 ± 0.16^g	19.36 ± 0.12^{de}	35.91 ± 0.04^{de}
3ANN-12	42.54 ± 0.19^h	18.51 ± 0.23^e	38.03 ± 0.16^c
3ANN-14	35.85 ± 0.12^k	20.07 ± 0.38^{cd}	43.11 ± 0.50^a

Data values are presented as mean ± standard deviation. Data with different alphabetic superscript in the same column are statistically significant ($p < 0.05$).

4B.12 Bibliography

[1]   Almeida, M.C.B.d.M., Costa, S.d.S., Cavalcanti, M.T., and Almeida, E.L., Characterization of Prata Banana (*Musa* AAB-*Prata*) Starch: Native and Modified by Annealing. *Starch-Stärke,* 72(3-4):1900137, 2020.

[2]   Amani, N.G.G., Buléon, A., Kamenan, A., and Colonna, P., Variability in starch physicochemical and functional properties of yam (*Dioscorea* sp) cultivated in Ivory Coast. *Journal of the Science of Food and Agriculture,* 84(15):2085-2096, 2004.

[3]   Barua, S., Tudu, K., Rakshit, M., and Srivastav, P.P., Characterization and digestogram modeling of modified elephant foot yam (*Amorphophallus paeoniifolius*) starch using ultrasonic pretreated autoclaving. *Journal of Food Process Engineering,* 44(11):e13841, 2021.

[4]   BeMiller, J.N., *Physical modification of starch*, in *Starch in food.* Elsevier, 223-253, 2018.

[5]   Bharti, I., Singh, S., and Saxena, D., Exploring the influence of heat moisture treatment on physicochemical, pasting, structural and morphological properties of mango kernel starches from Indian cultivars. *LWT-Food Science and Technology,* 110:197-206, 2019.

[6]   Chakraborty, I., Govindaraju, I., Rongpipi, S., Mahato, K.K., and Mazumder, N., Effects of hydrothermal treatments on physicochemical properties and in vitro digestion of starch. *Food Biophysics,* 16(4):544-554, 2021.

[7]   Chen, L., Tian, Y., Bai, Y., Wang, J., Jiao, A., and Jin, Z., Effect of frying on the pasting and rheological properties of normal maize starch. *Food Hydrocolloids,* 77:85-95, 2018.

[8]   Chung, H.-J., Liu, Q., and Hoover, R., Impact of annealing and heat-moisture treatment on rapidly digestible, slowly digestible and resistant starch levels in native and gelatinized corn, pea and lentil starches. *Carbohydrate Polymers,* 75(3):436-447, 2009.

[9]   Colussi, R., Kringel, D., Kaur, L., da Rosa Zavareze, E., Dias, A.R.G., and Singh, J., Dual modification of potato starch: Effects of heat-moisture and high pressure treatments on starch structure and functionalities. *Food Chemistry,* 318:126475, 2020.

[10]   da Rosa Zavareze, E. and Dias, A.R.G., Impact of heat-moisture treatment and annealing in starches: A review. *Carbohydrate Polymers,* 83(2):317-328, 2011.

[11]   Falade, K.O. and Ayetigbo, O.E., Effects of annealing, acid hydrolysis and citric acid modifications on physical and functional properties of starches from four yam (*Dioscorea* spp.) cultivars. *Food Hydrocolloids,* 43:529-539, 2015.

[12]   Fonseca, L.M., El Halal, S.L.M., Dias, A.R.G., and da Rosa Zavareze, E., Physical modification of starch by heat-moisture treatment and annealing and their applications: A review. *Carbohydrate Polymers,* 274:118665, 2021.

[13]   Goel, C., Semwal, A.D., Khan, A., Kumar, S., and Sharma, G.K., Physical modification of starch: changes in glycemic index, starch fractions, physicochemical and functional properties of heat-moisture treated buckwheat starch. *Journal of Food Science and Technology,* 57(8):2941-2948, 2020.

[14]   Gunaratne, A., *Heat-moisture treatment of starch*, in *Physical modifications of starch.* Springer, 15-36, 2018.

[15]   Hoover, R. and Vasanthan, T., The flow properties of native, heat-moisture treated, and annealed starches from wheat, oat, potato and lentil. *Journal of Food Biochemistry,* 18(2):67-82, 1994.

[16]   Huang, C.-C., Lin, M.-C., and Wang, C.-C., Changes in morphological, thermal and pasting properties of yam (*Dioscorea alata*) starch during growth. *Carbohydrate Polymers,* 64(4):524-531, 2006.

[17]   ISI, Specifications for tapioca starch for use in cotton textile industry. 1970.

[18]   Iuga, M. and Mironeasa, S., A review of the hydrothermal treatments impact on starch based systems properties. *Critical Reviews in Food Science and Nutrition,* 60(22):3890-3915, 2020.

[19]   Jayakody, L., Hoover, R., Liu, Q., and Donner, E., Studies on tuber starches. II. Molecular structure, composition and physicochemical properties of yam (*Dioscorea* sp.) starches grown in Sri Lanka. *Carbohydrate Polymers,* 69(1):148-163, 2007.

[20]   Jiang, Q., Gao, W., Li, X., Wang, H., Xia, Y., and Xiao, P., Comparison of starches separated from different *Dioscorea bulbifera* Linn. cultivars. *Starch-Stärke,* 64(7):531-537, 2012.

[21]   Karwasra, B.L., Gill, B.S., and Kaur, M., Rheological and structural properties of starches from different Indian wheat cultivars and their relationships. *International Journal of Food properties,* 20(sup1):S1093-S1106, 2017.

[22]   Kaur, M. and Singh, S., Influence of heat-moisture treatment (HMT) on physicochemical and functional properties of starches from different Indian oat (*Avena sativa* L.) cultivars. *International Journal of Biological Macromolecules,* 122:312-319, 2019.

[23]   Lee, H. and Yoo, B., Effect of hydroxypropylation on physical and rheological properties of sweet potato starch. *LWT-Food Science and Technology,* 44(3):765-770, 2011.

[24]   Lee, J.-S., Akanda, J.H., Fong, S.L., Siew, C.K., and Ho, A.L., Effects of Annealing on the Properties of Gamma-Irradiated Sago Starch. *Molecules,* 27(15):4838, 2022.

[25]   Liao, L., Liu, H., Gan, Z., and Wu, W., Structural properties of sweet potato starch and its vermicelli quality as affected by heat-moisture treatment. *International Journal of Food Properties,* 22(1):1122-1133, 2019.

[26]   Liu, H., Guo, X., Li, W., Wang, X., Peng, Q., and Wang, M., Changes in physicochemical properties and in vitro digestibility of common buckwheat starch by heat-moisture treatment and annealing. *Carbohydrate Polymers,* 132:237-244, 2015.

[27]   Liu, H., Lv, M., Wang, L., Li, Y., Fan, H., and Wang, M., Comparative study: How annealing and heat-moisture treatment affect the digestibility, textural, and physicochemical properties of maize starch. *Starch-Stärke,* 68(11-12):1158-1168, 2016.

[28]   Liu, H., Yu, L., Simon, G., Dean, K., and Chen, L., Effects of annealing on gelatinization and microstructures of corn starches with different amylose/amylopectin ratios. *Carbohydrate Polymers,* 77(3):662-669, 2009.

[29]   Marboh, V. and Mahanta, C.L., Physicochemical and rheological properties and in vitro digestibility of heat moisture treated and annealed starch of sohphlang (*Flemingia vestita*) tuber. *International Journal of Biological Macromolecules,* 168:486-495, 2021.

[30]   Megusar, P., Stopar, D., Poklar Ulrih, N., Dogsa, I., and Prislan, I., Thermal and Rheological Properties of Gluten-Free, Starch-Based Model Systems Modified by Hydrocolloids. *Polymers,* 14(16):3242, 2022.

[31]   Punia Bangar, S., Nehra, M., Siroha, A.K., Petrů, M., Ilyas, R.A., Devi, U., and Devi, P., Development and characterization of physical modified pearl millet starch-based films. *Foods,* 10(7):1609, 2021.

[32]   Radley, J.A. *Starch production technology.* Applied Science Publishers, 1976.

[33]   Sandhu, K.S., Siroha, A.K., Punia, S., and Nehra, M., Effect of heat moisture treatment on rheological and in vitro digestibility properties of pearl millet

starches. *Carbohydrate Polymer Technologies and Applications,* 1:100002, 2020.

[34]   Sharlina, M.E., Yaacob, W., Lazim, A.M., Fazry, S., Lim, S.J., Abdullah, S., Noordin, A., and Kumaran, M., Physicochemical properties of starch from *Dioscorea pyrifolia* tubers. *Food Chemistry,* 220:225-232, 2017.

[35]   Sindhu, R., Devi, A., and Khatkar, B., Morphology, structure and functionality of acetylated, oxidized and heat moisture treated amaranth starches. *Food Hydrocolloids,* 118:106800, 2021.

[36]   Sindhu, R., Devi, A., and Khatkar, B., Physicochemical, thermal and structural properties of heat moisture treated common buckwheat starches. *Journal of Food Science and Technology,* 56(5):2480-2489, 2019.

[37]   Su, C., Saleh, A.S., Zhang, B., Zhao, K., Ge, X., Zhang, Q., and Li, W., Changes in structural, physicochemical, and digestive properties of normal and waxy wheat starch during repeated and continuous annealing. *Carbohydrate Polymers,* 247:116675, 2020.

[38]   Sudheesh, C., Sunooj, K.V., Alom, M., Kumar, S., Sajeevkumar, V.A., and George, J., Effect of dual modification with annealing, heat moisture treatment and cross-linking on the physico-chemical, rheological and in vitro digestibility of underutilised kithul (*Caryota urens*) starch. *Journal of Food Measurement and Characterization,* 14(3):1557-1567, 2020.

[39]   Suriya, M., Reddy, C.K., and Haripriya, S., Functional and thermal behaviors of heat-moisture treated elephant foot yam starch. *International Journal of Biological Macromolecules,* 137:783-789, 2019.

[40]   Syarifin, A.N.K., Purnomo, A.S., and Fudholi, A., The effect of heat moisture treatment on crystallinity and physicochemical-digestibility properties of purple yam flour. *Food Hydrocolloids,* 120:106889, 2021.

[41]   Trung, P.T.B., Ngoc, L.B.B., Hoa, P.N., Tien, N.N.T., and Van Hung, P., Impact of heat-moisture and annealing treatments on physicochemical properties and digestibility of starches from different colored sweet potato varieties. *International Journal of Biological Macromolecules,* 105:1071-1078, 2017.

[42]   Vamadevan, V., Bertoft, E., and Seetharaman, K., On the importance of organization of glucan chains on thermal properties of starch. *Carbohydrate Polymers,* 92(2):1653-1659, 2013.

[43]   Van Hung, P., Chau, H.T., and Phi, N.T.L., In vitro digestibility and in vivo glucose response of native and physically modified rice starches varying amylose contents. *Food Chemistry,* 191:74-80, 2016.

[44]   Warren, F.J., Gidley, M.J., and Flanagan, B.M., Infrared spectroscopy as a tool to characterise starch ordered structure—a joint FTIR–ATR, NMR, XRD and DSC study. *Carbohydrate Polymers,* 139:35-42, 2016.

[45]   Watcharatewinkul, Y., Puttanlek, C., Rungsardthong, V., and Uttapap, D., Pasting properties of a heat-moisture treated canna starch in relation to its structural characteristics. *Carbohydrate Polymers,* 75(3):505-511, 2009.

[46]   Xie, S.X., Liu, Q., and Cui, S.W., Starch modification and applications. *Food carbohydrates: Chemistry, physical properties, and applications*:357-405, 2005.

[47]   Xu, M., Saleh, A.S., Gong, B., Li, B., Jing, L., Gou, M., Jiang, H., and Li, W., The effect of repeated versus continuous annealing on structural, physicochemical, and digestive properties of potato starch. *Food Research International,* 111:324-333, 2018.

[48]   Yao, T., Sui, Z., and Janaswamy, S., *Annealing*, in *Physical modifications of starch.* Springer, 37-49, 2018.

[49]   Zeng, F., Ma, F., Kong, F., Gao, Q., and Yu, S., Physicochemical properties and digestibility of hydrothermally treated waxy rice starch. *Food Chemistry,* 172:92-98, 2015.

[50]   Zhu, F., Isolation, composition, structure, properties, modifications, and uses of yam starch. *Comprehensive Reviews in Food Science and Food Safety,* 14(4):357-386, 2015.

[51]   Zhu, F. and Xie, Q., Structure and Physicochemical properties of starch. *Physical modifications of starch*:1-14, 2018.

Chapter 4C

Hydroxypropylation and cross-linking of underutilized yam starches and their physical and rheological properties

4C.1 Introduction

This chapter deals with the chemical modification of isolated starches from *Dioscorea esculenta* (Y1), *Dioscorea alata* (purple yam, Y2), and *Dioscorea alata* (yellow yam, Y3). There is a lack of adequate information on the chemical modification of yam starches, which is one of the limiting factors for industrial application of yam starches. Therefore, 1YNS, 2YNS and 3YNS, the isolated starches from Y1, Y2, and Y3, respectively, were chemically modified through hydroxypropylation using propylene oxide and cross-linking using sodium trimetaphosphate (STMP). The hydroxypropylated starches were named 1YHP-05, 1YHP-10, 2YHP-05, 2YHP-10, 3YHP-05 and 3YHP-10, where the prefix '1', '2', and '3' indicate the yam species *D. esculenta*, *D. alata* (purple yam), and *D. alata* (yellow yam) respectively, and the suffix –05 and –10 indicate starch modified with 5 ml and 10 ml propylene oxide, respectively. The cross-linked starches were named 1YCL-02, 2YCL-02, and 3YCL-02,, where the prefix '1', '2', and '3' indicate the yam species *D. esculenta*, *D. alata* (purple yam), and *D. alata* (yellow yam) respectively, and the suffix -02 indicates starch modified with 2 g STMP. The effect of both the chemical modifications on the physical and rheological properties of starch was investigated. The chemically modified starches was studied to drive desirable changes in the properties of starch that can help to determine the end use of the chemical modified starches.

4C.2 Molar substitution and Degree of substitution

The hydroxypropyl groups (HP), molar substitution (MS), phosphorus (P) content, and degree of substitution (DS) of the starches are shown in **Table 4C.1**. With the raise of propylene oxide from 5 ml to 10 ml, there was a corresponding increase in the MS value of the starches. Similarly, STMP increased the phosphorus content of the starches, which resulted in increased value of DS.

Table 4C.1: Hydroxypropyl groups (HP), molar substitution (MS), phosphorus (P) content, and degree of substitution (DS) of the yam starches

Samples	%HP	MS	P content	DS
1YNS	-	-	0.004 ± 0.001	-
1YHP-05	0.58 ± 0.025	0.0172 ± 0.0012	-	-
1YHP-10	1.023 ± 0.037	0.0358 ± 0.0018	-	-
1YCL-02	-	-	0.052 ± 0.012	0.0025 ± 0.0002
2YNS	-	-	0.005 ± 0.015	-
2YHP-05	0.67 ± 0.056	0.0184 ± 0.0016	-	-
2YHP-10	1.192 ± 0.048	0.0439 ± 0.0025	-	-
2YCL-02	-	-	0.061 ± 0.008	0.0029 ± 0.0003
3YNS	-	-	0.005 ± 0.003	-
3YHP-05	0.77 ± 0.019	0.0216 ± 0.0021	-	-
3YHP-10	1.325 ± 0.021	0.0523 ± 0.0015	-	-
3YCL-02	-	-	0.064 ± 0.011	0.0033 ± 0.0002

Data values are presented as mean ± standard deviation.

4C.3   Scanning electron microscopy

Fig. 4C.1 illustrates the SEM images of the native, hydroxypropylated, and cross-linked yam starches. *D. esculenta* (Y1) native starch micrographs presented irregular polygonal or polyhedral shaped starch granules with smooth surfaces. *D. alata* (purple yam, Y2) and *D. alata* (yellow yam, Y3) starch micrographs presented oval, elongated or lenticular shaped starch granules with smooth surface. Micrographs of 1YCL-02 showed the presence of agglomerated starch granules, which may increase the particle size of starch granules. Similar observations were reported for STMP modified commercial soluble starch, and this behavior may be related to the phosphorylation of starch, which can increase the intermolecular interactions between starch chains due to insertion of phosphate groups **[11]**. Moreover, after cross-linking with STMP, the surface of all the starch granules appear to be rougher and having surface dents.

1YNS	**1YHP-05**	**1YHP-10**	**1YCL-02**

2YNS	**2YHP-05**	**2YHP-10**	**2YCL-02**

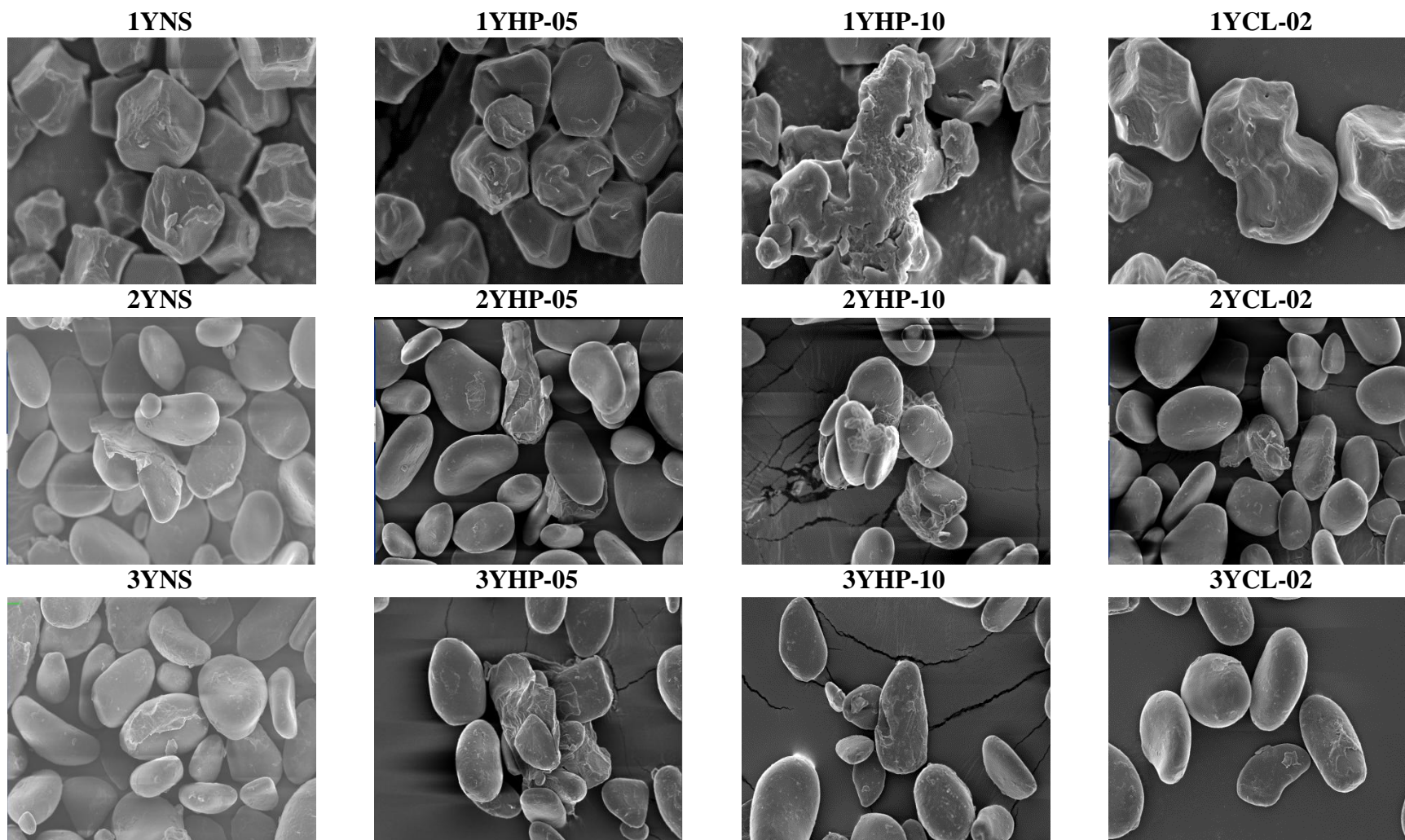| **3YNS**	**3YHP-05**	**3YHP-10**	**3YCL-02**

Fig. 4C.1: Scanning electron microscopy (SEM) of native and chemically modified yam starches at 15000x for yam species 1, and 2000x for yam species 2 and 3. YNS, YHP, and YCL indicate native, hydroxypropylated, and cross-linked yam starch, respectively. Prefix 1, 2 & 3 indicate the three yam species. Suffix –05, –10, and –02 indicate starch modified with 5 ml propylene oxide, 10 ml propylene oxide, and 2 g STMP, respectively.

Similar starch granules with rough surface and dents were observed after cross-linking of corn starch using STMP **[3]**. Hydroxypropylated starch showed the presence of small attachments around the starch granules and some indents, which may be due to the damage caused by sodium hydroxide. The starch granules were found to be rough in surface, and some granules melted together and lost their structural integrity after hydroxypropylation. Similar micrographs of hydroxypropylated starch for rice was observed by **Shen et al. [12]**.

(A)

(B)

(C)
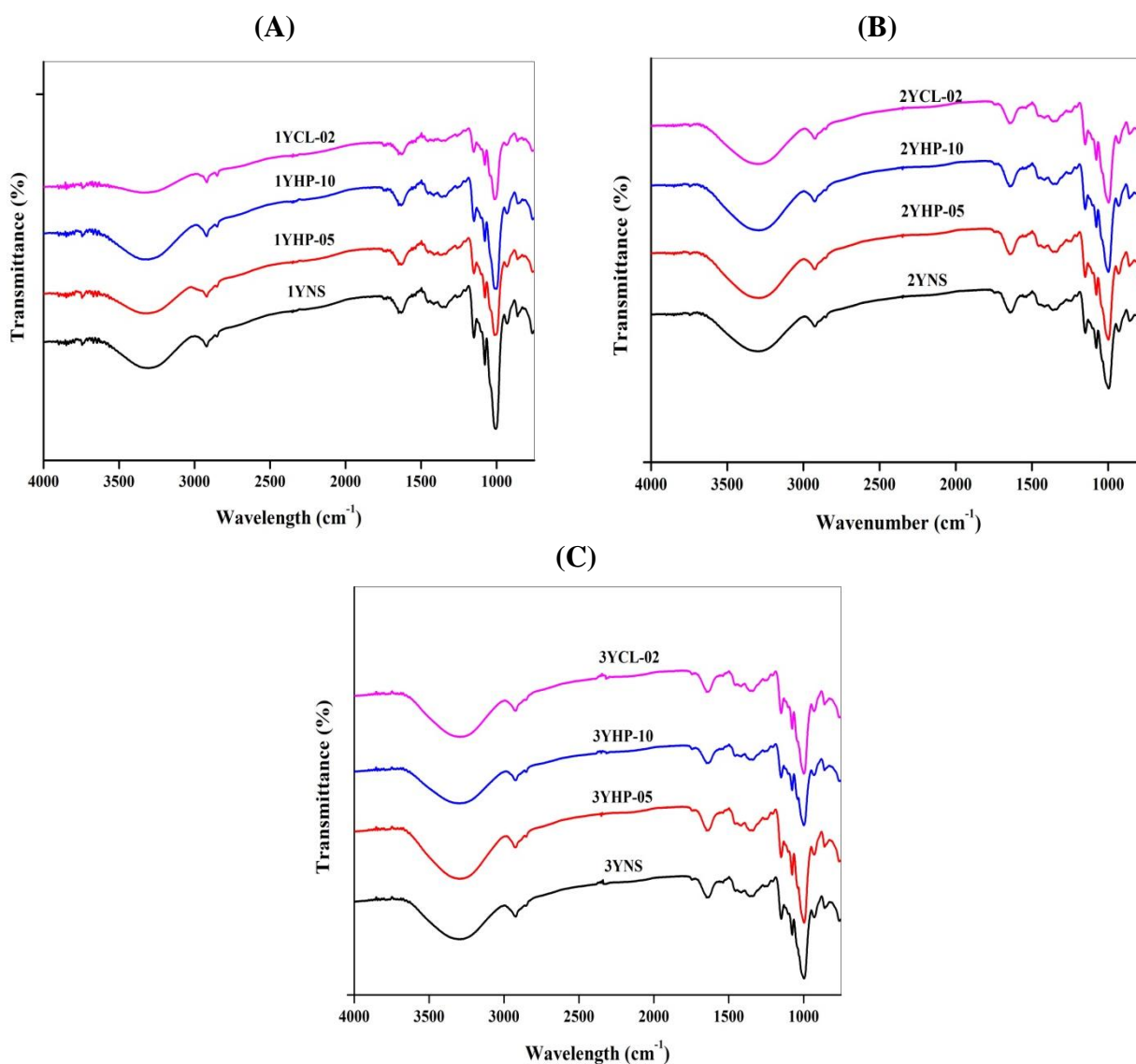
Fig. 4C.2: ATR-FTIR spectra of native and chemically modified yam starches. YNS, YHP, and YCL indicate native, hydroxypropylated, and cross-linked yam starch, respectively. Prefix 1, 2 & 3 indicate the three yam species. Suffix –05, –10, and –02 indicate starch modified with 5 ml propylene oxide, 10 ml propylene oxide, and 2 g STMP, respectively.

4C.4   ATR-FTIR spectroscopy

Fig. 4C.2 presents the ATR-FTIR spectra of the native, hydroxypropylated, and cross-linked yam starches. Hydroxypropylation and cross-linking did not alter the ATR-FTIR spectra of the samples, and exhibited similar absorption peaks at 860 cm^{-1} (C–H and CH2 deformations) 930 cm^{-1} (skeletal mode vibration of α-(1–4) glycosidic linkage), 1150 cm^{-1} and 1077 cm^{-1} (C-O, C-C, and C-O-H stretching), 1641 cm^{-1} (H-O-H bending vibration), 2924 cm^{-1} (C-H stretching vibration), and 3293 cm^{-1} (O-H stretching vibrations) [5, 14, 15]. As shown in **Fig. 4C.2**, there is no clear difference between the O–H, C–H and C–O vibrational bands of native, hydroxypropylated and cross-linked starches. This may be attributed to the fact that the basic chemical structure of cross-linked starch, hydroxypropylated starch and native starch are similar, which are reflected in the similar absorption peaks. However, the peak intensity at 3293 cm^{-1} representing O-H stretching vibration was found to be lower for 1YCL-02 compared to the native and hydroxypropylated starches of Y1.

4C.5   Swelling power and solubility

The effect of temperature on swelling power and solubility of the native and chemically modified starches of the yam species is presented in **Fig. 4C.3 (A)-(F)**. The swelling power and solubility of all the starches increased as the temperature increased from 55 to 95 °C, due to the gelatinization of starch. There was a significant (p<0.5) increase in the swelling power and solubility of the hydroxypropylated starches compared to native, and increased with an increase in MS. Generally, hydroxypropylation increases the swelling power and solubility of starch by disrupting the intramolecular and intermolecular hydrogen bonds in starch chains, thereby weakening the granular structure of starch and increasing the water uptake [7]. Meanwhile, a decrease in the swelling power and solubility of the cross-linked starches was observed, which may be due to the increase in density of cross-links between the starch chains or formation of a hard crust around the starch granules that may restrict swelling [6].
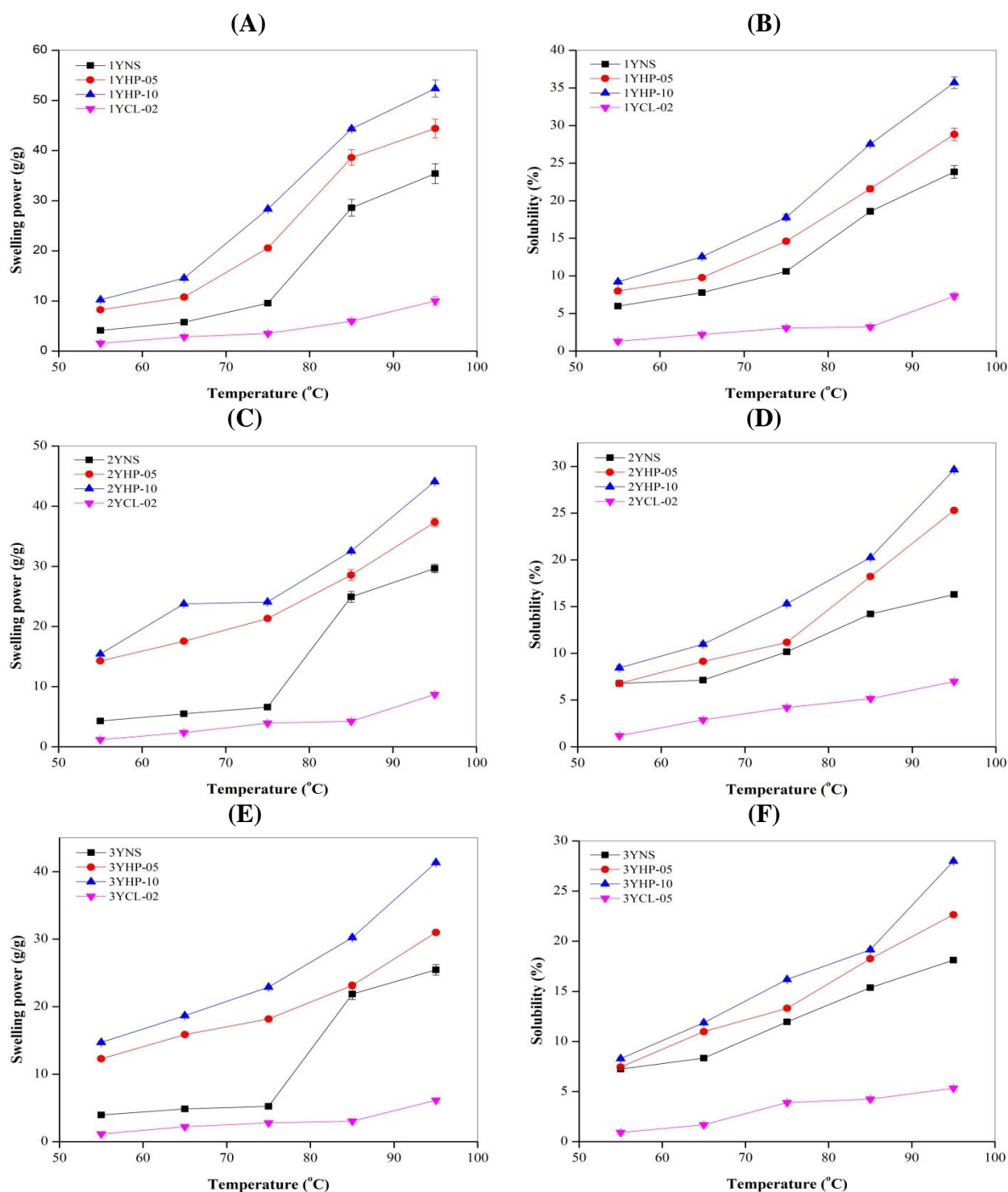
(A)

(B)

(C)

(D)

(E)

(F)

Fig. 4C.3: Effect of temperature on the swelling power and solubility of native and chemically modified yam starches. (A), (C), and (E) are the swelling power vs. temperature curve of Y1, Y2, and Y3 yam starches, respectively. (B), (D), and (F) are the solubility vs. temperature curve of Y1, Y2, and Y3 yam starches, respectively.

4C.6 Paste clarity and freeze thaw stability

Table 4C.2 presents the information on the paste clarity of the native and chemically modified yam starches. Hydroxypropylated yam starches exhibited a better clarity than the native starches. The high paste clarity of hydroxypropylated yam starches could be due to the incorporation of hydrophilic hydroxypropyl groups that inhibits association of the starch chains after pasting and have greater swelling than native starches, resulting in more light transmittance **[7]**. The paste clarity of cross-linked starches was found to be lower than those of native starches, which may be due to the generated covalent bonds between the starch chains that makes the paste hard to absorb water, resulting in incomplete gelatinization of granules **[6]**. A similar decrease in paste clarity of cross-linked elephant foot yam was reported by **Shukhija et al. [13]**.

Table 4C.2: Paste clarity and freeze thaw stability of chemically modified starches

Sample	Paste clarity	Syneresis (%)		
		1st FTC	2nd FTC	3rd FTC
1YNS	15.33 ± 0.05^i	41.36 ± 0.51^c	45.21 ± 0.66^c	48.24 ± 0.56^c
1YHP-05	23.51 ± 0.03^h	35.22 ± 0.33^d	37.46 ± 0.51^e	38.13 ± 0.25^e
1YHP-10	32.15 ± 0.03^f	26.39 ± 0.39^g	28.21 ± 0.34^h	30.91 ± 0.46^g
1YCL-02	5.12 ± 0.02^l	53.44 ± 0.44^a	57.33 ± 0.23^a	59.32 ± 0.54^a
2YNS	26.54 ± 0.06^g	36.27 ± 0.47^d	39.35 ± 0.39^d	41.12 ± 0.23^d
2YHP-05	34.23 ± 0.05^e	26.54 ± 0.54^g	29.33 ± 0.13^h	30.12 ± 0.28^g
2YHP-10	41.36 ± 0.06^c	21.48 ± 0.26^i	22.51 ± 0.53^j	23.17 ± 0.21^i
2YCL-02	8.22 ± 0.04^k	44.45 ± 0.12^b	48.29 ± 0.64^b	50.11 ± 0.19^b
3YNS	34.64 ± 0.07^d	32.46 ± 0.60^e	35.32 ± 0.32^f	38.93 ± 0.37^e
3YHP-05	42.82 ± 0.04^b	23.41 ± 0.21^h	26.47 ± 0.47^i	28.53 ± 0.41^h
3YHP-10	55.43 ± 0.10^a	18.31 ± 0.20^j	20.64 ± 0.44^k	20.87 ± 0.10^j
3YCL-02	10.35 ± 0.10^j	29.23 ± 0.14^f	33.74 ± 0.31^g	36.53 ± 0.54^f

Data values are presented as mean ± standard deviation. Data with different alphabetic superscript in the same column are statistically significant (p<0.05).

The data representing the syneresis (%) of the native and chemically modified yam starches are shown in **Table 4C.2**. Freeze thaw stability or syneresis is the tendency of starch paste or gel to exclude water from the gel due to increased molecular associations of starch chains [8]. Cross-linked starches showed a higher percentage of syneresis than the native and hydroxypropylated starches. Generally, cross-linked starch retards the association of starch chains, recrystallization, and mobility of amylopectin branches, resulting in higher syneresis from the crosslinked starch paste [1]. High freeze-thaw stability of hydroxypropylated starch gels may be attributed to the decreased retrogradation of starch caused by the incorporation of hydroxypropyl groups in the starch molecules [7]. The difference in the syneresis of starches from the yam species may be due to the size and amylose content of the starch granules [10]. There was an increase in the syneresis (%) with the increase in freeze thaw cycle (FTC) in all the starches.

4C.7   Steady shear testing

The steady-state flow behaviors of the native and chemically modified starch pastes at 25 ⁰C are shown in **Fig. 4C.4 (A), (B) & (C)**. The experimental data fitted with power-law models were used to explain the flow behavior of the sample pastes with high R^2 values (0.9851 – 0.9992). Consistency coefficient (k), flow behavior index (n), and determination coefficient were the model parameters used to accurately analyze the flow curve of each starch paste (**Table 4C.3**).   The flow curves of all the native and chemically modified starch pastes were non-linear and behaved as non-Newtonian fluids as shown in **Fig. 4C.4**. There was an increase in shear stress with an increase in the shear rate of all the sample pastes.

There was a significant (p<0.5) increase in the n values of hydroxypropylated starch pastes and with an increase in MS, compared to native starch pastes, indicating low shear thinning behavior of the hydroxypropylated starch pastes. The magnitudes of consistency coefficient (k) of the hydroxypropylated starch pastes was found to be lower than the native starch pastes, indicating a low structural strength of the hydroxypropylated starch pastes. This behavior of hydroxypropylated starch paste may be due to the incorporation of hydroxypropyl groups and disruption of hydrogen bonds in the starch molecules. Such flow properties of hydroxypropylated starch paste is consistent with previous reports on hydroxypropylated sweet potato starches with

different MS [7]. However, the *n* values of cross-linked starch pastes decreased significantly (p<0.5) compared to native starch pastes, indicating high shear thinning behavior of the cross-linked starch pastes. The magnitudes of consistency coefficient (*k*) of the cross-linked starch pastes were found to be much higher than those of the native starch pastes, indicating a high structural strength of the cross-linked starch pastes. This behavior of the cross-linked starch pastes may be attributed to the lower level of disruption of intermolecular and intramolecular bonds in the starch granules [2].

(A)

(B)

(C)
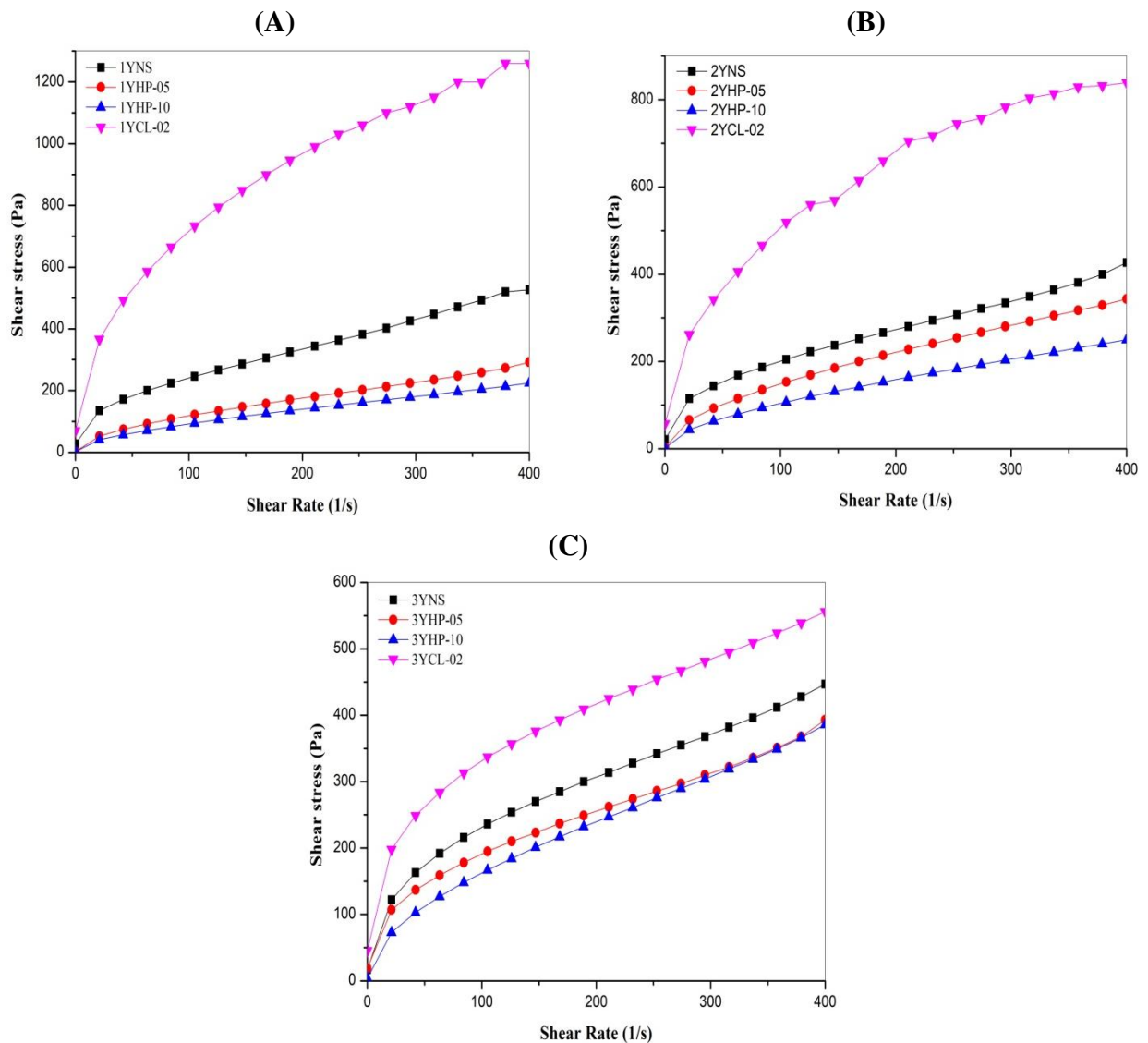
Fig. 4C.4: (A), (B) and (C) are the flow curves of steady shear testing of Y1, Y2 and Y3 yam starches, respectively. YNS, YHP, and YCL indicate native, hydroxypropylated, and cross-linked yam starch, respectively. Prefix 1, 2 & 3 indicate the three yam species. Suffix –05, –10, and –02 indicate starch modified with 5 ml propylene oxide, 10 ml propylene oxide, and 2 g STMP, respectively.

Table 4C.3: Power law fitted parameters of steady flow of Y1, Y2 and Y3 native and chemically modified starches

Sample	Flow behavior		
	k (Pa.s^n)	n	R^2
1YNS	19.84 ± 0.73^e	0.54 ± 0.005^c	0.9851
1YHP-05	6.60 ± 0.51^{fg}	0.62 ± 0.012^a	0.9947
1YHP-10	5.23 ± 0.26^g	0.62 ± 0.007^a	0.9978
1YCL-02	106.86 ± 1.81^a	0.41 ± 0.003^f	0.9974
2YNS	20.86 ± 0.56^e	0.49 ± 0.004^d	0.9856
2YHP-05	9.74 ± 0.36^f	0.59 ± 0.006^b	0.9990
2YHP-10	5.94 ± 0.49^g	0.62 ± 0.013^a	0.9992
2YCL-02	81.84 ± 0.74^b	0.39 ± 0.001^f	0.9927
3YNS	28.87 ± 0.99^d	0.45 ± 0.005^e	0.9950
3YHP-05	21.59 ± 0.94^e	0.47 ± 0.006^d	0.9872
3YHP-10	10.02 ± 0.28^f	0.60 ± 0.004^{ab}	0.9966
3YCL-02	65.96 ± 3.09^c	0.35 ± 0.009^g	0.9942

Data values are presented as mean ± standard deviation. Data with different alphabetic superscript in the same column are statistically significant (p<0.05).

4C.8   Oscillatory testing

Rheological properties such as dynamic moduli (storage modulus, G´; and loss modulus, G´´), and loss tangent (tan δ = G´´/ G´) as a function of frequency (ω) for the native and chemically modified starch pastes at 25 ºC are presented in **Fig. 4C.5 (A)-(F)**. A loss tangent (tan δ) value greater than one indicates the predominance of viscous properties (behavior like liquid), whereas a tan δ less than 1 indicates the predominance of elastic properties (behavior like solid) of a gel.

All the native and chemically modified starch pastes showed a predominance of G´ over G´´, and no crossover was evident at the tested frequency range of 0.1-100 rad/s. Both the moduli (G´ and G´´) increased with an increase in frequency, indicating weaker gel characteristics of the starch pastes. Both the moduli (G´ and G´´) of hydroxypropylated starch pastes were found to be lower than the moduli (G´ and G´´) of native starch pastes, and with an increase in MS. Lower dynamic moduli of hydroxypropylated starch paste may be due to the weak granular integrity of starch

molecules caused by the presence of hydroxypropyl groups in hydroxypropylated starch paste that increases the water uptake capacity of swollen granules in the paste **[7]**.
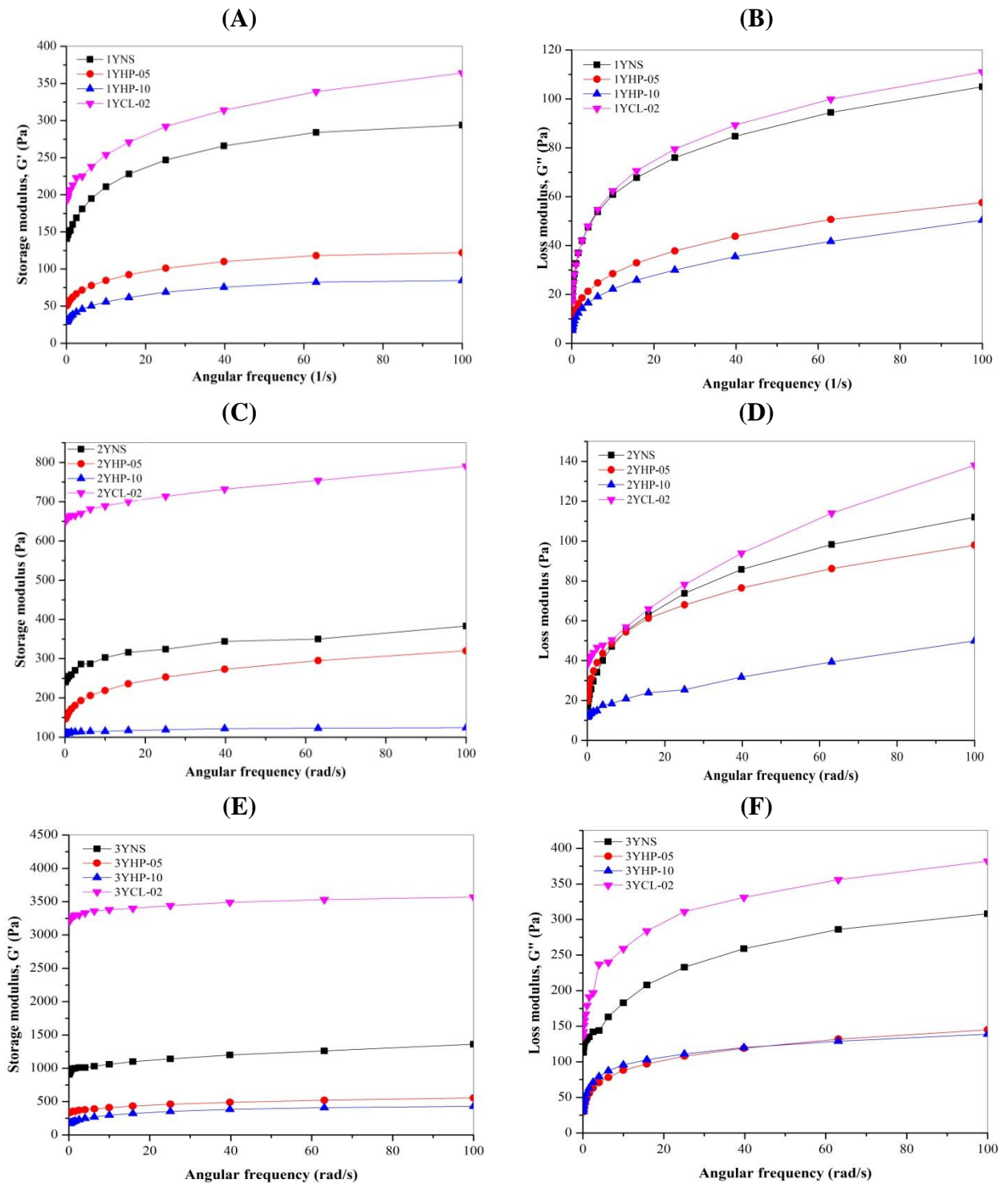

Fig. 4C.5: (A), (C) and (E) are the storage modulus vs. angular frequency curves for oscillatory testing of Y1, Y2 and Y3 starches, respectively. (B), (D) and (F) are the loss modulus vs. angular frequency curves for oscillatory testing of Y1, Y2 and Y3 starches, respectively.
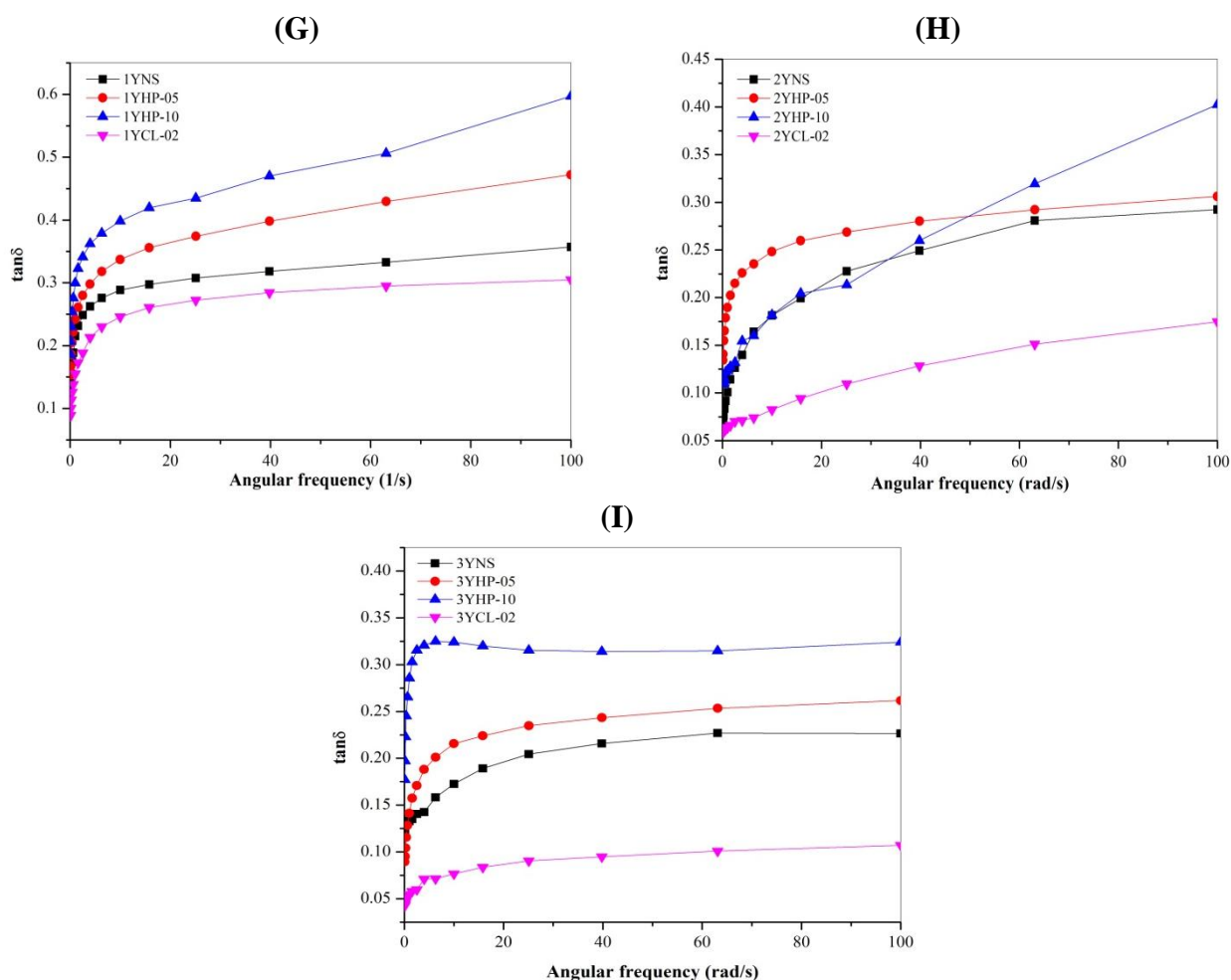
Fig. 4C.5: (continued) (G), (H) and (I) are the tanδ vs. angular frequency curves for oscillatory testing of Y1, Y2 and Y3 starches, respectively. YNS, YHP, and YCL indicate native, hydroxypropylated, and cross-linked yam starch, respectively. Prefix 1, 2 & 3 indicate the three yam species. Suffix –05, –10, and –02 indicate starch modified with 5 ml propylene oxide, 10 ml propylene oxide, and 2 g STMP, respectively.

However, the cross-linked starch HPSPS pastes showed a much higher value of both the moduli than the native starch paste. The tan δ (ratio of G''/G') values (**Fig. 4C.5 (G), (H) & (I)**) of all native and chemically modified starch paste indicated that all the sample pastes were more elastic than viscous. The hydroxypropylated starch pastes were found to be highly viscous compared to the native starch paste, as demonstrated by their higher tan δ values. Similar observations was previously reported on hydroxypropylated sweet potato with different MS **[7]** and potato starches with different MS **[9]**. Meanwhile, the cross-linked starch pastes were found to be highly elastic compared to the native starch paste, as evident by their lower tan δ values. Our results are consistent

with the previously reported results on dynamic rheological properties of cross-linked potato starch using STMP/STPP **[4]**.

4C.9   Bibliography

[1]   Chatakanonda, P., Varavinit, S., and Chinachoti, P., Effect of crosslinking on thermal and microscopic transitions of rice starch. *LWT-Food Science and Technology,* 33(4):276-284, 2000.

[2]   Cho, S.-A., Kim, B.-Y., and Yoo, B.-S., Flow behavior of sweet potato starch in mixed sugar systems. *Preventive Nutrition and Food Science,* 13(3):249-252, 2008.

[3]   Gao, F., Li, D., Bi, C.-h., Mao, Z.-h., and Adhikari, B., Preparation and characterization of starch crosslinked with sodium trimetaphosphate and hydrolyzed by enzymes. *Carbohydrate Polymers,* 103:310-318, 2014.

[4]   Heo, H., Lee, Y.-K., and Chang, Y.H., Rheological, pasting, and structural properties of potato starch by cross-linking. *International Journal of Food Properties,* 20(sup2):2138-2150, 2017.

[5]   Karwasra, B.L., Gill, B.S., and Kaur, M., Rheological and structural properties of starches from different Indian wheat cultivars and their relationships. *International Journal of Food Properties,* 20(sup1):S1093-S1106, 2017.

[6]   Kaur, L., Singh, J., and Singh, N., Effect of cross-linking on some properties of potato (*Solanum tuberosum* L.) starches. *Journal of the Science of Food and Agriculture,* 86(12):1945-1954, 2006.

[7]   Lee, H. and Yoo, B., Effect of hydroxypropylation on physical and rheological properties of sweet potato starch. *LWT-Food Science and Technology,* 44(3):765-770, 2011.

[8]   Liu, H., Ramsden, L., and Corke, H., Physical properties and enzymatic digestibility of hydroxypropylated waxy and normal maize starch. *Carbohydrate Polymers,* 40(3):175-182, 1999.

[9]   Morikawa, K. and Nishinari, K., Effects of concentration dependence of retrogradation behaviour of dispersions for native and chemically modified potato starch. *Food Hydrocolloids,* 14(4):395-401, 2000.

[10]   Otegbayo, B., Oguniyan, D., and Akinwumi, O., Physicochemical and functional characterization of yam starch for potential industrial applications. *Starch-Stärke,* 66(3-4):235-250, 2014.

[11]   Sechi, N.d.S.M. and Marques, P.T., Preparation and physicochemical, structural and morphological characterization of phosphorylated starch. *Materials Research,* 20:174-180, 2017.

[12]   Shen, Y., Zhang, N., Xu, Y., Huang, J., Wu, D., and Shu, X., Physicochemical properties of hydroxypropylated and cross-linked rice starches differential in amylose content. *International Journal of Biological Macromolecules,* 128:775-781, 2019.

[13]   Sukhija, S., Singh, S., and Riar, C.S., Effect of oxidation, cross-linking and dual modification on physicochemical, crystallinity, morphological, pasting and thermal characteristics of elephant foot yam (*Amorphophallus paeoniifolius*) starch. *Food Hydrocolloids,* 55:56-64, 2016.

[14]   Suriya, M., Reddy, C.K., and Haripriya, S., Functional and thermal behaviors of heat-moisture treated elephant foot yam starch. *International Journal of Biological Macromolecules,* 137:783-789, 2019.

[15]   Syarifin, A.N.K., Purnomo, A.S., and Fudholi, A., The effect of heat moisture treatment on crystallinity and physicochemical-digestibility properties of purple yam flour. *Food Hydrocolloids,* 120:106889, 2021.

Chapter 4D

Native and hydrothermally treated yam starch-based edible film incorporated with walnut oil and its coating to study the shelf life of grapes

4D.1   Introduction

This chapter presents the results and discussion on the characterization and starch-based edible films with and without walnut oil, and application of the film-forming solutions as coatings to study the shelf life of grapes. The native and hydrothermally treated *Dioscorea esculenta* starches were used for the film preparation. The characterization of the films were done, and various parameters such weight loss, pH, TSS, titratable acidity, DPPH scavenging activity, total phenolic content and total monomeric anthocyanin content of the uncoated and coated grapes were studied for investigating the effects of native and hydrothermally treated starch-based coatings with or without walnut oil on shelf life of grapes.

4D.2   Properties of films

4D.2.1 Thickness, moisture content, swelling index and solubility of films

The thickness, moisture content, swelling index, and solubility of the edible films (**Fig. 4D.1**) are shown in **Table 4D.1**.

Thickness is an important property of the film as it affects barrier properties such as water vapor permeability (WVP) and other gases. In particular, the thickness affects the water vapor transmission rate due to the difference in water vapor pressure and moisture accumulation at the film-air interface **[10]**.

It was observed that the thickness of the native film increased significantly from 0.18 ± 0.02 to 0.22 ± 0.03 with the addition of walnut oil (WO). A similar trend was observed for millet starch edible film incorporated with clove essential oil, and increasing material concentration when using different components in edible films can increase film thickness **[9]**.

NS0F   **NSWF**   **H1WF**

H2WF   **A1WF**   **A2WF**
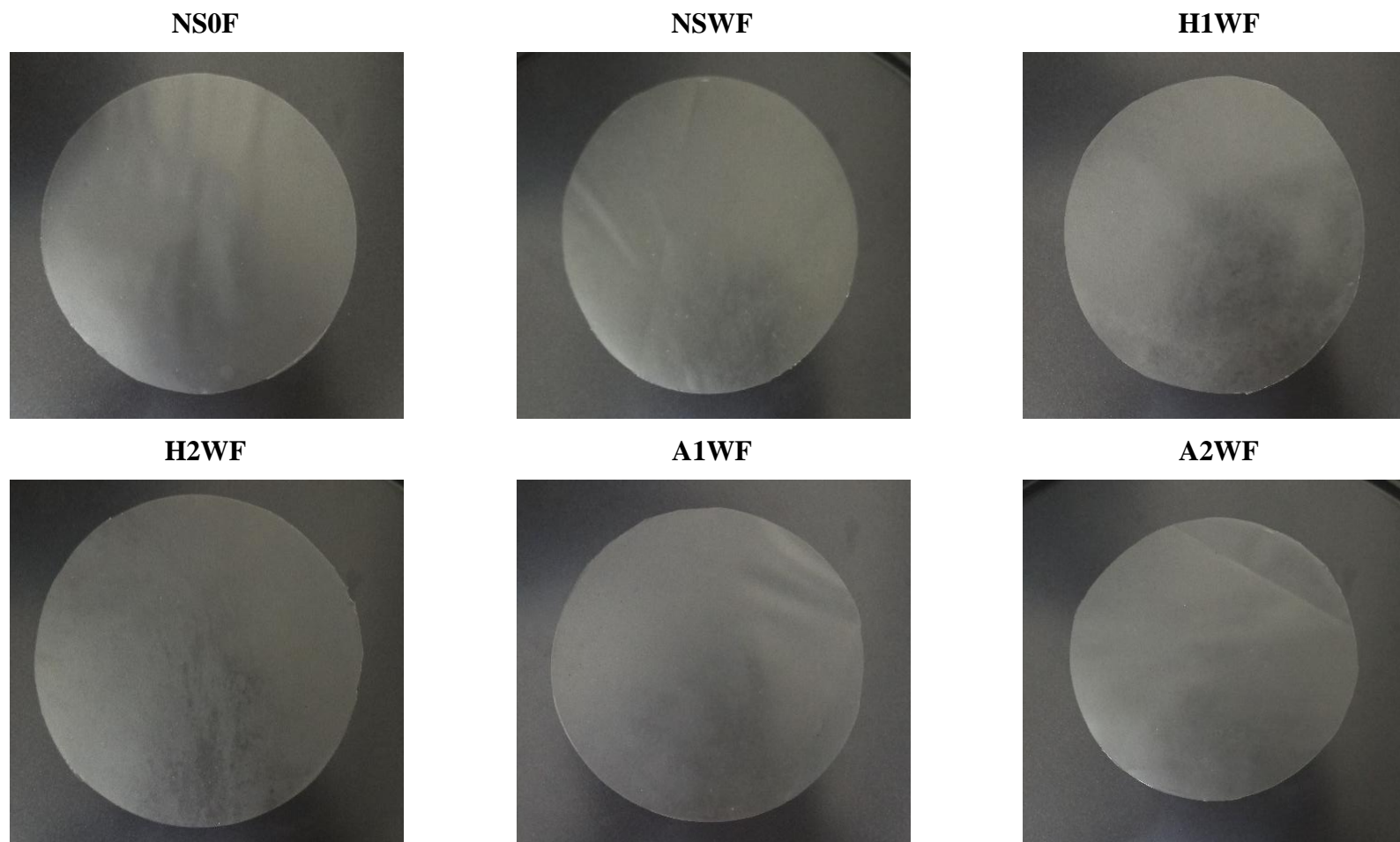

Fig. 4D.1: Edible films prepared from native and hydrothermally modified starches. NS0F: native starch film without walnut oil; NSWF: native starch film with walnut oil; H1WF and H2WF: films prepared from HMT starch with 20% moisture level and 30% moisture level, respectively, and walnut oil; A1WF and A2WF: films prepared from annealed starch with 1:2 and 1:4 starch to moisture ratio, respectively, and walnut oil.

Table 4D.1: Thickness, moisture content, swelling index and solubility of edible films

Sample	Thickness (mm)	Moisture content (%)	Swelling index	Solubility (%)
NS0F	0.18 ± 0.02^b	21.53 ± 0.16^a	0.77 ± 0.02^a	20.00 ± 0.49^a
NSWF	0.22 ± 0.03^a	20.26 ± 0.11^b	0.67 ± 0.02^b	18.37 ± 0.55^b
H1WF	0.19 ± 0.02^b	18.09 ± 0.42^c	0.44 ± 0.02^d	16.36 ± 0.35^c
H2WF	0.18 ± 0.02^b	16.60 ± 0.73^{de}	0.52 ± 0.02^c	18.60 ± 0.39^b
A1WF	0.18 ± 0.02^b	17.37 ± 0.40^{cd}	0.63 ± 0.01^b	18.56 ± 0.55^b
A2WF	0.18 ± 0.02^b	15.79 ± 0.11^e	0.45 ± 0.01^d	18.41 ± 0.38^b

Data values are presented as mean ± standard deviation. Data with different alphabetic superscript in the same column are statistically significant ($p<0.05$). NS0F: native starch film without walnut oil; NSWF: native starch film with walnut oil; H1WF and H2WF: films prepared from HMT starch with 20% moisture level and 30% moisture level, respectively, and walnut oil; A1WF and A2WF: films prepared from annealed starch with 1:2 and 1:4 starch to moisture ratio, respectively, and walnut oil.

In addition, the physical bonding between film and oil, and the formation of micro-droplets from hydrophobic oil during film-forming solution homogenization can also increase the thickness of the film [32]. Meanwhile, no significant ($p<0.05$) variation in the thickness between the hydrothermally treated starch films with walnut oil (H1WF, H2WF, A1WF, and A2WF) and native starch film (NS0F) was noticed. Compared to native starch film with walnut oil (NSWF), significant ($p<0.05$) decrease in the thickness of hydrothermally treated starch films with walnut oil may be due to the greater degree of interaction and rearrangement of amylose and amylopectin molecules of hydrothermally treated starches within the film matrix [28].

The highest moisture content of the native starch film was due to the higher mass fraction of starch and glycerol that has a greater affinity for water and can form hydrogen bonds with water. The incorporation of walnut oil significantly decreased the moisture content of the films, possibly due to the decrease in hydrophilicity of the membranes caused by the addition of oil, which can reduce the hydroxyl groups' interaction with water [23].

A significant decrease in swelling index and solubility was observed for the hydrothermally treated starch films with walnut oil (H1WF, H2WF, A1WF, and A2WF) and native starch film with walnut oil (NSWF) compared to the native starch film (NS0F). This decrease in swelling index and solubility can be credited to the hydrophobic nature of walnut oil, which possibly can cause interaction between oil and starch matrix, resulting in low swelling index and solubility. Moreover, the formation of a tight helical structure due to formed links between amylose-lipid complexes and hydrophobic oil can also contribute to the low swelling power and solubility shown by oil-incorporated starch films [9]. Among all the films, H1WF and A2WF showed the lowest swelling index, which may be due to the higher degree of crystallinity of the films shown by the XRD analysis (**Fig. 4D.4**). A decrease in swelling power with an increase in the crystallinity of wheat starch samples was observed and may be linked to the fact that higher fractions of small crystalline granules exhibit low swelling power [30].

4D.2.2 Transparency and color of films

Transparency is a key characteristic of film that affects its overall appearance and determines its application. The starch film without walnut oil (NS0F) was more transparent (indicated by lower transparency value) as compared to films incorporated with walnut oil (**Table 4D.2**). The results demonstrated that the transparency value of the native film markedly increased from 1.47 to 3.53 due to the addition of oil, giving more-opaque films. This behavior may be due to a change in the film's refractive index at the polymer interface facilitated by the addition of oil, where oil dispersed in the polymer matrix promotes increased light scattering, resulting in increased film opacity [8, 26]. Transparency values of HMT starch films with WO were found to be higher than all other films, indicating lower transparent films. The transparency value was found to be in the order as follows: H2WF> H1WF > A1WF > A2WF > NSWF > NS0F. This reduction in transparency of the HMT starch films with WO may be due to the higher surface roughness as observed in the SEM images (**Fig. 4D.2**). Furthermore, the transparency of starch films can be linked to the compactness of the matrix, and the greater the intermolecular interactions between glycerol and modified starch chains, the denser and more opaque the formed films [3, 31].

The color parameters (*L**, *a** and *b**) of the native and modified starch films with or without WO (**Fig. 4D.1**) are listed in **Table 4D.2**. A non-significant decrease in the

brightness ($L*$ value) of the films (except H2WF and A2WF) was observed with the addition of WO in the starch films. The films with WO (except H1WF) showed a lower $a*$ value indicating a tendency to green. The addition of WO to the starch films led to a significant increase in the yellowness ($b*$) of the films. Similar trends of color parameters were reported due to addition of essential oils to films [8, 18, 32].

Table 4D.2: Transparency and color values of edible films

Samples	Transparency (mm^{-1})	Color values		
		$L*$	$a*$	$b*$
NS0F	1.47 ± 0.01^e	91.33 ± 0.25^a	2.57 ± 0.12^a	-12.60 ± 0.26^a
NSWF	2.99 ± 0.01^d	90.63 ± 0.55^{ab}	1.70 ± 0.04^d	-9.50 ± 0.50^{bc}
H1WF	3.30 ± 0.02^b	89.83 ± 0.68^{abc}	2.43 ± 0.06^{ab}	-10.60 ± 0.26^b
H2WF	3.53 ± 0.02^a	88.70 ± 0.96^c	2.10 ± 0.10^c	-8.87 ± 0.60^c
A1WF	3.22 ± 0.08^{bc}	90.01 ± 0.30^{abc}	2.23 ± 0.12^{bc}	-10.71 ± 0.70^b
A2WF	3.14 ± 0.02^c	89.33 ± 0.21^{bc}	2.30 ± 0.09^{bc}	-10.43 ± 0.21^b

Data values are presented as mean $\pm$ standard deviation. Data with different alphabetic superscript in the same column are statistically significant (p<0.05). NS0F: native starch film without walnut oil; NSWF: native starch film with walnut oil; H1WF and H2WF: films prepared from HMT starch with 20% moisture level and 30% moisture level, respectively, and walnut oil; A1WF and A2WF: films prepared from annealed starch with 1:2 and 1:4 starch to moisture ratio, respectively, and walnut oil.

4D.2.3 SEM morphology of films

SEM micrographs of the of the starch films with and without WO (**Fig. 4D.1**) are presented in **Fig. 4D.2**. The native starch film without WO (NS0F) presented a homogenous and uniform surface. However, the addition of WO to native and modified starch films reduced the homogeneity of the surface. The increase in roughness shown by the WO incorporated films may be due to the hydrophobicity of oil and its density difference with the aqueous starch solution that could affect the stability of the film forming solution, and thus can form heterogeneous structures due to phase separation [8].
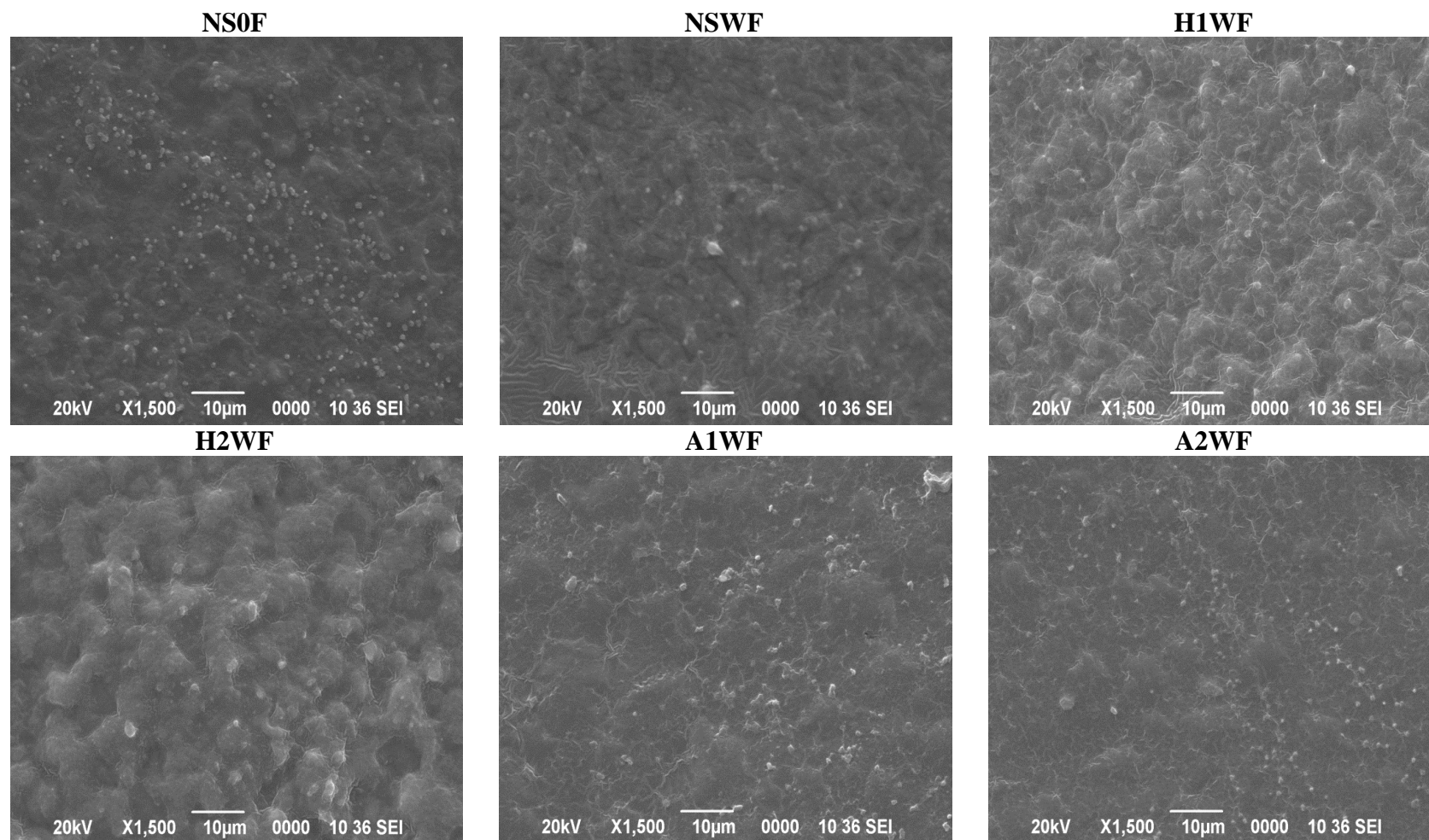
NS0F

NSWF

H1WF
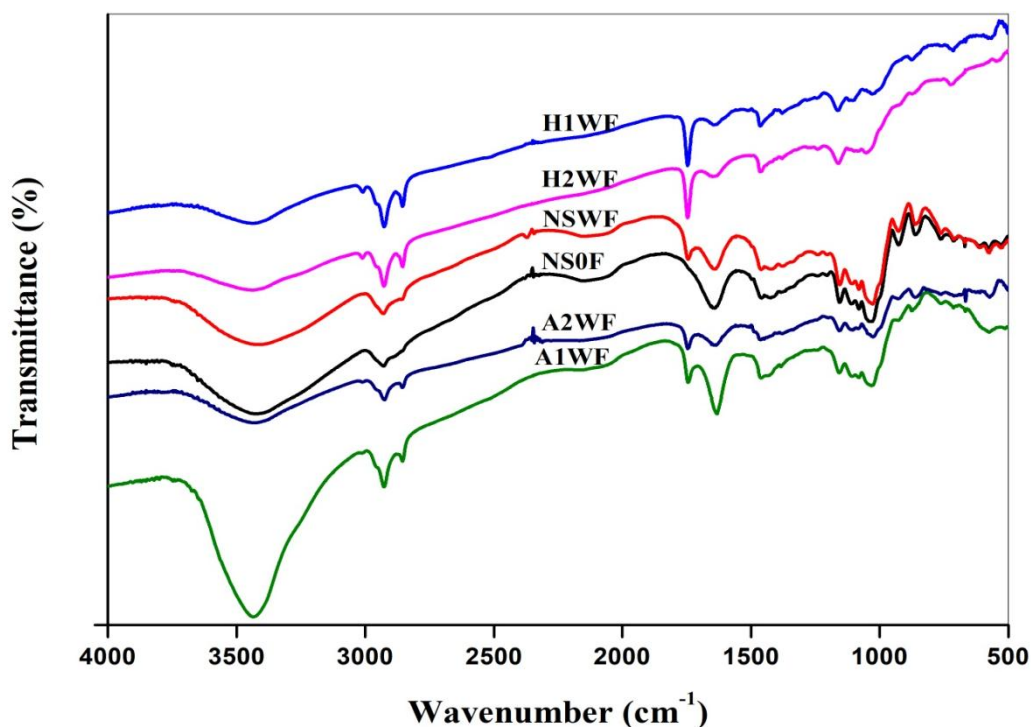
H2WF

A1WF

A2WF

Fig. 4D.2: SEM images of edible films. NS0F: native starch film without walnut oil; NSWF: native starch film with walnut oil; H1WF and H2WF: films prepared from HMT starch with 20% moisture level and 30% moisture level, respectively, and walnut oil; A1WF and A2WF: films prepared from annealed starch with 1:2 and 1:4 starch to moisture ratio, respectively, and walnut oil.

In addition, the surface roughness or heterogeneity of HMT starch films with WO (H1WF and H2WF) was found to be higher, which could be attributed to the increase in surface roughness due to evaporation of water from the surface of starch granules and partial gelatinization of the starch granules during HMT **[5]**.

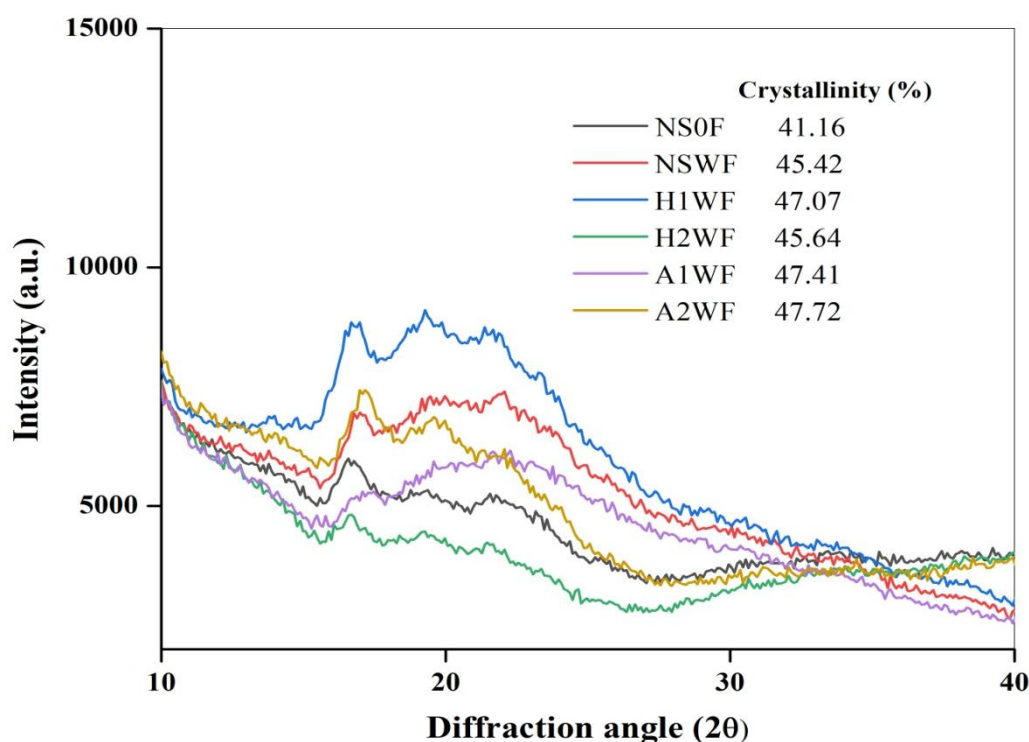## 4D.2.4 FTIR spectra of films

Fig. 4D.3: FTIR spectra of edible films. NS0F: native starch film without walnut oil; NSWF: native starch film with walnut oil; H1WF and H2WF: films prepared from HMT starch with 20% moisture level and 30% moisture level, respectively, and walnut oil; A1WF and A2WF: films prepared from annealed starch with 1:2 and 1:4 starch to moisture ratio, respectively, and walnut oil.

Fig. 4D.3 illustrates the FTIR spectra of starch films with or without WO in the spectral range from 500 to 4000 cm^{-1}. The band at 3421 cm^{-1} corresponds to the stretching vibrations of OH groups that are abundant in water, glycerol and starch **[2]**. The band at 2925 cm^{-1} and 2853 cm^{-1} can be associated with the symmetric and asymmetric stretching CH2 vibrations, respectively **[17]**. The increase in band intensity at 2925 cm^{-1} and a slight shift to a higher wave number may be due to the possibility of interaction between the starch and walnut oil chains **[6]**. A new bandwidth with a peak at

1745 cm^{-1} was observed in the walnut oil starch film possibly due to the presence of saturated aldehyde functional groups [17]. The peak at 1640 cm^{-1} indicates H-O-H bending vibrations. Additionally, the peak at 1640 cm^{-1} can be associated with ester bond and more intense reaction between starch and the walnut oil [2]. The peak at 1461 cm^{-1} represents the bending vibrations of CH$_2$ and CH$_3$ groups [29]. The decrease in peak intensity at ~1000 cm^{-1} is a consequence of the interaction between the starch hydroxyls and stretching of the ether bond C=O of walnut oil [6]. The peaks at 926, 860 and 763 cm^{-1} are likely related to α-1,4-glycosidic bonds, C–H bending and C–C stretching of starch chains [12, 15].

4D.2.5 XRD spectra of films

Fig. 4D.4: XRD spectra of edible films. NS0F: native starch film without walnut oil; NSWF: native starch film with walnut oil; H1WF and H2WF: films prepared from HMT starch with 20% moisture level and 30% moisture level, respectively, and walnut oil; A1WF and A2WF: films prepared from annealed starch with 1:2 and 1:4 starch to moisture ratio, respectively, and walnut oil.

XRD diffraction pattern of the starch films with or without WO are shown in **Fig. 4D.4**. The main peaks of the pure starch film at 16.7°, 19.3° and 21.8° can be attributed

to the type B polymorphisms. The addition of WO in the starch film induced a slight peak shift (~1°) at 16.7°, 19.3° and 21.8°, indicating changes in the crystallization of the amylopectin chain [6, 15].

The native and modified starch films with walnut oil exhibited a higher crystallinity compared to the native starch film without WO. One reason could be that the essential oil has partially evaporated, with little effect on crystallinity. Another possibility is that the essential oil interacts with the starch matrix, reducing phase separation and facilitating plasticization [20]. Hence, the annealed starch films with WO that showed higher crystallinity, was observed to be smoother and uniform in surface than HMT starch films with WO in the SEM micrographs (**Fig. 4D.2**). The relative crystallinity (percentage) was found to be in the order as follows: A2WF>A1WF > H1WF> H2WF > NSWF > NS0F. The increased crystallinity of the modified films may be due to the strengthened association between starch chains and the realignment of disrupted double helices within the crystalline regions, resulting in increased crystalline perfection [14].

4D.2.6 Tensile strength of films

Mechanical properties describe the film's resistance to normal stresses encountered during transportation, application, and handling to maintain food integrity and properties [22]. According to **Table 4D.3**, the addition of WO affected the tensile strength of the starch films. XRD patterns (**Fig. 4D.4**) of the films indicated a higher crystallinity of the films with the addition of WO, and this result is consistent with the high tensile strength obtained for films with higher crystallinity. Similar behavior was shown by cassava starch films loaded with lemongrass essential oil [20]. The starch-starch interactions might have been partially replaced by starch-WO interactions that formed a strengthened associative network, leading to increase in tensile strength of films. Moreover, droplet size of the WO could also influence the tensile strength, as small droplets having higher surface area can increase the level of interactions with the starch matrix, whereas large droplets disturbs the film formation process [4]. The increase in tensile strength in the modified starch films may be due to the increase in coherent forces between starch molecules, and formation of a better-packed crystalline structure caused by the displacement and arrangement of double helices between starch

crystals. Similar results was reported for modified sweet potato starch films and higher crystallinity of the films promoted compactness of the film structure [11].

Table 4D.3: Tensile strength and water vapor permeability of edible films

Sample	Tensile strength (N/mm^2)	Water vapor permeability (10^{-6} g day^{-1} m^{-1} Pa^{-1})
NS0F	4.41 ± 0.51^b	4.28 ± 0.10^a
NSWF	4.75 ± 0.56^b	3.69 ± 0.09^b
H1WF	5.07 ± 0.45^b	2.14 ± 0.18^d
H2WF	4.90 ± 0.41^b	2.79 ± 0.17^c
A1WF	6.64 ± 0.86^a	2.11 ± 0.10^d
A2WF	6.92 ± 0.56^a	1.64 ± 0.19^e

Data values are presented as mean ± standard deviation. Data with different alphabetic superscript in the same column are statistically significant ($p<0.05$). NS0F: native starch film without walnut oil; NSWF: native starch film with walnut oil; H1WF and H2WF: films prepared from HMT starch with 20% moisture level and 30% moisture level, respectively, and walnut oil; A1WF and A2WF: films prepared from annealed starch with 1:2 and 1:4 starch to moisture ratio, respectively, and walnut oil.

4D.2.7 Water vapor permeability (WVP) of films

A packaging film's WVP is one of the most important properties for determining its suitability for use as a packaging material [25]. WVP is one of the important properties among the various water resistance properties of a film and indicates the film's ability to cope with the high humidity environment around and on the food surface [16]. As shown in **Table 4D.3**, the addition of WO in the starch films resulted in decrease of WVP values of the films 4.28 ± 0.10 to 3.69 ± 0.09 (10^{-6} g day^{-1} m^{-1} Pa^{-1}), indicating a continuous network of starch matrix formed by the hydrophobic WO [20], which increased the cohesive force and reduced the transport phenomenon of the film matrix. WVP generally occurs through the hydrophilic portion of films, and so the hydrophobic nature of WO was effective in decreasing the WVP of the films [22]. In the modified starch films, the WVP values increased linearly with the increase in crystallinity as observed from XRD pattern (**Fig. 4D.4**) of the films, and this increase in crystallinity is linearly related to the compactness of the films and can minimize moisture transfer [11].

The WVP values were found to be in the order as follows: A2WF<A1WF<H1WF<H2WF<NSWF<NS0F.

4D.3   Shelf life study of grapes

4D.3.1 Weight loss, pH and TSS

The weight loss, pH and TSS of grapes coated with different coating solutions (**Fig. 4D.5**) during a 15 days storage period are presented in **Fig. 4D.6**, **7** and **8**, respectively.

The native starch and modified starch-based coatings with or without WO significantly decreased the weight loss of grapes (**Fig. 4D.6**) during the 15 days storage period compared to uncoated grapes, indicating that the starch-based coatings enabled the epidermis layer to control water loss associated with weight loss and reduce the respiratory exchange. Moreover, water loss to the atmosphere can take place through the pores present in the grapes, and the starch-based coatings were able to block the pores, thereby preventing humidity loss and reducing respiratory rate.

The uncoated grapes (UC) had the highest percentage of weight loss, with a significant increase from 3.65 % at day 3 to 14.83 % at day 15 at 4 ℃ during refrigerated storage. However, porosity of coatings can also promote the water loss leading to weight loss. The weight loss of UC stored at 4 ℃ for 15 days was less than the weight loss of control grapes stored at 25 ℃ for 12 days reported by **de Souza et al. [7]**, and this difference in weight loss can be attributed to the storage temperature as high temperature favors rapid water evaporation.

The modified starch-based coatings with WO more effectively protected the grapes from weight loss compared to UC and NS0F. ANN starch-based coatings showed a reduced value of weight loss than the HMT starch-based coatings, and the results are consistent with the results of film properties. Our findings have shown A2WF as the best coating for minimizing weight loss (1.84 % at day 3 to 11.58 % at day 15) compared to all other coatings during the storage period. These results demonstrated that modified starch and WO in coating solutions could form a better protective barrier against water evaporation associated with weight loss of grapes.
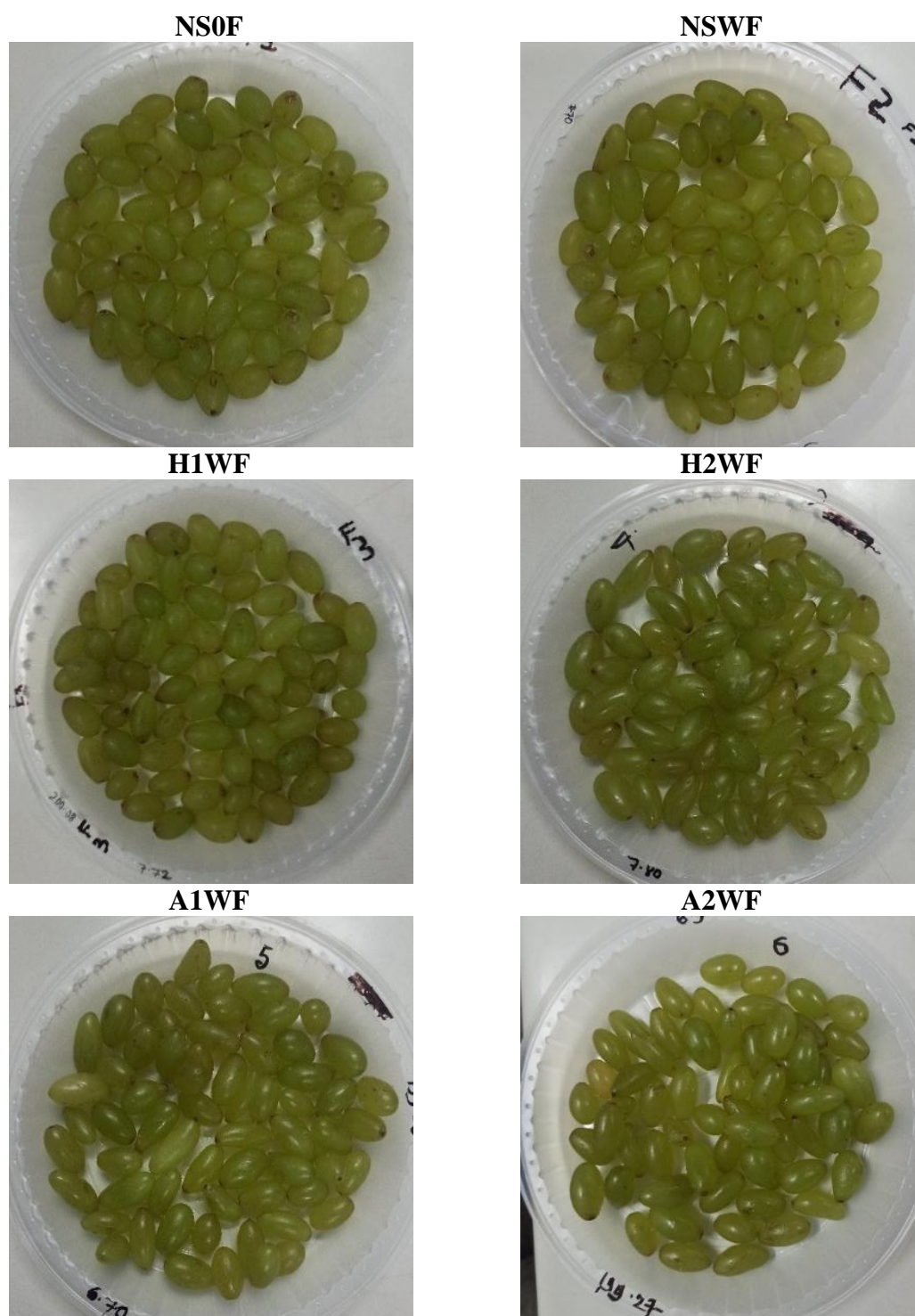
NS0F

NSWF

H1WF

H2WF

A1WF

A2WF

Fig. 4D.5: Grapes coated with different film-forming solutions of NS0F & NSWF: native starch without and with walnut oil, respectively; H1WF and H2WF: HMT starch with 20% and 30% moisture level, respectively, and walnut oil; A1WF and A2WF: annealed starch with 1:2 and 1:4 starch to moisture ratio, respectively, and walnut oil.
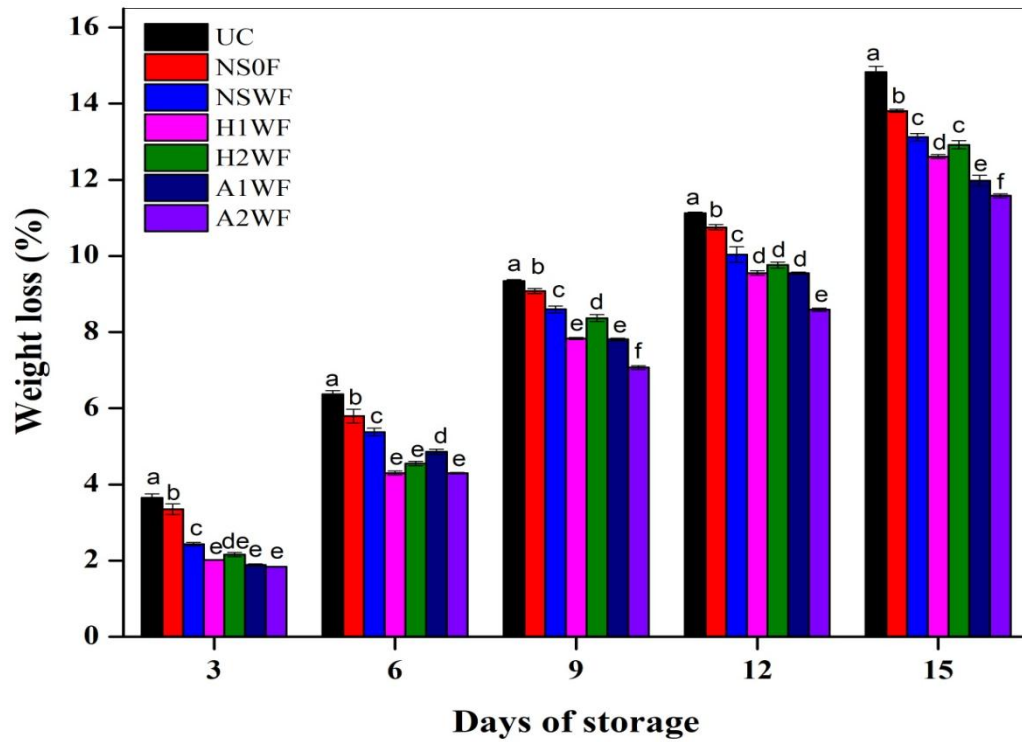
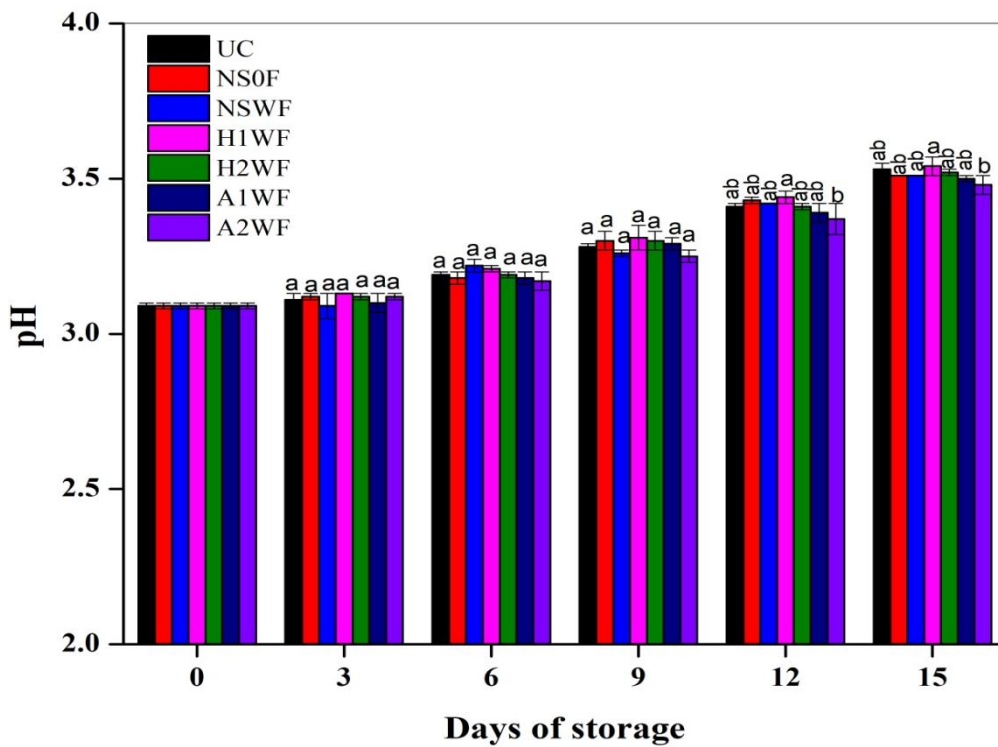**Fig. 4D.6:** Weight loss of grapes with different coatings of film-forming solutions during storage.

Fig. 4D.7: pH of grapes with different coatings of film-forming solutions during storage.

As shown in (**Fig. 4D.6**), there was no significant difference in pH values between the grapes coated with different coating solutions during the storage period, and presented the same variation pattern. The pH values ranged from 3.09 to 3.54 for all the groups during the 15 days of storage period. Treatments applied such as type of edible coatings do not affect the pH of grapes, rather the natural variability of the fruits are responsible for such changes **[13, 19]**. A slight pH change may be due to natural organic acids that maintain the fruit's pH **[27]**.
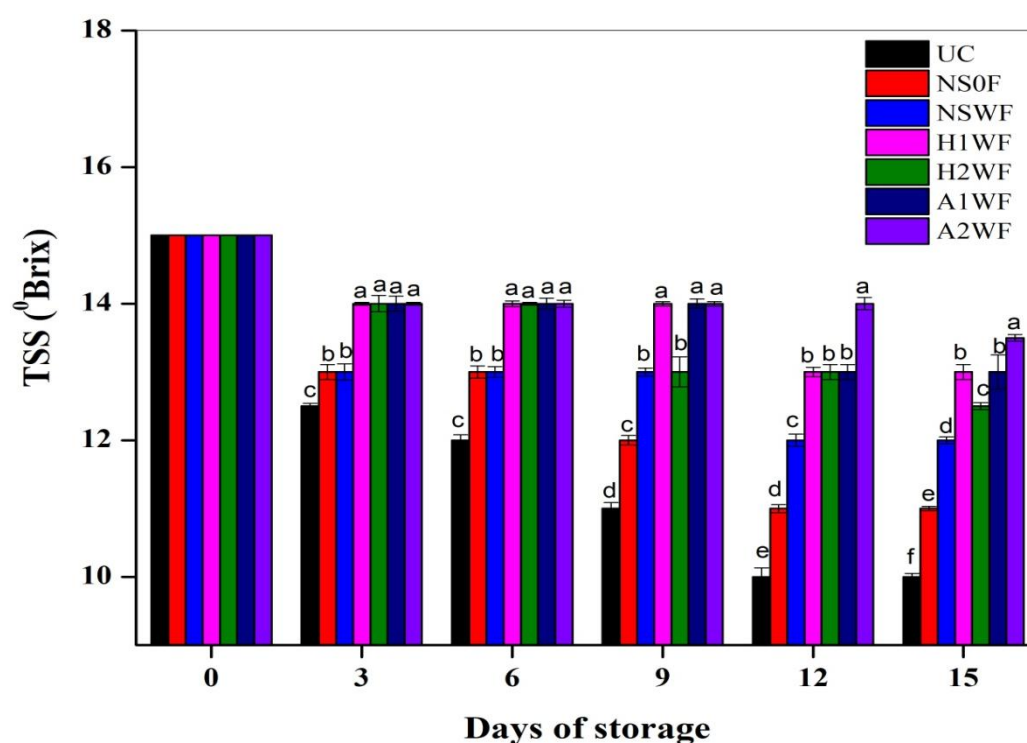
Fig. 4D.8: Total soluble solids (TSS) of grapes with different coatings of film-forming solutions during storage.

TSS content of the uncoated and coated grapes gradually decreased during the 15 days storing period **(Fig. 4D.8)**. This behavior indicates an increase in soluble solids consumption with maturation and the possible initiation of senescence in these samples **[7]**. In addition, the consumption of soluble solids by the respiratory process leads to a decrease in SSC of fruit metabolic activity **[21]**. The modified starch-based coatings with WO significantly reduced the decrease in TSS compared to uncoated and native starch-based coatings with/without WO. This positive effect could be due to the decrease in respiration process caused by WO that forms a gaseous environment at the surface of fruit **[24]**, and the reduced WVP shown by the modified starch-based films with WO.

Similar decrease in TSS have been reported for table grapes coated with chitosan edible nanoparticles that delayed the ripening process due to slow respiration and metabolic activity in the fruit [19].

4D.3.2 Titratable acidity

The titratable acidity (TA) of the uncoated and all the coated grapes decreased during the 15 days storage period (**Fig. 4D.9**). A decrease in TA is associated with the maturation process as organic acids, mainly malic acid, are metabolized as energy in the Krebs cycle [7, 24]. The modified starch based coatings with WO showed a high value of TA than the UC and NS0F at the end of 15-day storage period, indicating their efficacy to control maturation process by forming an effective barrier to gases. Therefore, the modified starch based coatings with WO was effective in delaying the ripening process of grapes by reducing the rate of organic acid biodegradation.
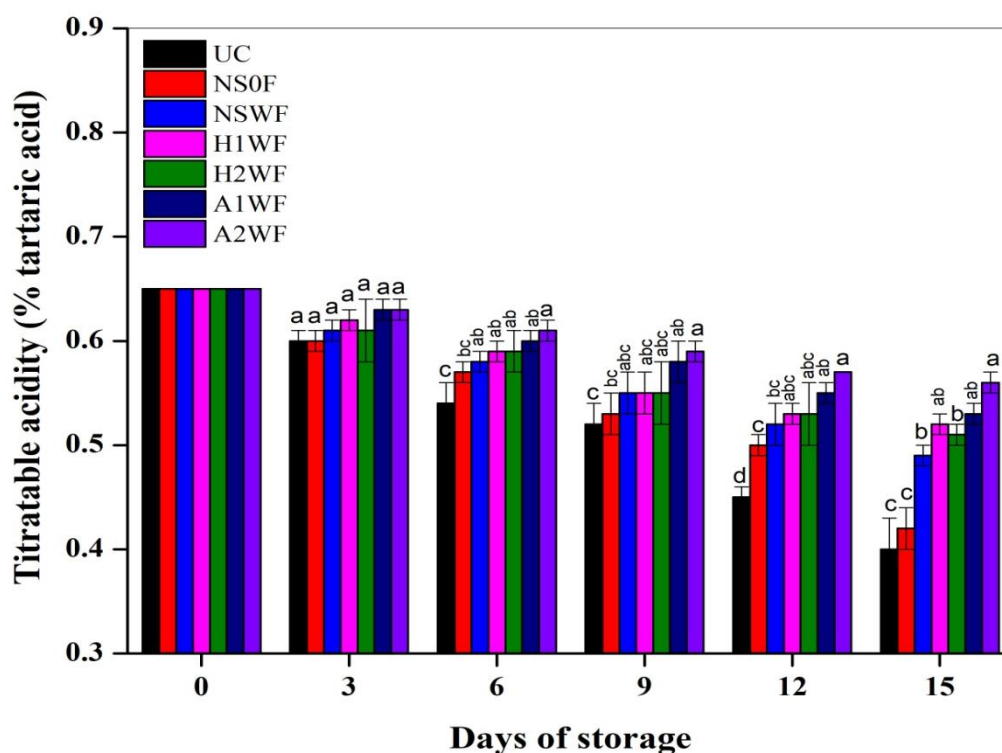

Fig. 4D.9: Titratable acidity of grapes with different coatings of film-forming solutions during storage.

4D.3.3 Total phenolic content and antioxidant activity

Phenolic compounds, distributed in different parts of grapes such as stalks, skin, pulp and seeds, could be positively correlated with the antioxidant activity of grapes.

Results of total phenolic content (TPC) and antioxidant activity (DPPH scavenging activity) are shown in **Fig. 4D.10** and **11**, respectively.
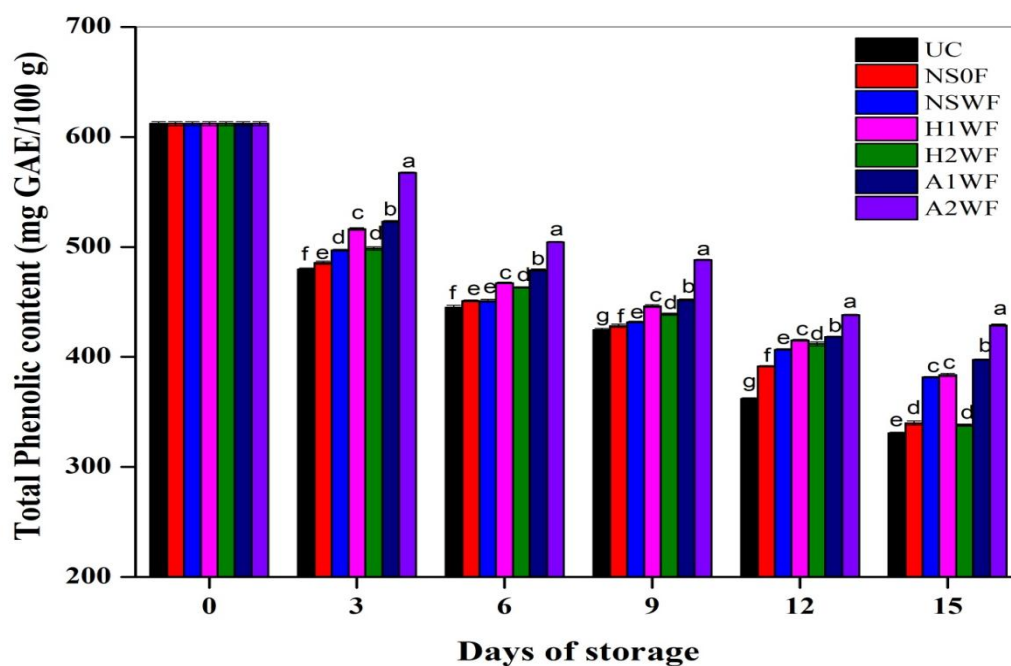

Fig. 4D.10: Total phenolic content (TPC) of grapes with different coatings of film-forming solutions during storage.
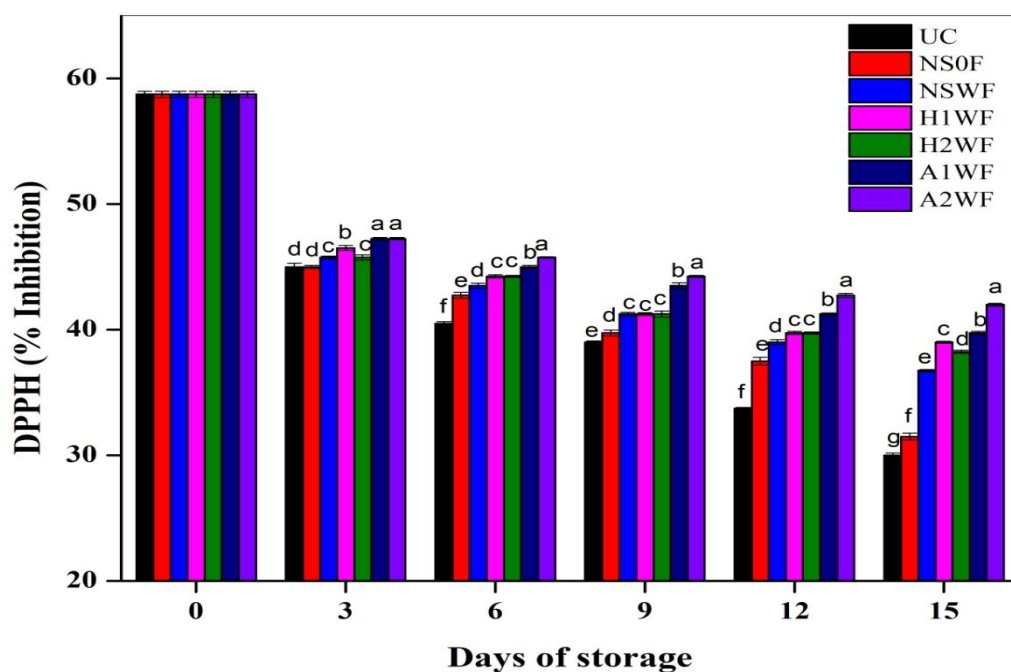

Fig. 4D.11: DPPH scavenging activity (% inhibition) of grapes with different coatings of film-forming solutions during storage.

TPC and DPPH scavenging activity values in all the samples gradually decreased with increase in the storage period. The decline in TPC (**Fig. 4D.10**) and antioxidant activity (**Fig. 4D.11**) was efficiently prevented by the modified starch-based coatings with WO, indicated reduced loss of phenolic compounds during the storage. Similar observation has been reported for table grapes coated with alginate solutions enriched with vanillin [24].

A2WF had the highest TPC and DPPH scavenging activity (428.95 ± 0.92 mg GAE/100 g and 42.01 ± 0.15 % , respectively), while UC had the lowest TPC and DPPH scavenging activity (330.90 ± 0.85 mg GAE/100 g and 30.00 ± 0.18 %, respectively) at the day 15 of storage.
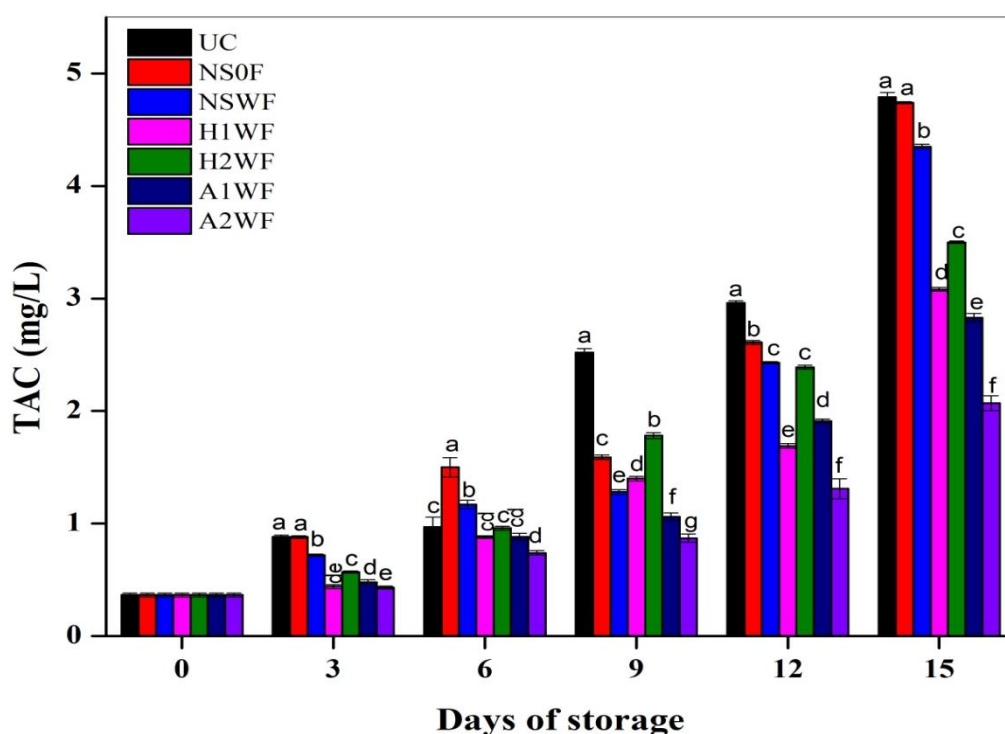
4D.3.4 Total monomeric anthocyanin content

Fig. 4D.12: Total monomeric anthocyanin content (TAC) of grapes with different coatings of film-forming solutions during storage.

Fig. 4D.12 illustrates the total monomeric anthocyanin content (TAC) of the uncoated and coated grapes during the 15 days storing period. Anthocyanins, polyphenolic compounds that are found in table grapes, have essential functional properties that promote human health [1]. However, more accumulation of anthocyanins

in grapes is associated to advanced maturity, which involves synthesis of this pigment from glucose.

The TAC values of all the samples significantly increased during the storage period of 15 days. After 15 days of storage, grapes with annealed starch-based coatings with WO showed the lowest TAC (2.07 ± 0.07, mg/L) compared to all other samples, indicating an inhibitory effect of the coatings on fruit senescence **[19]**.

Studies on reduction of anthocyanin content of grapes has been reported for grapes coated with lemongrass oil nanoemulsion **[13]** and strawberries coated with chitosan-oliec acid **[27]**. Therefore, we conclude that the modified starch-based coatings with WO can effectively prevent fruit ripening and can have anti-aging effect on the grapes during cold storage.

4D.4   Bibliography

[1]   Champa, W.H., Gill, M., Mahajan, B., and Arora, N., Postharvest treatment of polyamines maintains quality and extends shelf-life of table grapes (*Vitis vinifera* L.) cv. Flame Seedless. *Postharvest Biology and Technology,* 91:57-63, 2014.

[2]   Cruz-Tirado, J., Ferreira, R.S.B., Lizárraga, E., Tapia-Blacido, D.R., Silva, N., Angelats-Silva, L., and Siche, R., Bioactive Andean sweet potato starch-based foam incorporated with oregano or thyme essential oil. *Food Packaging and Shelf Life,* 23:100457, 2020.

[3]   Dai, L., Zhang, J., and Cheng, F., Effects of starches from different botanical sources and modification methods on physicochemical properties of starch-based edible films. *International Journal of Biological Macromolecules,* 132:897-905, 2019.

[4]   De Moura, M.R., Aouada, F.A., Avena-Bustillos, R.J., McHugh, T.H., Krochta, J.M., and Mattoso, L.H., Improved barrier and mechanical properties of novel hydroxypropyl methylcellulose edible films with chitosan/tripolyphosphate nanoparticles. *Journal of Food Engineering,* 92(4):448-453, 2009.

[5]   de Oliveira, C.S., Bet, C.D., Bisinella, R.Z.B., Waiga, L.H., Colman, T.A.D., and Schnitzler, E., Heat-moisture treatment (HMT) on blends from potato starch (PS) and sweet potato starch (SPS). *Journal of Thermal Analysis and Calorimetry,* 133(3):1491-1498, 2018.

[6]   de Souza, A.G., Dos Santos, N.M.A., da Silva Torin, R.F., and dos Santos Rosa, D., Synergic antimicrobial properties of Carvacrol essential oil and montmorillonite in biodegradable starch films. *International Journal of Biological Macromolecules,* 164:1737-1747, 2020.

[7]   de Souza, W.F.C., de Lucena, F.A., da Silva, K.G., Martins, L.P., de Castro, R.J.S., and Sato, H.H., Influence of edible coatings composed of alginate, galactomannans, cashew gum, and gelatin on the shelf-life of grape cultivar 'Italia': Physicochemical and bioactive properties. *LWT-Food Science and Technology,* 152:112315, 2021.

[8]   do Evangelho, J.A., da Silva Dannenberg, G., Biduski, B., El Halal, S.L.M., Kringel, D.H., Gularte, M.A., Fiorentini, A.M., and da Rosa Zavareze, E., Antibacterial activity, optical, mechanical, and barrier properties of corn starch films containing orange essential oil. *Carbohydrate Polymers,* 222:114981, 2019.

[9]   G. Al-Hashimi, A., Ammar, A.B., Cacciola, F., and Lakhssassi, N., Development of a millet starch edible film containing clove essential oil. *Foods,* 9(2):184, 2020.

[10]   Gutiérrez, T.J., Tapia, M.S., Pérez, E., and Famá, L., Structural and mechanical properties of edible films made from native and modified cush-cush yam and cassava starch. *Food Hydrocolloids,* 45:211-217, 2015.

[11]   Indrianti, N., Pranoto, Y., and Abbas, A., Preparation and characterization of edible films made from modified sweet potato starch through heat moisture treatment. *Indonesian Journal of Chemistry,* 18(4):679-687, 2018.

[12]   Kang, J.-H. and Song, K.B., Characterization of Job's tears (*Coix lachryma-jobi* L.) starch films incorporated with clove bud essential oil and their antioxidant effects on pork belly during storage. *LWT-Food Science and Technology,* 111:711-718, 2019.

[13]   Kim, I.-H., Oh, Y.A., Lee, H., Song, K.B., and Min, S.C., Grape berry coatings of lemongrass oil-incorporating nanoemulsion. *LWT-Food Science and Technology,* 58(1):1-10, 2014.

[14]   Klein, B., Pinto, V.Z., Vanier, N.L., da Rosa Zavareze, E., Colussi, R., do Evangelho, J.A., Gutkoski, L.C., and Dias, A.R.G., Effect of single and dual heat–moisture treatments on properties of rice, cassava, and pinhao starches. *Carbohydrate Polymers,* 98(2):1578-1584, 2013.

[15]   Kumar, R., Ghoshal, G., and Goyal, M., Moth bean starch (*Vigna aconitifolia*): isolation, characterization, and development of edible/biodegradable films. *Journal of Food Science and Technology,* 56(11):4891-4900, 2019.

[16]   Li, J., Ye, F., Lei, L., and Zhao, G., Combined effects of octenylsuccination and oregano essential oil on sweet potato starch films with an emphasis on water resistance. *International Journal of Biological Macromolecules,* 115:547-553, 2018.

[17]   Liang, P., Chen, C., Zhao, S., Ge, F., Liu, D., Liu, B., Fan, Q., Han, B., and Xiong, X., Application of Fourier transform infrared spectroscopy for the oxidation and peroxide value evaluation in virgin walnut oil. *Journal of Spectroscopy,* 2013, 2013.

[18]   Mehdizadeh, T., Tajik, H., Langroodi, A.M., Molaei, R., and Mahmoudian, A., Chitosan-starch film containing pomegranate peel extract and Thymus kotschyanus essential oil can prolong the shelf life of beef. *Meat Science,* 163:108073, 2020.

[19]   Melo, N.F.C.B., de MendonçaSoares, B.L., Diniz, K.M., Leal, C.F., Canto, D., Flores, M.A., da Costa Tavares-Filho, J.H., Galembeck, A., Stamford, T.L.M., and Stamford-Arnaud, T.M., Effects of fungal chitosan nanoparticles as eco-friendly edible coatings on the quality of postharvest table grapes. *Postharvest Biology and Technology,* 139:56-66, 2018.

[20]   Mendes, J., Paschoalin, R., Carmona, V., Neto, A.R.S., Marques, A., Marconcini, J., Mattoso, L., Medeiros, E., and Oliveira, J., Biodegradable polymer blends based on corn starch and thermoplastic chitosan processed by extrusion. *Carbohydrate Polymers,* 137:452-458, 2016.

[21]   Özden, Ç. and Bayindirli, L., Effects of combinational use of controlled atmosphere, cold storage and edible coating applications on shelf life and quality attributes of green peppers. *European Food Research and Technology,* 214(4):320-326, 2002.

[22]   Pelissari, F.M., Grossmann, M.V., Yamashita, F., and Pineda, E.A.G., Antimicrobial, mechanical, and barrier properties of cassava starch− chitosan films incorporated with oregano essential oil. *Journal of Agricultural and Food Chemistry,* 57(16):7499-7504, 2009.

[23] Song, X., Zuo, G., and Chen, F., Effect of essential oil and surfactant on the physical and antimicrobial properties of corn and wheat starch films. *International Journal of Biological Macromolecules,* 107:1302-1309, 2018.

[24] Takma, D.K. and Korel, F., Impact of preharvest and postharvest alginate treatments enriched with vanillin on postharvest decay, biochemical properties, quality and sensory attributes of table grapes. *Food Chemistry,* 221:187-195, 2017.

[25] Turan, D., Water vapor transport properties of polyurethane films for packaging of respiring foods. *Food Engineering Reviews,* 13(1):54-65, 2021.

[26] Valencia-Sullca, C., Vargas, M., Atarés, L., and Chiralt, A., Thermoplastic cassava starch-chitosan bilayer films containing essential oils. *Food Hydrocolloids,* 75:107-115, 2018.

[27] Vargas, M., Albors, A., Chiralt, A., and González-Martínez, C., Quality of cold-stored strawberries as affected by chitosan–oleic acid edible coatings. *Postharvest Biology and Technology,* 41(2):164-171, 2006.

[28] Viana, E.B.M., Oliveira, N.L., Ribeiro, J.S., Almeida, M.F., Souza, C.C.E., Resende, J.V., Santos, L.S., and Veloso, C.M., Development of starch-based bioplastics of green plantain banana (*Musa paradisiaca* L.) modified with heat-moisture treatment (HMT). *Food Packaging and Shelf Life,* 31:100776, 2022.

[29] Wen, Y., Zhou, S., Wang, L., Li, Q., Gao, Y., and Yu, X., New Method for the Determination of the Induction Period of Walnut Oil by Fourier Transform Infrared Spectroscopy. *Food Analytical Methods,* 15(3):833-843, 2022.

[30] Wong, R. and Lelievre, J., Comparison of the crystallinities of wheat starches with different swelling capacities. *Starch-Stärke,* 34(5):159-161, 1982.

[31] Yan, Q., Hou, H., Guo, P., and Dong, H., Effects of extrusion and glycerol content on properties of oxidized and acetylated corn starch-based films. *Carbohydrate Polymers,* 87(1):707-712, 2012.

[32] Zhou, Y., Wu, X., Chen, J., and He, J., Effects of cinnamon essential oil on the physical, mechanical, structural and thermal properties of cassava starch-based edible films. *International Journal of Biological Macromolecules,* 184:574-583, 2021.